



D3.1

Modelling, simulation and assessment of vehicle automations and automated vehicles' driver behaviour in mixed traffic

Project Acronym	TransAID
Project Title	Transition Areas for Infrastructure-Assisted Driving
Project Number	Horizon 2020 ART-05-2016 – GA Nr 723390
Work Package	WP3 Modelling and Impact Assessment of Automated Vehicles
Lead Beneficiary	CERTH - HIT (CRT)
Editor / Main Author	Evangelos Mintsis CRT
Reviewer	Sven Maerivoet TML
Dissemination Level	PU
Contractual Delivery Date	30/06/2018 (M10)
Actual Delivery Date	12/08/2018 (M12)
Version	V1.0



This project has received funding from the European Union's Horizon 2020 research and innovation programme under grant agreement No 723390.

Document revision history

Version	Date	Comments
v0.1	2018-05-15	Initial draft version including the structure of the deliverabel D3.1.
v0.2	2018-05-31	Chapter 1 “Introduction” and Section 2.1 “Adaptive Cruise Control Model” added.
v0.3	2018-06-14	Sub-section 2.2.1 “Parametrization of SUMO Lane Change Model (LC2013)” added.
v0.4	2018-06-28	Sections 3.1 – 3.4 of Chapter 3 “Simulation Experiments” added.
v0.5	2018-07-19	Chapters 1, 2, and 3 finalized.
v0.6	2018-07-31	Section 4.2 “Scenario 2.1 Prevent ToC/MRM by providing speed, headway and/or lane advice” and Appendix A added.
v0.7	2018-08-08	All chapters finalized apart from conclusions chpater.
v0.8	2018-08-09	Added conclusions chapter, checked all references (literature, figures, and tables).
v0.9	2018-08-10	TML review processed.
v1.0	2018-08-12	Final version

Editor / Main author

Evangelos Mintsis (CRT)

List of contributors

Evangelos Mintsis (CRT), Leonhard Luecken (DLR), Kallirroï Porfyri (CRT), Dimitris Koutras (CRT), Xiaoyun Zhang (DYN), Michele Rondinone (HYU), Julian Schindler (DLR), Sven Maerivoet (TML), Lars Akkermans (TML), Kristof Carlier (TML), Inge Mayeres (TML), Alejandro Correa (UMH), Evangelos Mitsakis (CRT)

List of reviewers

Sven Maerivoet (TML)

Dissemination level:

- PU : Public
- RE : Restricted to a group specified by the consortium (including the Commission Services)
- CO : Confidential, only for members of the consortium (including the Commission Services)

Table of contents

Document revision history	2
Table of contents	3
1. Introduction	6
1.1 About TransAID	6
1.1.1 Iterative project approach	6
1.2 Purpose of this document	6
1.3 Structure of this document	7
1.4 Glossary	7
2 Modelling of vehicle automations	9
2.1 Adaptive Cruise Control (ACC) Model	9
2.1.1 Background	9
2.1.2 ACC Controller	10
2.1.2.1 Speed Control Mode	10
2.1.2.2 Gap Control Mode	10
2.1.2.3 Gap-closing Control Mode	11
2.1.2.4 Collision Avoidance Mode	11
2.2 (C)AV/CV Lane Change Model	12
2.2.1 Parametrisation of SUMO Lane Change Model (LC2013)	12
2.2.2 Overview of LC2013 Model	13
2.2.2.1 Lane Change Intention	13
2.2.3 Sensitivity Analysis of LC2013 Model	20
2.2.3.1 Introduction	20
2.2.3.2 Variance-based sensitivity analysis	21
2.2.3.3 Application and Results	22
2.3 Simulation of Take-over Process	28
2.3.1 Structure of Take-over Events	28
2.3.2 Parametrisation of the ToC Model	29
2.3.3 Modelling of a Decreased Post-ToC Driver Performance	30
2.3.4 Implementation of the ToC Model in SUMO	37
3 Simulation Experiments	38
3.1 Dimensions of Simulation Experiments	38
3.2 Updated Actors Definition	38
3.3 Traffic Composition	39

3.4	Traffic Demand Levels.....	40
3.5	Driver Models Parametrisation	41
3.5.1	Vehicle Properties	44
3.6	Simulation Runs	47
3.7	Simulation Output	47
4	Baseline Simulation Scenarios.....	50
4.1	Scenario 1.1 Provide path around road works via bus lane.....	50
4.1.1	Scenario Description	50
4.1.2	Results.....	51
4.1.2.1	Impacts on Traffic Efficiency.....	51
4.1.2.2	Impacts on Traffic Dynamics	55
4.1.2.3	Impacts on Traffic Safety	56
4.1.2.4	Environmental Impacts.....	57
4.2	Scenario 2.1 Prevent ToC/MRM by providing speed, headway and/or lane advice.....	59
4.2.1	Scenario Description	59
4.2.2	Results.....	62
4.2.2.1	Impacts on Traffic Efficiency.....	62
4.2.2.2	Impacts on Traffic Dynamics	67
4.2.2.3	Impacts on Traffic Safety	68
4.2.2.4	Environmental Impacts.....	70
4.3	Scenario 3.1 Apply traffic separation before motorway merging/diverging.....	72
4.3.1	Scenario Description	72
4.3.2	Results.....	73
4.3.2.1	Impacts on Traffic Efficiency.....	73
4.3.2.2	Impacts on Traffic Dynamics	76
4.3.2.3	Impacts on Traffic Safety	77
4.3.2.4	Environmental Impacts.....	78
4.4	Scenario 4.2: Safe spot in lane of blockage.....	80
4.4.1	Scenario Description	80
4.4.2	Results.....	82
4.4.2.1	Urban Network	82
4.4.2.2	Motorway Network.....	89
4.5	Scenario 5.1: Schedule ToCs before no AD zone	96
4.5.1	Scenario Description	96
4.5.2	Results.....	97

4.5.2.1	Impacts on Traffic Efficiency	97
4.5.2.2	Impacts on Traffic Dynamics	99
4.5.2.3	Impacts on Traffic Safety	100
4.5.2.4	Environmental Impacts	100
5	Conclusions	102
	References	104
	Appendix A	109

1. Introduction

1.1 About TransAID

As automated driving (AD) becomes feasible on interrupted and uninterrupted traffic flow facilities, it is important to assess its impacts on traffic safety, traffic efficiency, and the environment. During the early stages of AD market introduction, cooperative and automated vehicles (CAVs), automated vehicles (AVs) of different SAE levels, cooperative vehicles (CVs) able to communicate via vehicle-to-anything (V2X), and legacy vehicles (LVs) will share the same roads with varying penetration rates. In the course of this period, there will be areas and situations on the roads where high automation can be granted, and others where it will not be allowed or feasible due to system failures, highly complex traffic situations, human factors and possibly other reasons. At these areas many AVs will have to change their level of automation. We refer to these areas as “Transition Areas” (TAs).

TransAID develops and demonstrates traffic management procedures and protocols to enable smooth coexistence of (C)AVs, CVs, and LVs, especially at TAs. A hierarchical and centralized approach is adopted, where control actions are implemented at different layers including traffic management centres, roadside infrastructure, and vehicles.

Initially, simulations will be run to investigate the efficiency of infrastructure-assisted traffic management solutions in controlling (C)AVs, CVs, and LVs at TAs, taking into account traffic safety, traffic efficiency and environmental metrics. Then, communication protocols for the cooperation between (C)AVs – CVs and the road infrastructure are going to be developed. Traffic measures to detect and inform LVs will be also addressed. The most promising solutions will be subsequently implemented as real world prototypes and demonstrated at a test track (1st project iteration), or possibly under actual urban traffic conditions (2nd project iteration). Finally, guidelines for advanced infrastructure-assisted driving will be formulated. These guidelines are going to include a roadmap defining necessary activities and upgrades of road infrastructure in the upcoming fifteen years to guarantee a smooth coexistence of (C)AVs, CVs, and LVs.

1.1.1 Iterative project approach

TransAID develops and tests infrastructure-assisted management solutions for mixed traffic ((C)AVs, CVs, and LVs) at TAs in two project iterations. Each project iteration lasts half of the total project duration. During the first project iteration, focus is placed on studying Transitions-of-Control (ToCs) and Minimum Risk Manoeuvres (MRMs) using simplified scenarios. To this end, models for AD and ToC/MRM are adopted and developed. The simplified scenarios are used for conducting several simulation experiments to analyse the impacts of ToCs at TAs, and the effects of the corresponding mitigating measures.

During the second project iteration, the experience accumulated during the first project iteration is used to refine/tune the driver models and enhance/extend the proposed mitigating measures. Moreover, the complexity/realism of the tested scenarios will be increased and the possibility of combining multiple simplified scenarios into one new more complex Use Case (UC) is considered.

1.2 Purpose of this document

This deliverable D3.1 encompasses the modelling of vehicle automations and automated vehicles’ driver behaviour in SUMO (Simulator of Urban MObility) (Task T3.1), as well as the simulation of baseline scenarios (Task T3.2) previously defined in D2.2. Initially, we provide a description of the first stable versions of the driver models emulating the longitudinal and lateral motion of (C)AVs

and CVs. These driver models dictate the motion of (C)AVs and CVs upstream and downstream of TAs where AD is feasible and allowed. Longitudinal motion is determined by an Adaptive Cruise Control (ACC) system, while the lateral motion is determined by the SUMO default lane change model (LC2013). The latter was parametrised to reflect actual (C)AV and CV lane change behaviour. (C)AVs' driver behaviour is also modelled when a take-over request (ToR) by the vehicle automation is issued. Based on driver's responsiveness, a ToC can either be successful or lead to the execution of an MRM. We also include a detailed description of a combined ToC/MRM model.

Vehicle demand levels and mixes were previously defined in deliverable D2.2 for the conduct of the baseline simulation experiments. D3.1 further elaborates the discussion on actors by proposing a new vehicle classification that represents actual driving conditions in a more comprehensive manner. We also present a parametrisation scheme of the driver models (ACC, LC2013, ToC/MRM) that accounts for simulation experiments that have different effects on traffic safety and efficiency. Moreover, this document includes the results of the baseline simulation experiments. Simulation results were analysed using a subset of the Key Performance Indicators (KPIs) defined in D2.1. D3.1 establishes the basis for the conduct of the subsequent simulation experiments both in WP3 and WP6. We expect it to unravel limitations of the simulated driver models, demonstrate the impacts of ToCs and possible MRMs at TAs, and identify the UCs and scenarios where ToCs/MRMs play a major role in traffic operations. Thus, this deliverable will provide valuable information for the development of the TransAID measures and the set up of the more detailed simulations (encompassing communication aspects) that will be run on the iTETRIS Platform (WP6).

1.3 Structure of this document

This document is comprised of five chapters and one Appendix. Chapter 1 is the introductory chapter where we present a summary of the project, describe the purpose of this document, and provide the structure of D3.1 and the Glossary. The driver models developed to emulate the longitudinal and lateral motion of AVs, and the behaviour of automated vehicles drivers during ToC are outlined in Chapter 2. Chapter 3 includes the description of the simulation experiments (experiments dimensionality, driver models parametrisation, simulation input, simulation runs, and simulation output). We present and analyse the baseline simulation results in Chapter 4, and discuss relevant conclusions in Chapter 5. Finally, in Appendix A we present the information regarding the setup of the baseline simulation experiments.

1.4 Glossary

Abbreviation/Term	Definition
ACC	Adaptive Cruise Control
AD	Automated Driving
ADAS	Advanced Driver Assistance Systems
AV	Automated Vehicle
CAV	Cooperative Automated Vehicle
CV	Cooperative Vehicle

DVU	Driver-vehicle unit
DX.X	Deliverable X.X
HMI	Human Machine Interface
IDM	Intelligent Driver Model
KPI	Key Performance Indicator
LC2013	SUMO Lane Change Model (default)
LOS	Level of Service (from Highway Capacity Manual)
LV	Legacy Vehicle
MRM	Minimum Risk Manoeuvre
RSI	Road-side Infrastructure
SAE	Society of Automotive Engineers
SSM	Surrogate Safety Measure
SUMO	Simulation of Urban MObility
TA	Transition Area
ToC	Transition of Control
ToR	Take-over Request
TransAID	Transition Areas for Infrastructure-Assisted Driving
UC	Use Case
V2X	Vehicle-to-anything
VDIFF	Velocity Difference Model
VMS	Variable Message Signs
WP	Work Package

2 Modelling of vehicle automations

The modelling requirements (WP3) for the conduct of the simulation analysis (with abstract communications) during the first project iteration were specified in D2.2. In line with these specifications, we extended an ACC model adopted from a previous study in order to replicate the longitudinal motion of (C)AVs/CVs. In addition we parametrised the SUMO LC2013 model to reflect the lateral motion of (C)AVs/CVs, and finally we developed a ToC/MRM model to mimic automated vehicles driver behaviour during ToC, and the (C)AVs MRM in case of driver's unresponsiveness. A detailed description of the latter driver models is presented subsequently.

2.1 Adaptive Cruise Control (ACC) Model

2.1.1 Background

Advanced Driver Assistance Systems (ADAS) have been designed to increase road safety and driving comfort (Blythe & Curtis, 2004). In the past decade, the automobile industry has been deploying ADAS at an increasing rate on new vehicles. ACC is one such a benchmark ADAS, being heavily studied and currently tested in real-world conditions to unravel its impacts on the traffic flow.

ACC systems that are currently available on the market enable automatic following of a preceding vehicle by controlling the throttle and/or the brake actuators of the ACC vehicle. Specifically, using range sensors, such as radar, lidar and video camera, an ACC system is able to measure the distance and the relative velocity with respect to a preceding vehicle. If the ACC sensors detect a slower preceding vehicle, it automatically adjusts the speed to maintain a desired space headway (gap-control mode). In the absence of a preceding vehicle, the ACC vehicle operates under the speed-control mode, maintaining the user's chosen desired speed.

Many studies address the impacts of ACC vehicles on traffic flow dynamics with the use of traffic simulation, mainly because large-scale field tests have not been implemented. However, some investigations predict a positive effect of ACC (Davis, 2004; Hasebe et al., 2003; Naus et al., 2010; Treiber & Helbing, 2001; van Arem et al., 2006), whereas others are more conservative on the stabilisation results of ACC systems (Marsden et al., 2001; Milanés et al., 2014).

In (Liang & Peng, 1999) the authors suggested a two-level ACC synthesis method based on optimal control theory. The upper level calculates the desired acceleration rate depending on measurements of the vehicle range (inter-vehicle distance in terms to its predecessor) and range rate (difference in the corresponding speeds), whereas the lower (servo) level deals with the accurate conversion of the higher-level acceleration command into brake or throttle commands. Given that the control signal optimises the range and range errors rate of all vehicles in a platoon, string stability is guaranteed.

In (VanderWerf et al., 2001) a mathematical model that incorporates ACC functionality was developed, aiming to predict the effects of the ACC vehicles on overall traffic flow dynamics and safety. A year later this model was used to investigate the effects of different vehicle types (manually driven vehicles and ACC vehicles) on traffic flow capacity, for different market penetration rates (VanderWerf et al., 2002). The study showed that conventional ACC systems are unlikely to have significant positive or negative effects on traffic flow.

In (Kesting et al., 2008) the Intelligent Driver Model (IDM) introduced by (Treiber et al., 2000) was used as a reference for incorporating ACC behaviour in traffic flow simulations. According to the simulation results, traffic congestion was eliminated with a low ACC market penetration (25%)

while significant improvements in travel times were produced for much lower penetration rates (5%).

A car-following control algorithm for ACC equipped vehicles was presented in (Shladover et al., 2012). The algorithm was developed based on field data collected through experiments conducted with ACC equipped vehicles proprietary to Nissan. The authors proposed two modes in the developed ACC control algorithm: the speed control and the gap control mode. The former enables vehicles to maintain their speed close to the desired speed limit, while the latter aims to maintain the desired gap between the controlled vehicle and the preceding one. Simulation results demonstrated that the increase in the number of ACC vehicles is unlikely to increase the capacity of the freeway significantly.

Within the context of modelling vehicle automations in WP3 (Task T3.1), we integrated a car-following model reflecting ACC behaviour in the microscopic traffic simulator SUMO (Behrisch et al., 2011); it builds upon recent work from (Xiao et al., 2017), where an ACC simulation model originating from a commercial ACC controller (Milanes et al., 2014) was established to guarantee the full-speed range operation of equipped vehicles while considering the collision avoidance constraint.

2.1.2 ACC Controller

The selected ACC driving model is based on (Liu et al., 2018; Milanés & Shladover, 2014, 2016; Milanes et al., 2014; Xiao et al., 2017), whereby the developed control law in the ACC control algorithm is explicitly divided into three modes based on three different motion purposes: (i) speed (or cruising) control, (ii) gap-closing control, and (iii) gap control. More specifically, the speed control mode is designed to maintain the by the driver chosen desired speed, the gap control mode aims to maintain a constant time gap between the controlled vehicle and its predecessor, while the gap-closing controller enables the smooth transition from speed control mode to gap control mode. In addition, TransAID has introduced a fourth mode (i.e. collision avoidance mode) to the latter controller that prevents rear-end collisions when safety critical conditions prevail. In the following text we present the basic definitions and equations for these four ACC control modes.

2.1.2.1 Speed Control Mode

The feedback control law in speed mode is activated when there are no preceding vehicles in the range covered by the sensors, or preceding vehicles exist in a spacing larger of 120 m (Liu et al., 2018; Xiao et al., 2017). This mode aims to eliminate the deviation between the vehicle speed and the desired speed and is given as:

$$a_{i,k+1} = k_1(v_d - v_{i,k}), k_1 > 0 \quad (1)$$

where $a_{i,k+1}$ represents the acceleration recommended by the speed control mode of the i -th consecutive (subject) vehicle for the next time step $k + 1$; v_d and $v_{i,k}$ indicates the desired cruising speed and the speed of the i -th vehicle at the current time step k , respectively; k_1 is the control gain determining the rate of speed deviation for acceleration. Typical values for this gain range between $0.3 - 0.4 \text{ s}^{-1}$ according to (Xiao et al., 2017); in this study we selected 0.4 s^{-1} .

2.1.2.2 Gap Control Mode

When the gap control mode is activated, the acceleration in the next time step $k + 1$ is modelled as a second-order transfer function based on the gap and speed deviations with respect to the preceding vehicle; it is defined as:

$$a_{i,k+1} = k_2 e_{i,k} + k_3 (v_{i-1,k} - v_{i,k}), k_2, k_3 > 0 \quad (2)$$

in which $e_{i,k}$ is the gap deviation of the i -th consecutive vehicle at the current time step k , and $v_{i-1,k}$ is the current speed of the preceding vehicle (index $i - 1$ refers to the leader of vehicle i); k_2 and k_3 are the control gains on both the positioning and speed deviations, respectively. The proposed optimal values for the gains are $k_2 = 0.23 \text{ s}^{-2}$ and $k_3 = 0.07 \text{ s}^{-1}$ (Xiao et al., 2017). The gap control mode is activated when the gap and speed deviations are concurrently smaller than 0.2 m and 0.1 m/s respectively (Xiao et al., 2017).

Moreover, in this study, and following from (Milanés & Shladover, 2014, 2016; Milanés et al., 2014), the gap deviation of the i -th consecutive vehicle ($e_{i,k}$) is defined as:

$$e_{i,k} = x_{i-1,k} - x_{i,k} - t_d v_{i,k} \quad (3)$$

According to Equation (3), the gap deviation is calculated by the current position of the preceding vehicle $x_{i-1,k}$, the current position of the subject vehicle $x_{i,k}$, the current speed of the subject vehicle $v_{i,k}$ and the desired time gap t_d of the ACC controller.

2.1.2.3 Gap-closing Control Mode

The initial ACC car-following models by (Milanés & Shladover, 2016) considered the gap-closing controller, but the ACC longitudinal vehicle response under this mode was not modelled in their study. This shortcoming was overcome in (Xiao et al., 2017), where the gap-closing controller was derived by tuning the parameters of the existing gap controller. We also adopted this approach in the current study. In this case, the gap-closing control mode is triggered when the spacing to the preceding vehicle is smaller than 100 m, with the control gains of Equation (2) are set as $k_2 = 0.04 \text{ s}^{-2}$ and $k_3 = 0.8 \text{ s}^{-1}$. If the spacing is between 100 m and 120 m, the controlled vehicle retains the previous control strategy to provide hysteresis in the control loop and perform a smooth transfer between the two strategies (Liu et al., 2018; Xiao et al., 2017).

2.1.2.4 Collision Avoidance Mode

We introduced the collision avoidance mode into the ACC car-following model to prevent rear-end collisions occurring during simulations. These may be due to safety critical conditions, i.e. low time-to-collision (TTC) values, or a follower's speed significantly higher than its leader's. We derived the collision avoidance controller by tuning the parameters of the existing gap controller. It is triggered when the spacing to the preceding vehicle is smaller than 100 m, the gap deviation is negative, and the speed deviation is smaller than 0.1 m/s. In this case, the control gains of Equation (2) are set as $k_2 = 0.8 \text{ s}^{-2}$ and $k_3 = 0.23 \text{ s}^{-1}$ to ensure that ACC vehicles can brake hard enough to avoid an imminent collision. Similar to the gap-closing control mode, the controlled vehicle retains the previous control strategy to provide hysteresis in the control loop and perform a smooth transfer between the two strategies (Liu et al., 2018; Xiao et al., 2017) if the spacing is between 100 m and 120 m.

2.2 (C)AV/CV Lane Change Model

2.2.1 Parametrisation of SUMO Lane Change Model (LC2013)

In TransAID we develop driver models for (C)AVs/CVs in SUMO to reflect their car-following and lane-change behaviour. SUMO's inherent default lane change model (i.e. the LC2013 model) was developed to mimic the lane change behaviour of LVs. It is a sophisticated model that accounts for lane changes due to different reasons (i.e. strategic, cooperative, tactical, right-of-way, etc.) and assesses the feasibility of lane changes based on traffic conditions in the surrounding LV road environment. However, (C)AVs/CVs are expected to deviate from human lane change behaviour due to the capabilities of automated driving systems. Currently, the lane change behaviour of CAVs/CVs is OEM-specific.

Parametrisation of the SUMO LC2013 model is an approach that can render the model capable to mimic the lane change behaviour of (C)AVs/CVs in SUMO. Within the context of TransAID the LC2013 lane-change model is parametrized to reflect (C)AVs/CVs lane-change behaviour based on information provided by Hyundai Motor Europe Technical Center (HMETC). The parametrisation process encompasses the adjustment of SUMO's lane change calibration parameters to attain the desired lane change behaviour in terms of SUMO lane change output (**Table 1**).

Table 1. SUMO lane change output.

Name	Description
id	The id of the vehicle.
type	The type id of the vehicle.
time	The time at which the change took place.
from	The id of the source lane.
to	The id of the destination lane.
pos	The position where the lane-change took place (offset from lane start).
reason	The reason for changing.
dir	The direction of the change (difference in lane indices when staying within one edge).
speed	The current speed of the vehicle.
leaderGap	The longitudinal gap to the nearest leader in the target lane (bumper to bumper) or 'None' if there was no leader.
leaderSecureGap	The required longitudinal gap to the nearest leader to fulfil deceleration constraints or 'None' if there was no leader.
followerGap	The longitudinal gap to the nearest follower in the target lane (bumper to bumper) or 'None' if there was no follower.
followerSecureGap	The required longitudinal gap to the nearest follower to fulfil deceleration

constraints or ‘None’ if there was no follower.

origLeaderGap The longitudinal gap to the nearest leader on the vehicle's original lane (bumper to bumper) or ‘None’ if there was no leader.

origLeaderSecureGap The required longitudinal gap to the nearest leader to fulfil deceleration constraints or ‘None’ if there was no leader.

The accomplishment of the parametrisation task presumes:

1. Knowledge regarding the logic of the LC2013 model.
2. Information about the lane change behaviour of (C)AVs/CVs in the real world.

The latter information has to be translated into SUMO lane change output for the effective LC2013 model parametrisation. To this end, HMETC provided information with respect to (C)AVs/CVs desired lane change gaps for two specific speed ranges (0 – 30 km/h & 30 – 60 km/h) based on the behaviour of their test vehicles (automation ready).

2.2.2 Overview of LC2013 Model

A description of the LC2013 model is provided subsequently, encompassing the model’s logic for determining the intention to change lanes (cf. strategic, cooperative, tactical, right-of-way, etc.).

2.2.2.1 Lane Change Intention

The LC2013 model considers three main reasons (strategic, cooperative, and tactical) for changing lanes (either right or left) per simulation time step. The ego vehicle initially checks if a right lane change is mandatory¹ or desired based on the logic depicted in **Figure 1**. If a right lane change is not mandatory or desired, a left lane change motivation is determined based on the same rules.

¹ Hence, we assume traffic laws dictating right-hand driving, with overtaking/passing mandatory on the left side.

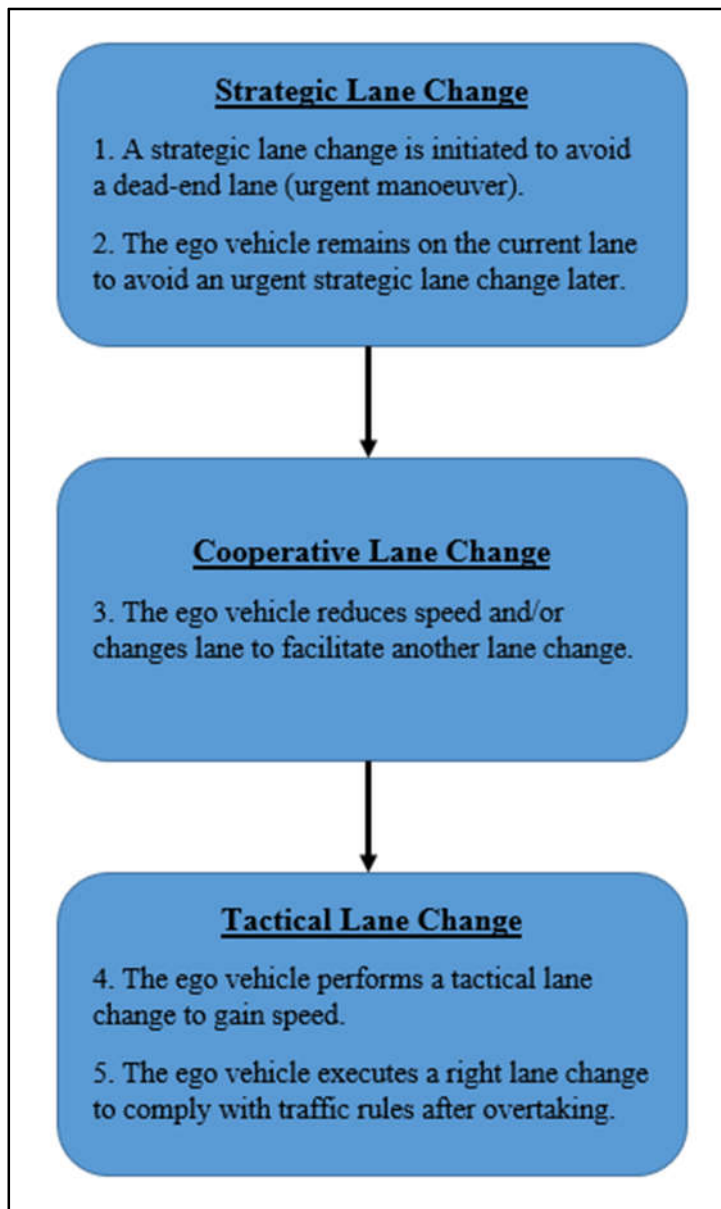


Figure 1. Hierarchy of lane change logic.

Strategic Lane Changes

An ego vehicle approaching a dead-end lane might stay in the strategically advisable lane (if it is already travelling on it), or it might change lanes to the strategically advisable lane (if it is driving in a dead-end lane). The urgency for initiating a strategic lane change manoeuvre is related to the following factors (**Table 2**):

Table 2. SUMO parameters related to urgency for strategic lane-changing.

Parameter Name	Parameter Description
myLookAheadSpeed (mLAS)	Virtual speed, used to calculate the ideal distance required for the execution of a lane change manoeuvre. It is increasing proportionally to the ego vehicle’s current speed. It decays slowly with decreasing vehicle speed, to stimulate an urgent lane change from the ego vehicle.

bestLaneOffset (bLO)	Indicates the number of lane changes required by the ego vehicle to reach an advisable lane. The higher the value the more lanes the ego vehicle should change to continue along its desired path.
miniGap (MG)	Safe bumper-to-bumper vehicle distance at standstill.
laneOccupation (Occ)	The occupied space in a lane by all vehicles (including their miniGap) downstream of the ego vehicle.
freeSpace (FS)	The available free space on a lane downstream of the ego vehicle.
usableDist	The available distance on a dead-end lane where the ego vehicle can drive unimpeded at its desired speed.
laDist	The ideal longitudinal distance for the ego vehicle to execute a lane change manoeuvre.

A physical representation of parameters *MG*, *Occ*, *FS*, and *usableDist* is depicted in Figure 2.

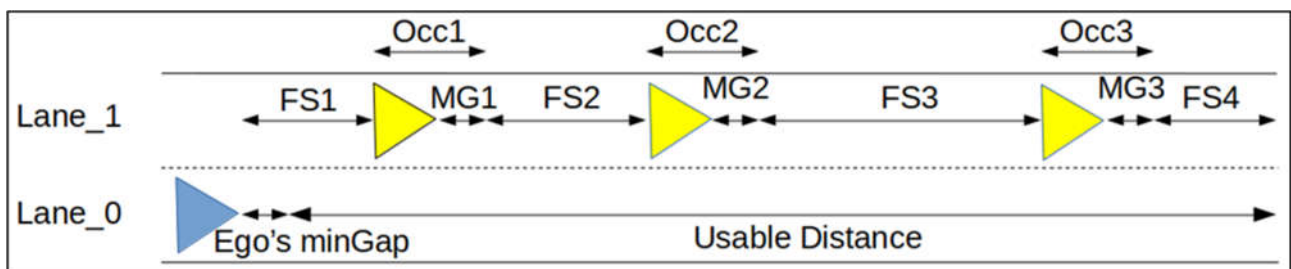


Figure 2. Physical representation of parameters *MG*, *Occ*, *FS*, and *usableDist*.

A strategic lane change manoeuvre is urgent when the available distance is lesser than the ideal:

$$usableDist < laDist \Leftrightarrow RD - Occ < mLAS \times |bLO| \times f \quad (4)$$

where parameters *mLAS*, *bLO*, and *Occ* are defined in **Table 2**, *RD* is the remaining distance between the ego vehicle and the lane end, and *f* is a factor that encodes the time typically needed to perform a successful change manoeuvre (set to 10 s for right lane changes to right and to 20 s for left lane changes).

The relationship between parameters *usableDist* and *laDist* is illustrated for two different cases. One that encompasses an ego vehicle target lane that is free (**Figure 3**), and one where the ego vehicle target lane is occupied by other vehicles (**Figure 4**). In **Figure 3a** an ego vehicle travels unimpeded on a dead-end lane. The vehicle approaches the end of the lane (**Figure 3b**) and is not changing lane unless the ideal distance to change lanes is shorter than the available (*usableDist* < *laDist*) (**Figure 3c**). If the target lane is occupied by other vehicles, then the free space on the target lane (*usableDist*) is reduced based on the occupation length of each vehicle (**Figure 4**).

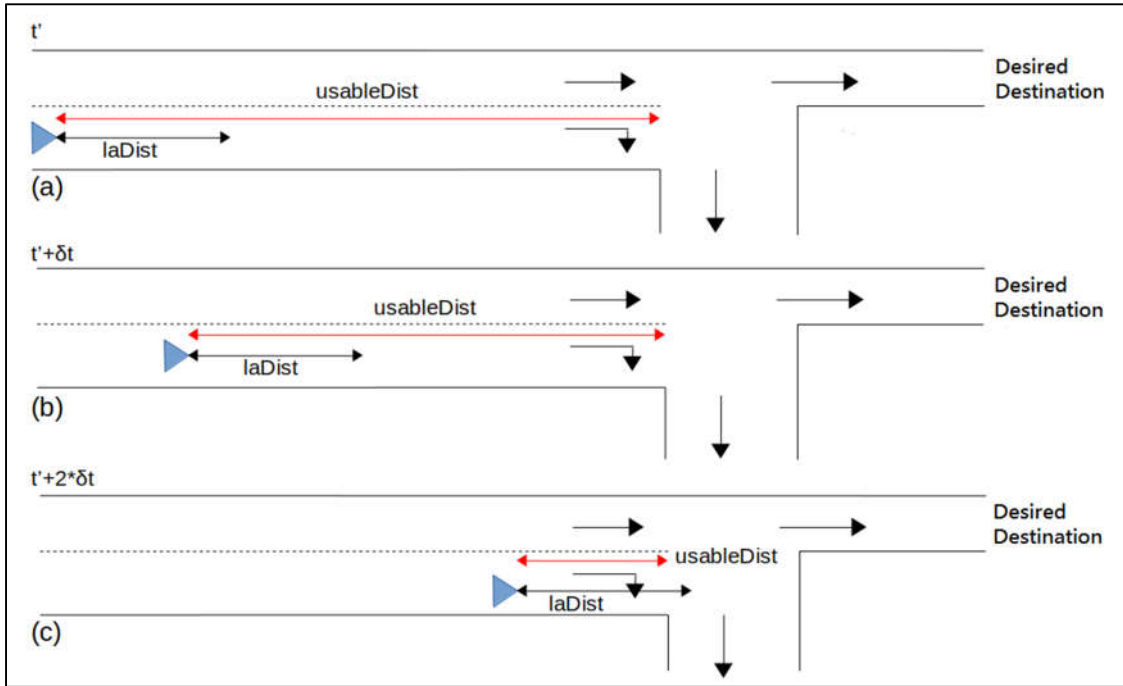


Figure 3. (a) The ego vehicle travels at constant speed on a dead-end lane. (b) The available distance on the target lane decreases as the ego vehicle drives towards the dead-end lane. (c) The ego vehicle initiates a lane change manoeuvre to the target lane when its ideal distance to perform a lane change ($laDist$) is shorter compared to the available distance on the target lane ($usableDist$).

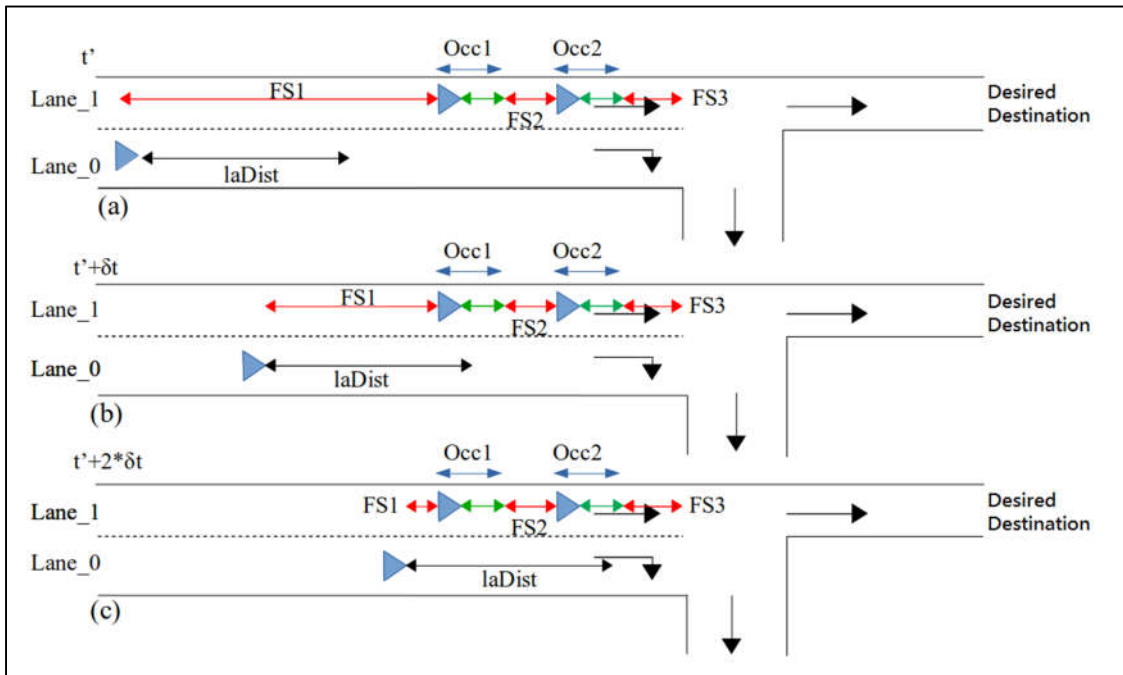


Figure 4. (a) The ego vehicle travels on a dead-end lane and the target lane is partially occupied by other vehicles. (b) The available distance for a lane change manoeuvre on the target lane is affected by the presence of other vehicles. (c) The ego vehicle performs a lane change when its ideal distance for performing a lane change is lesser than the available free space ($usableDist = FS1 + FS2 + FS3$) on the target lane.

Strategic lane changes might be executed as a consequence of preceding tactical lane changes. Namely, if the ego vehicle performs a lane change for tactical reasons, it might enter into an undesired situation where it will have to execute a strategic lane change manoeuvre soon to avoid a dead-end lane. In this case, the ego vehicle might lose the speed advantage that it gained due to the latter tactical lane change and be finally significantly delayed. Therefore, it would be best in this situation if the ego vehicle stays in the current lane and does not perform a tactical lane change.

Whenever the ego vehicle considers shifting away from the lane with the *bestLaneOffset*, the LC2013 model assesses if the free space on the target lane is sufficient for the imminent strategic lane change. In these cases, the LC2013 model assesses the following inequality to decide upon the feasibility of the tactical lane change:

$$2 \times laDist < neighLeftPlace \tag{5}$$

where *neighLeftPlace* is the total free space, that the ego vehicle can use on the target dead-end lane to perform a strategic lane change. If the total free space (*neighLeftPlace*) is less than twice the desired distance to change lanes (*laDist*), the ego vehicle will stay in its current lane.

In **Figure 5a** the ego vehicle should stay in Lane_1 in order to reach its desired destination since $2 \times laDist > FS1 + FS2$. However, if the opposite was true and the vehicle could perform a tactical lane change (**Figure 5b**), then it would have to return to Lane_1 based on the aforementioned strategic lane change logic.

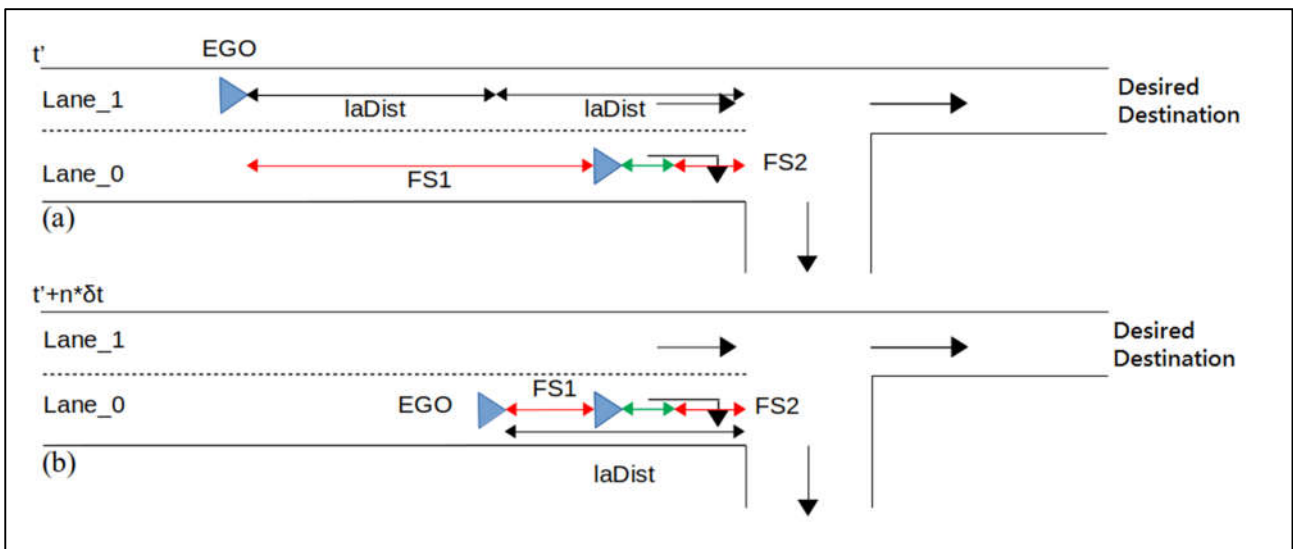


Figure 5. (a) The ego vehicle stays on the current lane since the free space on the neighbouring lane is insufficient to let it move back and forth. (b) The ego vehicle has shifted to the dead-end lane and will return based on the strategic lane change logic.

Cooperative Lane Changes

Vehicles also perform cooperative lane changes to facilitate nearby vehicles moving into their desired lanes. When the ego vehicle blocks a nearby vehicle and there are no strategic constraints against lane-changing, the ego vehicle may change lanes to create a gap for the blocked vehicle. Ego vehicles that cannot perform a cooperative lane change manoeuvre may adjust their speed to increase the probability of a successful lane change from a vehicle in a neighbouring lane. However, the ego vehicle shall not adjust speed if leading or following vehicles in the same lane are blocking it.

Tactical Lane Changes

Tactical lane changes take place for speed gains when the ego vehicle is blocked by a slower leader. The decision to execute a tactical lane-change is based on the expected speed gains. Keeping the overtaking lane free (keep right rule) should also be considered apart from the expected speed gains when performing a tactical lane change. Otherwise, slow moving vehicles with minor speed differences might significantly impede traffic flow.

The probability of a tactical lane change (right or left), is reflected by the parameter *speedGainProbability* for each vehicle. If the magnitude of this parameter exceeds a pre-specified threshold value (*speedGainProbabilityRight* for right lane changes and *speedGainProbabilityLeft* for left lane changes), a tactical lane change is desired. The relative gain for moving to the target lane (right or left) is calculated as the relative difference between the expected ego speed for moving to the candidate lane and the expected ego speed for remaining in the current lane:

$$rg = \frac{(neighV - defaultV)}{neighV} \quad (6)$$

where *rg* is the relative gain from the tactical lane change, *neighV* is the expected (virtual) ego vehicle speed for moving to the candidate lane, and *defaultV* is the expected ego speed for remaining in the current lane.

The parameter *speedGainProbability* is updated per time step based on the estimated relative gain:

$$speedGainProbability = speedGainProbability + rg \times timeStep \quad (7)$$

where *timeStep* is the time interval between consecutive simulation steps.

If the relative gain is less than a pre-specified threshold value the *speedGainProbability* value decays. A small relative gain or a negative one indicates that a lane change manoeuvre towards the candidate lane will not only prevent an ego vehicle from increasing speed, but it may finally slow it down. In these cases, *speedGainProbability* decays according to **Equation 8**:

$$speedGainProbability = speedGainProbability \times SPEEDGAIN_DECAY_FACTOR^{timeStep} \quad (8)$$

where *SPEEDGAIN_DECAY_FACTOR* is a factor that indicates the rate of *speedGainProbability* decay.

In **Figure 2.6**, a heavy vehicle (bus) is preceding a passenger car in Lane_0 and its desired speed is lower than the passenger car's speed. The passenger car is in car-following mode and adjusts its speed based on the actions of the bus. However, since Lane_1 is free, the relative gain for a left lane change is high and *speedGainProbability* increases until it exceeds *speedGainProbabilityLeft* and the ego vehicle performs the lane change manoeuvre.



Figure 6. (a) The ego vehicle is in the car-following mode behind a bus. **(b)** The ego vehicle performs a tactical lane-change to gain speed.

However, if a slow-moving leading vehicle exists on Lane_1 as well (**Figure 7**), then the relative gain for a left lane change will be small and thus the ego vehicle will gain no advantage if it makes a left lane change.

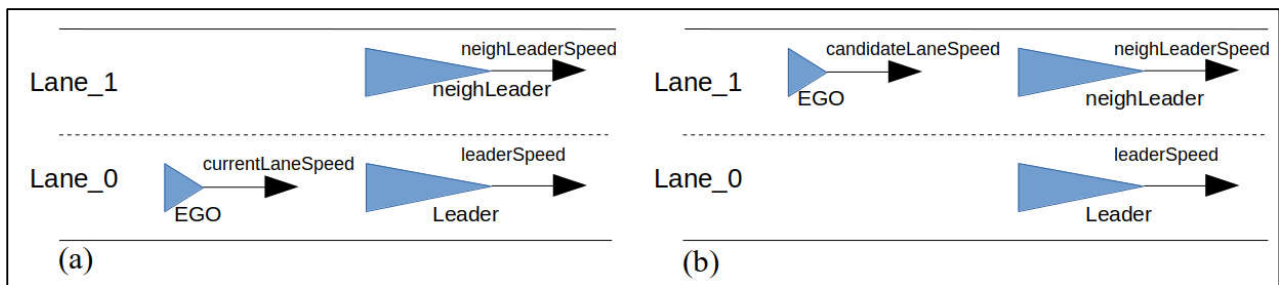


Figure 7. (a) The ego vehicle’s speed is impeded by the leader in Lane_0. **(b)** The ego vehicle will be impeded by the leader in the neighbouring lane if it performs a left lane change to Lane_1.

The lane change model initially examines if a right lane change manoeuvre is necessary, after which it investigates whether a left lane change is beneficial. The obligation to clear the overtaking lane is mandatory due to traffic regulations. The probability to make a right lane change after an overtaking manoeuvre is determined by the parameter *keepRightProbability*. When it exceeds a pre-specified threshold value, a right lane change is initiated (**Figure 8**). The threshold value is the maximum between the value of a constant pre-set parameter *myChangeProbabilityThresholdRight*, and *speedGainProbabilityLeft*. Namely, if the ego vehicle gains speed advantage by traveling on the left lane compared to clearing the overtaking lane by making a right lane change, it will keep on travelling in the left lane.

The ego vehicle determines if an overtaking manoeuvre is advantageous in terms of speed gains based on the gap and speed difference to the leading vehicle on the right. The parameter *keepRightProbability* is updated accordingly:

$$keepRightProbability = keepRightProbability + \frac{(t \times IV)}{(Vmax \times currentV \times T)} \quad (9)$$

where, *IV* is the legal speed limit for the current lane, *Vmax* is the maximum desired speed of the ego vehicle, *currentV* is the ego vehicle’s current speed, *T* is a calibration parameter set equal to 7 s, and *t* is the time interval that the ego vehicle can drive at its maximum desired speed in the right lane prior to an overtaking manoeuvre.

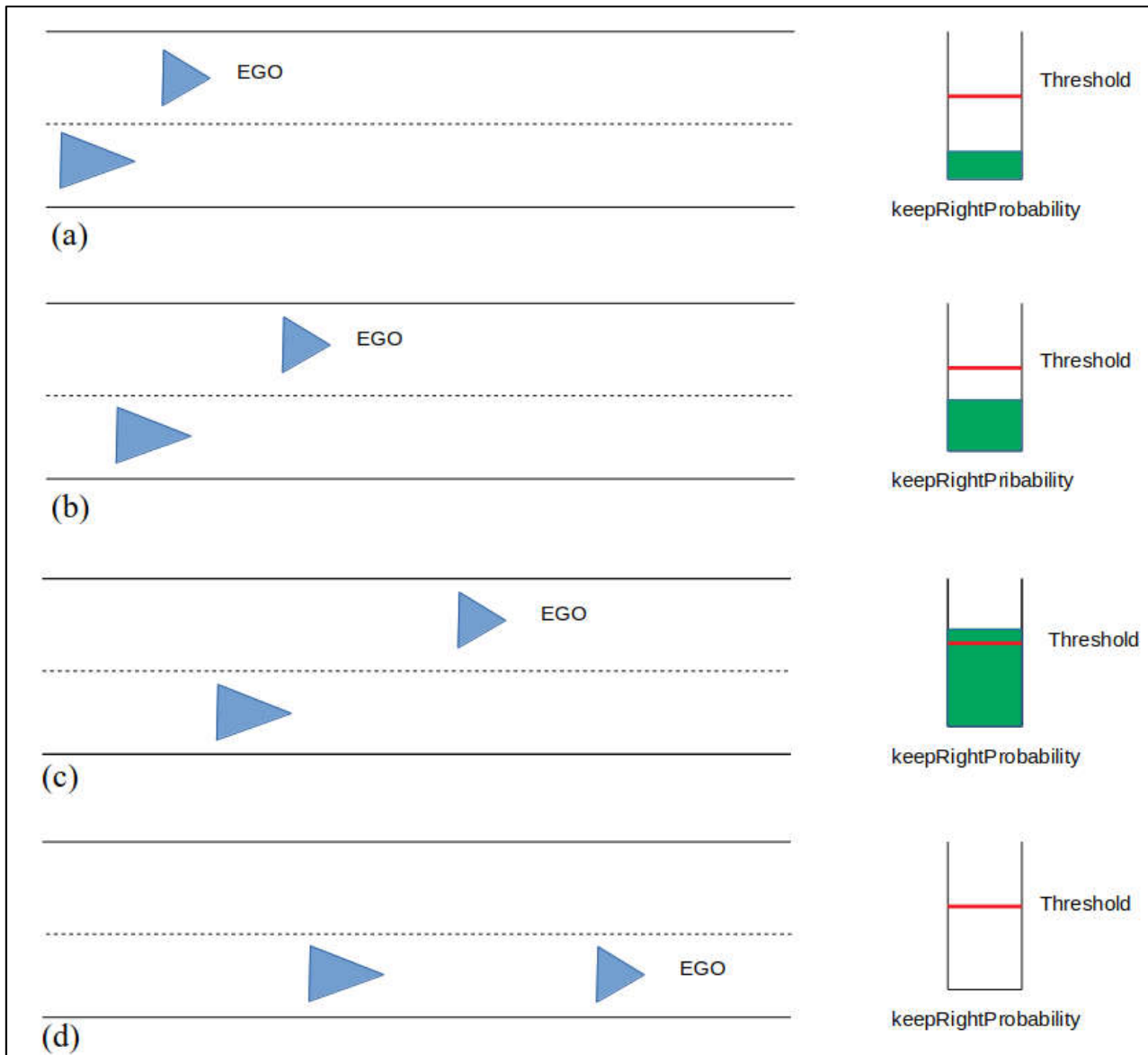


Figure 8. (a) The ego vehicle performed a lane change and is overtaking its previous leader (*keepRightProbability* is low). (b) The ego vehicle has overtaken its previous leader and accelerates to merge safely into the right-most lane (*keepRightProbability* close to the threshold value). (c) The ego vehicle can merge safely into the right-most lane (*keepRightProbability* exceeded the threshold value). (d) The ego vehicle has merged into the right-most lane (*keepRightProbability* is set equal to zero).

2.2.3 Sensitivity Analysis of LC2013 Model

2.2.3.1 Introduction

We conducted a sensitivity analysis to facilitate the parametrisation of the LC2013 model for the emulation of (C)AVs/CVs lane change behaviour in SUMO. The sensitivity analysis examines the behaviour of the LC2013 model by identifying the calibration parameters that exhibit the highest impact on its performance. Lane change outputs (**Table 1**) are mapped for predefined calibration parameter spaces and compared to actual (C)AV/CV lane change data to determine the parameters values that demonstrate the desired model behaviour.

A sensitivity analysis investigates the relationships between inputs and outputs of highly complex mathematical models or systems. It studies the uncertainty in the output of the mathematical model or system as a function of the uncertainty in the inputs. There are many available techniques that can be used to examine the sensitivity of a model. Typical techniques are: (i) one-at-a-time (OAT/OFAT), (ii) local methods, (iii) regression analysis, (iv) variance-based methods, (v) Monte Carlo filtering, and (vi) meta-modelling. Comprehensive information about sensitivity analysis can be found in (Saltelli, 2008; Saltelli et al., 2002), which are the main sources used in this study.

In microscopic traffic simulation modelling, sensitivity analysis was mainly used to analyse car-following models. A one-dimensional scan of the Intelligent Driver Model (IDM) and Velocity Difference (VDIFF) car-following model parameters was conducted to assess the models' parameter properties and sensitivity (Kesting & Treiber, 2008). Variance-based sensitivity analysis was applied to the IDM and the Gipps model to identify model parameters that highly contribute to the output uncertainty and thus need to be calibrated (Punzo & Ciuffo, 2011). The Monte Carlo framework was redesigned for variance-based sensitivity analysis of car-following models to estimate the least number of parameters required for credibly replicating actual car-following behaviour (Punzo et al., 2015).

This study also applies variance-based sensitivity analysis to analyse the LC2013 model. Variance-based sensitivity analysis is a global sensitivity analysis method (measures sensitivity across the whole input space). It can apportion the variance in the output of a mathematical model or system to inputs or input sets (interaction between inputs is accounted for). For instance, assuming a model with two inputs and one output, the method can determine that x % of the output variance is attributed to the first input, y % to the second, and z % due to the interaction between the two (percentages can be read as measures of sensitivity). Finally, variance-based sensitivity analysis can be applied to nonlinear and non-additive systems.

2.2.3.2 Variance-based sensitivity analysis

The sensitivity analysis method used in this study was initially introduced by (Cukier et al., 1973), generalised by (Sobol, 1993; Sobol et al., 2007) with a Monte Carlo-based implementation of the concept, and then improved by (Saltelli et al., 2010) to increase computational efficiency. The existing literature on the topic (Saltelli, 2008; Saltelli et al., 2010, 2002) shows that variance-based methods can overcome the limitations of most commonly used methods, such as OAT/OFAT analysis, local methods, and regression analysis.

This method assumes that variance can credibly represent uncertainty in the outputs and is based on the variance decomposition formula. For a model $Y = f(X_1, X_2, \dots, X_k)$, where $X_i \forall i \in [1, k]$ are the input stochastic variables, called *factors*, and Y is the output stochastic variable, the variance of the model can be decomposed as:

$$V(Y) = V_{X_i} \left(E_{\bar{X}_{\sim i}}(Y|X_i) \right) + E_{X_i} \left(V_{\bar{X}_{\sim i}}(Y|X_i) \right) \quad (10)$$

where X_i is the i -th factor, and $\bar{X}_{\sim i}$ denotes the vector of all factors but X_i .

The first component $V_{X_i} \left(E_{\bar{X}_{\sim i}}(Y|X_i) \right)$ is called the “main (or first-order) effect” of X_i . The associated sensitivity measure S_i , called the “first-order sensitivity index” is equal to the first-order effect normalised over the total (or unconditional) variance:

$$S_i = \frac{V_{X_i} \left(E_{\bar{X}_{\sim i}}(Y|X_i) \right)}{V(Y)} \quad (11)$$

It can be explained as the portion of the output variance that is only ascribed to the variation of the input factor X_i . Thus, the first order sensitivity index captures only the effect of a single input factor to the model output. However, for non-additive models, the input factor X_i affects the output variance also when interacting with other input factors. Namely, the joint variation of X_i with all (or some of) the input factors may influence the variation of the output. This influence is called the interaction (or higher order) effect related to X_i . The sum of the first-order and higher order effects for all the input factors explains all the output variance. Therefore, when the terms are normalised over the unconditional variance, such summation is equal to 1:

$$\sum_{i=1}^k S_i + \sum_{i=1}^k \sum_{\substack{j=1 \\ j \neq i}}^k S_{i,j} + \sum_{i=1}^k \sum_{\substack{j=1 \\ j \neq i}}^k \sum_{\substack{l=1 \\ l \neq \{i,j\}}}^k S_{i,j,l} + \dots + \sum_{i=1}^k \sum_{\substack{j=1 \\ j \neq i}}^k \dots \sum_{\substack{m=1 \\ m \neq \{i,\dots\}}}^k S_{i,j,\dots,m} = 1 \quad (12)$$

where $\sum_{i=1}^k S_i$ is the contribution of all the main effects, whereas $1 - \sum_{i=1}^k S_i$ is the contribution of all the interaction effects across all the input factors. It is worth noting that in the case of the additive models, there are no interaction effects and $\sum_{i=1}^k S_i = 1$, whereas in the case of non-additive models, it results in $\sum_{i=1}^k S_i < 1$.

Based on the latter decomposition, the number of higher order effects to calculate would be very high, i.e. $2^k - 1 - k$, with k being the number of factors. Thus, to estimate the total effect of a factor, the “total sensitivity index” is introduced:

$$ST_i = \frac{E_{\bar{X}_{\sim i}}(V_{X_i}(Y|\bar{X}_{\sim i}))}{V(Y)} = 1 - \frac{V_{\bar{X}_{\sim i}}(E_{X_i}(Y|\bar{X}_{\sim i}))}{V(Y)} \quad (13)$$

which is the sum of the first-order effect of X_i and of all the higher order effects that involve X_i . Since higher order effects are computed more times, i.e. in the ST of each factor involved in the interaction (e.g. $S_{i,j} = S_{j,i}$ in both ST_i and ST_j), it results in $\sum_{i=1}^k S_i \geq 1$, where the equality holds only for perfectly additive models (for which $S_i = ST_i, \forall i = 1, \dots, k$).

According to the aforementioned methodology, it becomes evident that the total sensitivity index is the appropriate measure to identify the factors that significantly influence the output variance. Indeed, $ST_i = 0$ is a necessary and sufficient condition for X_i to be non-influential.

2.2.3.3 Application and Results

The LC2013 model encompasses seven calibration parameters that can be modified to alter lane change behaviour in SUMO. Four of these parameters (**Table 2**) were finally analysed within the context of the current sensitivity analysis, per advice of the LC2013 model developers (DLR), based on the parameters’ expected influence on the model output. The simulation network of Scenario 2.1 (Prevent ToC/MRM by providing speed, headway, and/or lane advice) was used for the sensitivity analysis, which is a typical motorway merge section where lane changes occur for all the possible reasons considered by the LC2013 model:

- Strategic (on-ramp vehicles to enter the mainline lanes)
- Cooperative (mainline vehicles facilitate on-ramp vehicles’ lane changes)
- Tactical (both mainline and on-ramp vehicles to gain speed advantage)
- Right-of-way (both mainline and on-ramp vehicles due to the obligation to keep right)

Thus, the effects of the different calibration parameters on the lane change output can be effectively captured, since a significant number of lane changes will be executed for each reason.

Table 2. LC2013 model calibration parameters encompassed in sensitivity analysis.

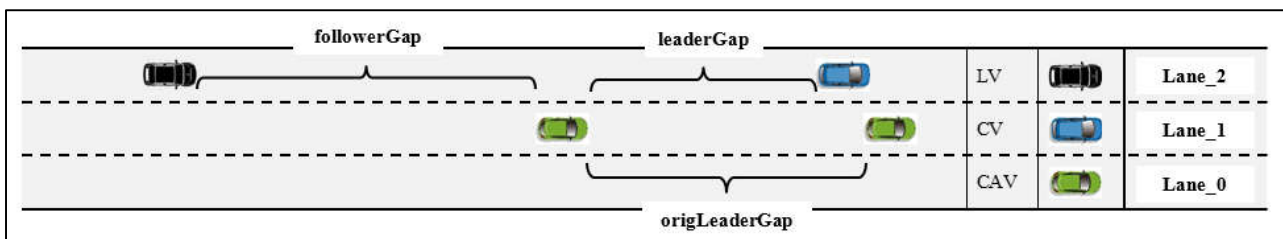
Parameter Name	Parameter Definition	Input Range
<i>lcStrategic</i>	The eagerness for performing strategic lane-changing. Higher values result in earlier lane-changing.	[0, inf)
<i>lcKeepRight</i>	The eagerness for following the obligation to keep right. Higher values result in earlier lane-changing.	[0, inf)
<i>lcSpeedGain</i>	The eagerness for performing lane-changing to gain speed. Higher values result in more lane-changing.	[0, inf)
<i>lcAssertive</i>	Willingness to accept lower front and rear gaps on the target lane. The required gap is divided by this value.	Positive reals

The sensitivity analysis was conducted using the SALib library (open source Python library for performing sensitivity analysis). SALib offers a decoupled workflow (it does not directly interface with the mathematical or computational model), where sample functions generate the model inputs, and analyse functions compute the sensitivity indices.

Input samples are generated using a quasi-random sampling technique with low discrepancy sequences (the so-called Sobol’s sequences), guaranteeing faster convergence for the indices calculation than other sampling strategies (Saltelli et al., 2010). The generated samples are iteratively input into SUMO and the model is run for the estimation of the lane change output. The first-order and total sensitivity indices are computed for the following lane change output:

- Safe longitudinal gap to leading vehicle in the ego lane (*origLeaderSecureGap*).
- Safe longitudinal gap to leading vehicle in the target lane (*leaderSecureGap*).
- Safe longitudinal gap to following vehicle in the target lane (*followerSecureGap*).

Safe longitudinal gaps to surrounding vehicles for an ego vehicle that is initiating a lane change manoeuvre are depicted in **Figure 11**.

**Figure 11.** Illustration of SUMO lane change output.

The latter lane change outputs (per input sample) are loaded into SALib, and the corresponding sensitivity indices are estimated per examined model output. The formulas for the estimation of the first-order and total sensitivity indices are obtained by (Saltelli et al., 2010). The values of the first-order (S_i) and total (ST_i) sensitivity indices for the aforementioned lane change output are presented in **Table 3**. Previously it was shown that an appropriate measure for identifying the non-influential parameters is the “total sensitivity index” ST_i , and that $ST_i = 0$ is both necessary and sufficient for the factor X_i to be non-influential. However, in practical applications, a threshold on

ST_i higher than zero is generally set, under which the parameter is considered non-influential (Punzo et al., 2015). In this study, we considered a value of 5% as an acceptable threshold.

Therefore, it becomes clear that the *lcStrategic* parameter has very limited influence on the output unconditional variance, since ST_i is less than 5 % for all the examined output. The *lcKeepRight* parameter is only influential for the safe longitudinal gaps between the leading vehicle in the target lane and the ego vehicle. However, since it does not affect the other two types of gaps considered prior to lane-changing, and the ST_i value is close to the specified threshold ($ST_i = 7.57$), this calibration parameter is also fixed in its default value ($lcKeepRight = 1.0$) for the baseline simulations experiments. The *lcSpeedGain* parameter is found to be influential for two model outputs (the safe gap to leading vehicle in the current lane, and the safe gap to the leading vehicle in the target lane). For the first model output $ST_i = 8.12$, while for the second $ST_i = 22.26$ (i.e. *lcSpeedGain* is influencing gaps to leading vehicles on the target lane more). Nonetheless, the first-order sensitivity indices are very low for *lcStrategic*, *lcKeepRight*, and *lcSpeedGain*, while being very high for *lcAssertive*. Thus, it is implied that high ST_i values for *lcSpeedGain* can be ascribed to its interaction with *lcAssertive*. According to the aforementioned considerations, the calibration parameter *lcAssertive* is explicitly adjusted for the parametrisation of the LC2013 model to reflect (C)AV/CV lane change behaviour.

Table 3. First-order and total sensitivity indexes per calibration parameter and lane change output.

Parameter	Speed Range [0, 100] (km/h)					
	Leader gap (ego lane)		Leader gap (target lane)		Follower gap (target lane)	
	S_i [%]	ST_i [%]	S_i [%]	ST_i [%]	S_i [%]	ST_i [%]
<i>lcStrategic</i>	0.39	0.62	0.74	2.62	1.14	0.47
<i>lcKeepRight</i>	1.08	0.83	3.32	7.57	1.13	2.26
<i>lcSpeedGain</i>	0.90	8.12	10.92	22.26	0.77	1.37
<i>lcAssertive</i>	59.15	77.03	61.26	80.17	91.40	95.56

The LC2013 model behaviour is mapped (in terms of the aforementioned lane change output) for different values of the *lcAssertive* parameter. However, information about the actual (C)AV/CV desired gaps (with surrounding vehicles) for lane-changing is necessary, so that it can be compared with the lane change output for different values of *lcAssertive*. Thus, scanning the parameter space of the *lcAssertive* calibration parameter and comparing against actual lane change data, renders the selection of the *lcAssertive* values that reproduce the actual (C)AV/CV lane change behaviour feasible. Moreover, we must consider the fact that desired gaps for lane change are a function of the ego vehicle's current speed and its relative speed with its surrounding vehicles that affect the lane change manoeuvre (leader in the current lane, leader in the target lane, and follower in the target lane). Given the latter consideration, actual lane change data for (C)AVs/CVs were provided by HMETC for the parametrisation of the LC2103 model. These data correspond to two different speed ranges (0 – 30 km/h, and 30 – 60 km/h), and represent highly conservative lane change behaviour as stressed by HMETC (Table 4 – 5). This information was used to select appropriate values for the *lcAssertive* parameter.

Table 4. OEM proposed minimum longitudinal gaps for CAV/CV lane-changing (0 – 30 km/h).

Speed Range (0, 30] (km/h)		
Subject Vehicle	Relative Speed ($v_{ego} - v_{obstacle}$)	Desired Gaps [m]
Leader gap (ego lane)	Positive	22
	Neutral	< 22
	Negative	< 22
Leader gap (target lane)	Positive	17
	Neutral	15
	Negative	< 15
Follower gap (target lane)	Positive	7
	Neutral	20
	Negative	44

Table 5. OEM proposed minimum longitudinal gaps for CAV/CV lane-changing (30 – 60 km/h).

Speed Range (30, 60] (km/h)		
Subject Vehicle	Relative Speed ($v_{ego} - v_{obstacle}$)	Desired Gaps [m]
Leader gap (ego lane)	Positive	50
	Neutral	< 50
	Negative	< 50
Leader gap (target lane)	Positive	35
	Neutral	30
	Negative	< 30
Follower gap (target lane)	Positive	20
	Neutral	44
	Negative	70

Lane change outputs are mapped for $lcAssertive = \{0.5, 0.7, 0.9\}$ and relative speeds of $\pm 5.0 \text{ km/h}$. Desired safe gaps for lane-changing increase linearly with vehicle speed, while OEM proposed gaps appear as vertical lines since they are constant within the aforementioned speed ranges (Figures 10 – 12). Desired gaps to the follower in the target lane are shorter compared to the OEM proposed ones for all the tested $lcAssertive$ values and negative relative speed. On the contrary, they are larger for positive relative speeds. Thus, the model behaviour is aggressive compared to the OEM proposed gaps for negative relative speeds, but is conservative for positive relative speeds.

The latter behaviour is not observed though for the other two types of gaps considered in this study (distance to the leader in the current and the target lane). With respect to longitudinal gaps between the ego vehicle and the target leader, $lcAssertive = 0.7$ reproduces actual vehicle behaviour at 30 km/h and 60 km/h respectively (desired gaps coincide at the upper bounds of the speed ranges, and it is reasonable to assume that they would decrease at speeds lower than 30 km/h and 60 km/h). For longitudinal gaps between the ego vehicle and the current leader, $lcAssertive = 0.9$ better emulates LC2013 model behaviour with actual vehicle behaviour.

The LC2013 model does not encompass a calibration parameter that can affect different longitudinal gap types (ego vehicle to target leader, current leader, and target follower) separately. Thus, if a calibration parameter is scaled, then all different gaps considered by the model for the lane change manoeuvre execution are scaled as well. Moreover, no existing calibration parameter can scale desired gaps explicitly for negative or positive relative speeds (even when considering only one type of gap). Therefore, adjusting $lcAssertive$ and/or other calibration parameters to reproduce the given actual (C)AV/CV lane change behaviour in this study is not a possibility according to the current model structure. As a result, the aforementioned $lcAssertive$ values that can replicate OEM proposed behaviour for different types of gaps are used for the baseline simulation experiments.

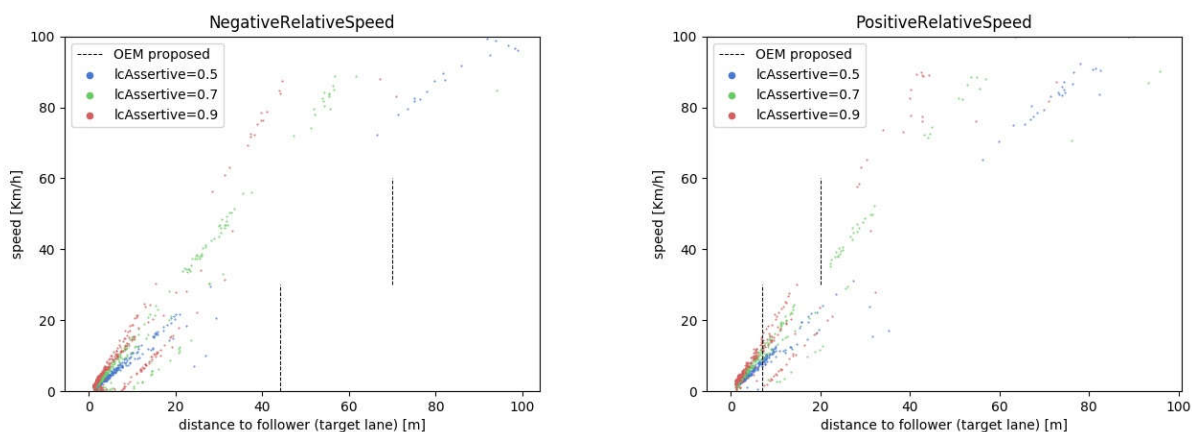


Figure 10. Safe longitudinal gaps to follower (target lane) for different values of $lcAssertive$.

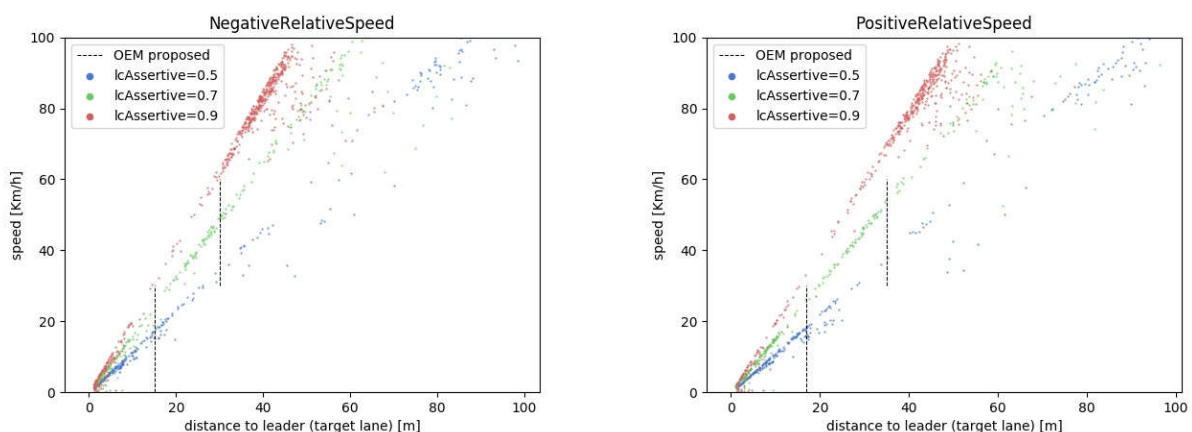


Figure 11. Safe longitudinal gaps to leader (target lane) for different values of *lcAssertive*.

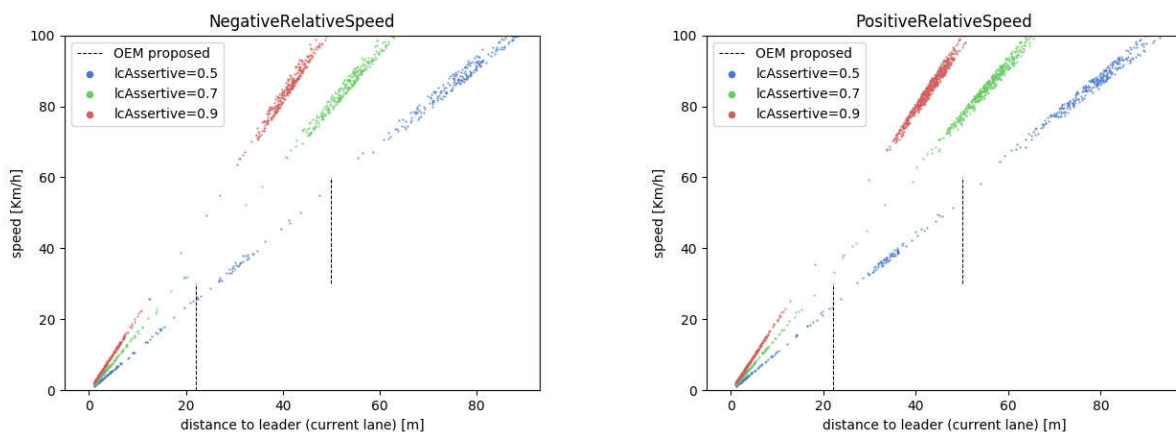


Figure 12. Safe longitudinal gaps to leader (ego lane) for different values of *lcAssertive*.

2.3 Simulation of Take-over Process

In this section we give an overview of the important aspects that are considered when modelling ToCs for (C)AVs. We provide details of the implementation in SUMO and propose parameter ranges for parameters to be adopted in baseline simulations of the TransAID project.

2.3.1 Structure of Take-over Events

ToCs in (C)AVs can be classified according to several characteristics (Eriksson & Stanton, 2017; Lu et al., 2016). The class of passive, downward transitions is likely to be the most critical as these pose high demands on a potentially distracted human driver in terms of time constraints for the take-over (D2.1).

For simulative studies on the impact of cumulative occurrences of ToCs in TAs, simulation models need to be developed, being capable of reproducing the important processes during such events. **Figure 13** shows a schematic representation of the presumed phases during a downward ToC (Gold et al., 2013).

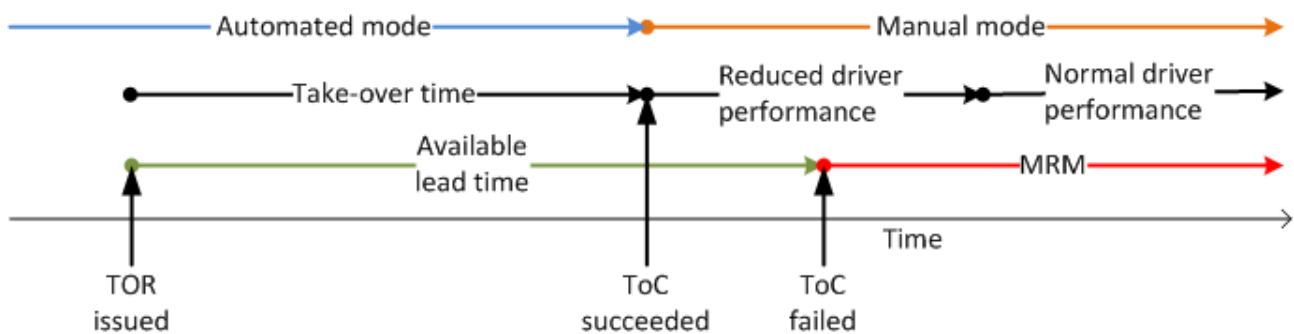


Figure 13. Timeline of a downward transition.

Even though the processes can be described to a higher detail, especially the driver (re)actions prior to the ToC are important (Gold et al., 2013). the level of granularity depicted in **Figure 13** suffices the modelling needs for the purposes in TransAID.

From a modelling perspective it is clear that the time point of switching between automated and manual driving mode requires a careful handling as the model features a discontinuity here. For the implementation, the car-following and lane-change models of the simulated driver-vehicle-unit (DVU) are substituted at this moment and we must ensure that this does not introduce unnaturally high brake rates or similar artefacts.

For the assessment of the impacts of ToCs on traffic safety and efficiency, the choice of parameters of the automated and manual mode is crucial. Especially the phase of reduced driving performance may be conjectured to imply an adverse effect due to irregular or erroneous behaviour, which disturbs a smooth traffic flow. Considerable evidence has been presented to claim that measures of driving performance may drop when a take-over is requested with an insufficient lead time (Blommer et al., 2017; de Winter et al., 2014; Eriksson & Stanton, 2017). Mostly, the available studies are concerned with Level 3 automation and urgency ToCs, and aim at estimating the lead time that permits drivers to operate their vehicle safely after performing the ToC. In general, this lead time was found to be significantly longer if the driver disengages from the driving process, i.e. more distracted or out of the loop for a longer period of time (de Winter et al., 2014; Louw et al. 2015; Merat et al., 2012). This observation is especially important for the case of highly automated

vehicles since the driver is likely to engage in other activities, which distract further from the driving process. Indicators, which were used to quantify the driving performance and are directly related to the driving process, are for instance *speed variation / throttle input* (Blommer et al., 2017; Clark & Feng, 2017), lane keeping (Clark & Feng, 2017; Mok et al., 2017), braking precision / overbraking (Clark & Feng, 2017; Louw et al., 2015; Young & Stanton, 2007), and the type of evasive manoeuvre applied in case of an urgent ToC (Blommer et al., 2017). But also, indirect indicators of attentiveness and situation awareness were studied, e.g. the driver’s ability to reconstruct a depicted situation after looking at it for different amounts of time (Lu et al., 2017), and the frequency and type of glances and eye movements (Samuel et al., 2016; Zeeb et al., 2015; Ziegler et al., 2014).

Figure 14 shows a diagram for a model capturing the essential phases and transition during the ToC process. Both driving modes, automated and manual, have a state of normal operation, which corresponds to a normal driver performance for the manual mode and undisrupted functioning for the automated mode. After a take-over request (ToR) has been issued, the model for automated control enters the “Prepare ToC” state, where it resides until the driver responds to the ToR, or until the lead time has elapsed, in case of which it initiates an MRM. The entry point to the manual mode is the “Post-ToC Recovery” period during which a decreased driver performance is assumed. This state is modelled as described in the subsequent Section 2.3.3.

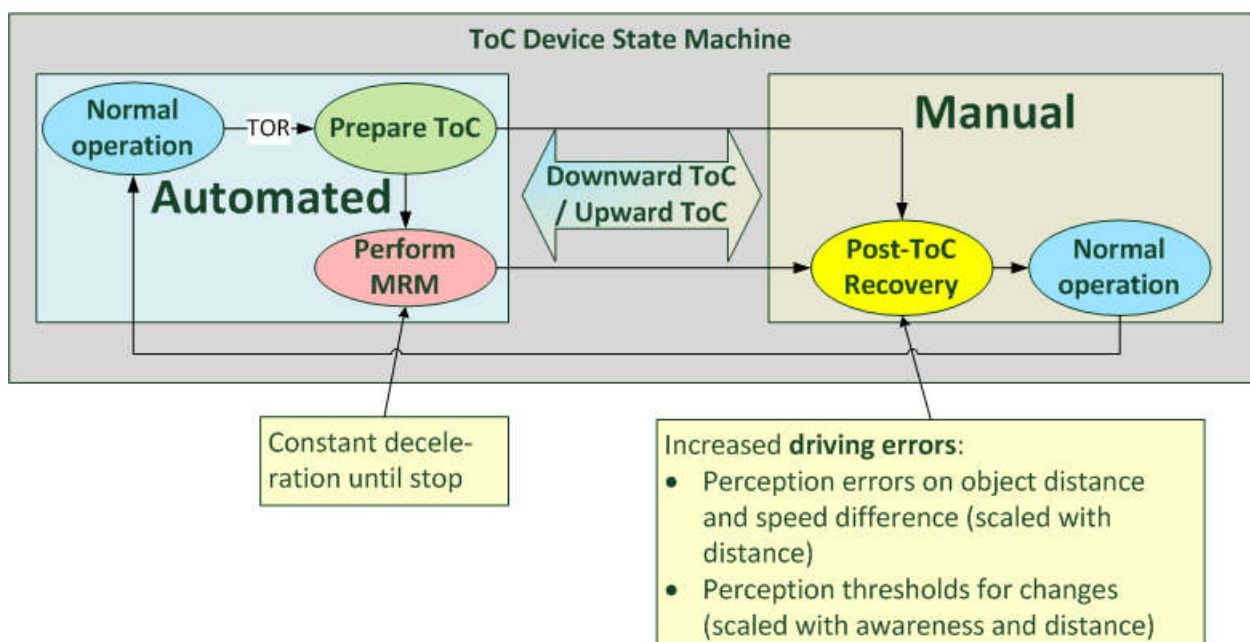


Figure 14. State machine for a ToC process model.

2.3.2 Parametrisation of the ToC Model

In TransAID we concentrate the research on situations where the need for a manual overtaking is foreseeable for a certain area. The ToR can be communicated to the driver with a relatively long lead time until the ToC is required to be executed. This means, that the transitions to be modelled are **not urgent but planned**. Unfortunately, the research body on planned ToCs is rather scarce in comparison to urgent ToCs (Eriksson & Stanton, 2017), which received the greatest attention so far because they are likely to lead to the most critical situations.

Due to the hypothetic nature of the parameter assumptions involved in the modelling, we strive to cover a range of possible scenarios by defining a set different parameter schemes (Section 3),

corresponding to major, moderate, and minor impacts of the ToC events. For the lead time we fixed a value of 10 seconds for the simulations, which has to be interpreted in conjunction with the distribution of driver response times. This distribution was modified between the different parameter schemes to affect the probability of an MRM being initiated, which presumably represents the largest impact of ToC processes on the traffic flow. **Figure 15** shows the cumulative distribution functions for the different parameter schemes. These are truncated normal distributions with a mean of 7 seconds and variances of 2.1 (minor impact), 2.5 (moderate impact), and 3.0 (major impact). This results in the following probabilities for MRMs:

- Minor impact: $P(\text{MRM}) = \sim 7.7\%$,
- Moderate impact: $P(\text{MRM}) = \sim 11.6\%$
- Major impact: $P(\text{MRM}) = \sim 16.2\%$

Note that a simulated DVU is assumed to switch immediately to the manual mode after the response time has elapsed, even if this requires an abort of an ongoing MRM. Therefore, not only the occurrence of an MRM is an important quantity but also its duration, which is the difference of the response time and the lead time. Thus, the most MRMs occurring in the simulations are of short duration ($> 85\%$ lie within $0 - 3$ s and $> 97.5\%$ within $0 - 5$ s for all parameter schemes) and are interrupted before the vehicle comes to a full stop.

Other important parameters are the initial awareness distribution affecting the driver state at the moment of performing the ToC, and the various coefficients for the driver state model error and perception mechanisms (Section 2.3.3).

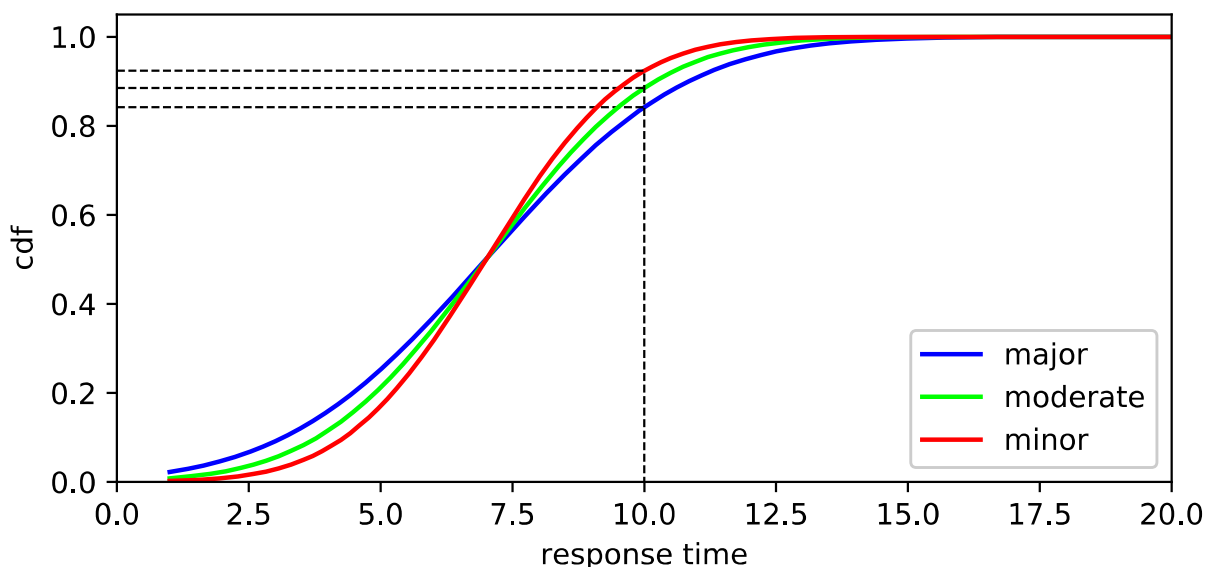


Figure 15. Cumulative distribution functions of the driver response time for the different parameter schemes employed in the baseline simulations. For the different parameter schemes, the intersections of the corresponding dashed lines with the ordinate indicate the probabilities that an AV, which requires a ToC, successfully performs it before initiating an MRM.

2.3.3 Modelling of a Decreased Post-ToC Driver Performance

The observations of increasing performance measures with increasing take over time (Section 2.3.1) can be attributed to an underlying recovery process of the driver's awareness and the mental

capacity available for the driving process (Fuller, 2005; Lu et al., 2017; Merat et al., 2014; Young & Stanton, 2002).

As this recovery process can be assumed to exhibit a high variability between different drivers and situations, it seems unavoidable that the level of disengagement will be elevated at least for some drivers of automated vehicles after the ToC, even if the granted lead time assures that a good performance can be expected after the ToC for most events.

We capture this assumption by randomly assigning a value for an *initial awareness* A_0 to the model of each DVU that is performing a ToC in the simulations. The variable A_0 is sampled from a distribution on the interval $[A_{min}, 1]$, see Section 3.5, where a value of $A_0 = 1$ corresponds to full awareness, i.e. normal driving performance, while $A_{min} > 0$ is the minimal level for the initial awareness. Further an *awareness recovery rate* r is given to the DVU controlling the post-ToC evolution of its awareness $A(t)$ according to $\dot{A}(t) = r$, until the awareness has completely recovered i.e. $A(t) = 1$.

For the period, where the awareness is reduced, i.e., $A(t) < 1$, we assume an increased error rate for the leading DVU. Although errors may enter the driving process at several stages (**Figure 16**), we restrict the modelling to one source, which is chosen to be the accuracy of the driver's perceptions, i.e. the perception errors. We follow this simplification since it is not obvious how a more detailed error mechanism would lead to a significant improvement of the model with respect to the modelling purposes within TransAID, because no driver error source specific countermeasures are developed here.

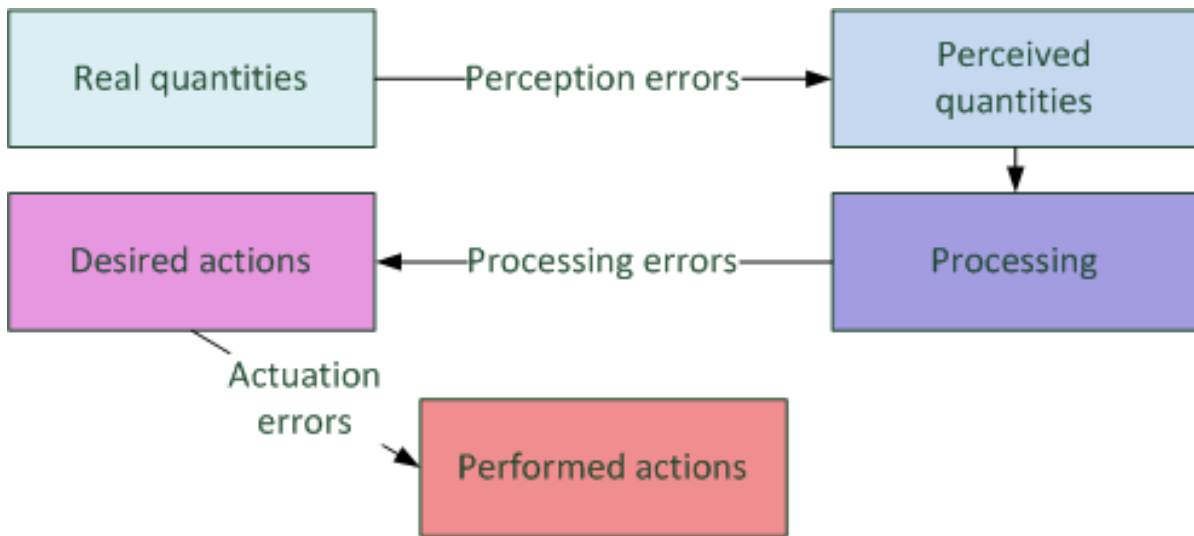


Figure 16. Errors entering the driving process.

Perception errors may be introduced to a car-following model in a generic way. Let us assume that a given model is of the form:

$$\dot{x}(t) = v(t) \quad (14)$$

$$\dot{v}(t) = a(\Delta x(t), \Delta v(t)) \quad (15)$$

where $x(t)$ is the vehicle's position and $v(t)$ its speed at time t . This form assumes that the quantities determining the acceleration $a(t) = a(\Delta x(t), \Delta v(t))$ are the gap $\Delta x(t)$ to the leading vehicle and the corresponding speed difference $\Delta v(t)$. This form is satisfied by a lot of commonly

applied car-following models (Treiber & Kesting, 2013), but a generalisation to other forms is not expected to be a difficult task.

Perception errors η_x regarding the gap Δx and η_v regarding the speed difference Δv are used to define the perceived gap $\Delta \tilde{x}$ and the perceived speed difference $\Delta \tilde{v}$ as:

$$\Delta \tilde{x} = \Delta x + \eta_x \quad (16)$$

$$\Delta \tilde{v} = v + \eta_v \quad (17)$$

The erroneous driving behaviour is then described by the equations:

$$\dot{x}(t) = v(t) \quad (18)$$

$$\dot{v}(t) = a(\Delta \tilde{x}(t), \Delta \tilde{v}(t)) \quad (19)$$

Both errors are derived from a scalar Ornstein-Uhlenbeck process H [Gardiner 2009, Kesting 2013] with time-dependent noise intensity σ_t and time scale θ_t . We favoured the implementation of this coloured noise over white noise to capture temporal autocorrelations in driver's deviances from ideal models (Wagner, 2012). The process H evolves according to:

$$dH_t = -\theta_t \cdot H_t \cdot dt + \sigma_t \cdot dW_t \quad (20)$$

The effective errors η_x and η_v are assumed to be proportional to the distance to the leading vehicle [Xin et al., 2008] and the main error term H_t , that is:

$$\eta_x(t) = c_x \cdot \Delta x(t) \cdot H_t \quad (21)$$

$$\eta_v(t) = c_v \cdot \Delta v(t) \cdot H_t \quad (22)$$

with constant coefficients c_x and c_v . The time scale θ and the noise drive σ of H follow the temporal changes of the awareness $A(t)$ as follows:

$$\theta_t = c_\theta \cdot A(t) \quad (23)$$

$$\sigma_t = c_\sigma \cdot (1 - A(t)) \quad (24)$$

Roughly speaking, this implies that the higher the awareness, the faster any errors decay and the smaller is their range.

As an additional generic mechanism for imperfect driving, we consider perception specific action points (Todosiev, 1963; Xin et al., 2008). An action point is an instant t where the acceleration $a(t)$ is changing its value according to the dynamical equation of the given car-following model.

Here we assume that a change in a perceived quantity is only recognised if its magnitude surpasses a certain threshold value. Accordingly, a corresponding change in action, here, a change of acceleration, is only taken out when the currently perceived speed difference $\Delta \tilde{v}(t)$ deviates sufficiently from the last recognised value $\Delta \tilde{v}_{\text{rec}}$ or the currently perceived gap $\Delta \tilde{x}(t)$ deviates from the value estimated based on the last recognised quantities. That is, instant t is assumed an action point if either:

$$|\Delta \tilde{x}_{\text{rec}} + (t - t_{\text{rec}}) \cdot \Delta \tilde{v}_{\text{rec}} - \Delta \tilde{x}(t)| > \theta_x, \text{ or } |\Delta \tilde{v}_{\text{rec}} - \Delta \tilde{v}(t)| > \theta_v. \quad (25)$$

Figures 17-19 compare data generated by SUMO's standard model, the proposed model and data from a real car-following episode of an approximate duration of 5.5 min. This episode was extracted from the sim^{TD} database².

The experimental setup entailed a simulated car-following situation, where a simulated, model-controlled following vehicle drove behind a simulated vehicle following exactly the recorded speed profile of the real leading vehicle. **Figure 17** shows the trajectory obtained from a Krauss model (the standard SUMO model), and **Figures 18 – 19** show trajectories of the model extended by the perception error mechanism as described above for two different parametrisations.

If not stated otherwise, the following parameter values were used for the driver state model of the following vehicle:

- $c_\theta \equiv 100$, and $c_\sigma = 0.2$
- $c_x = 0.75$, and $c_v = 0.15$
- $\theta_x = \theta_v = 0.1$

The underlying Krauss model had the following configuration parameters:

- $accel = 1.0$,
- $decel = 3.0$,
- $sigma = 0.0$, and
- $tau = 0.72$

The different charts (a)-(d) of Figures 17-19 show different aspects for the trajectory

² <https://www.sit.fraunhofer.de/de/simtd/>

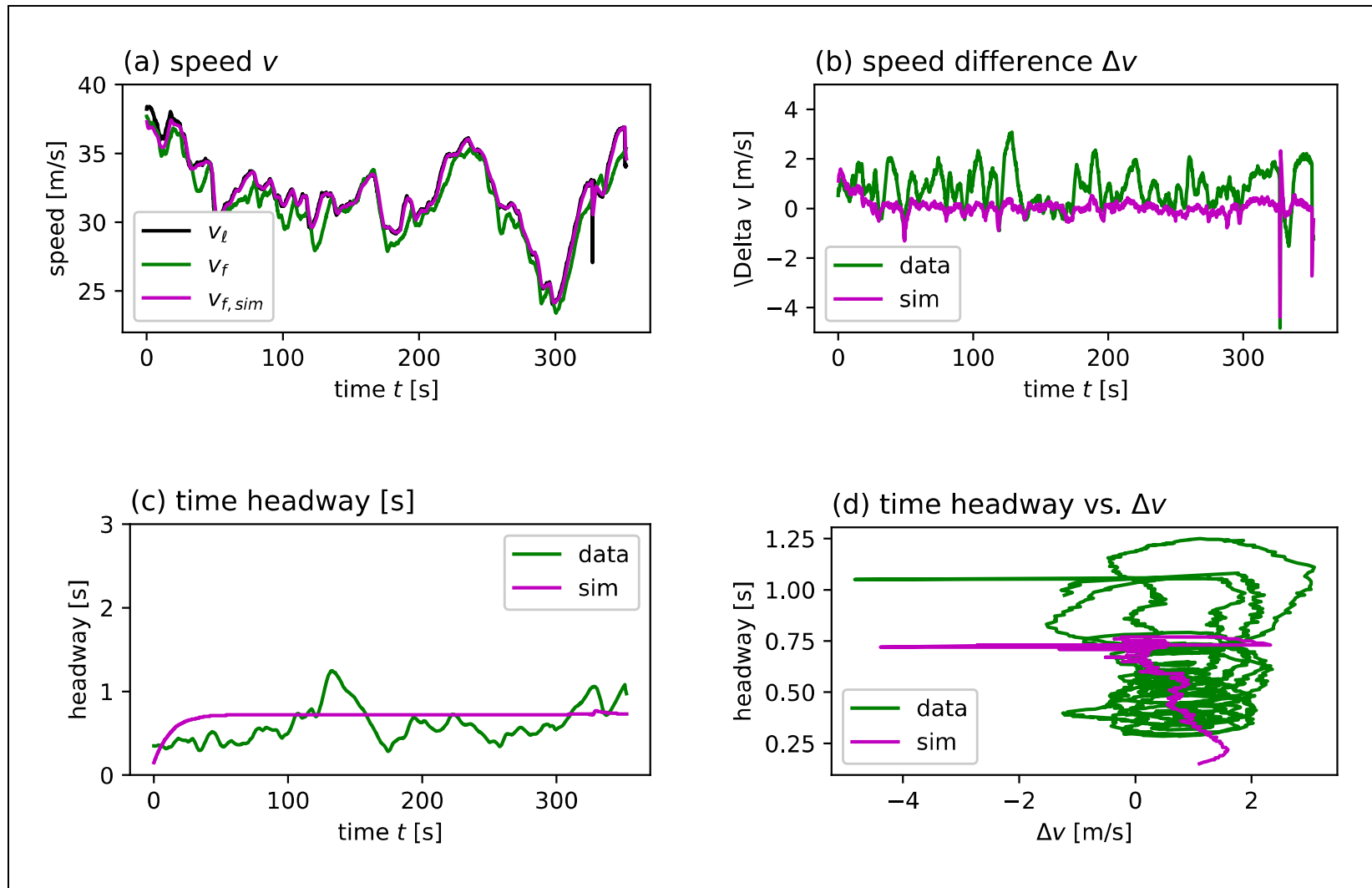


Figure 17. Comparison of SUMO's standard model (Krauss) without driver state extensions and real car-following data.

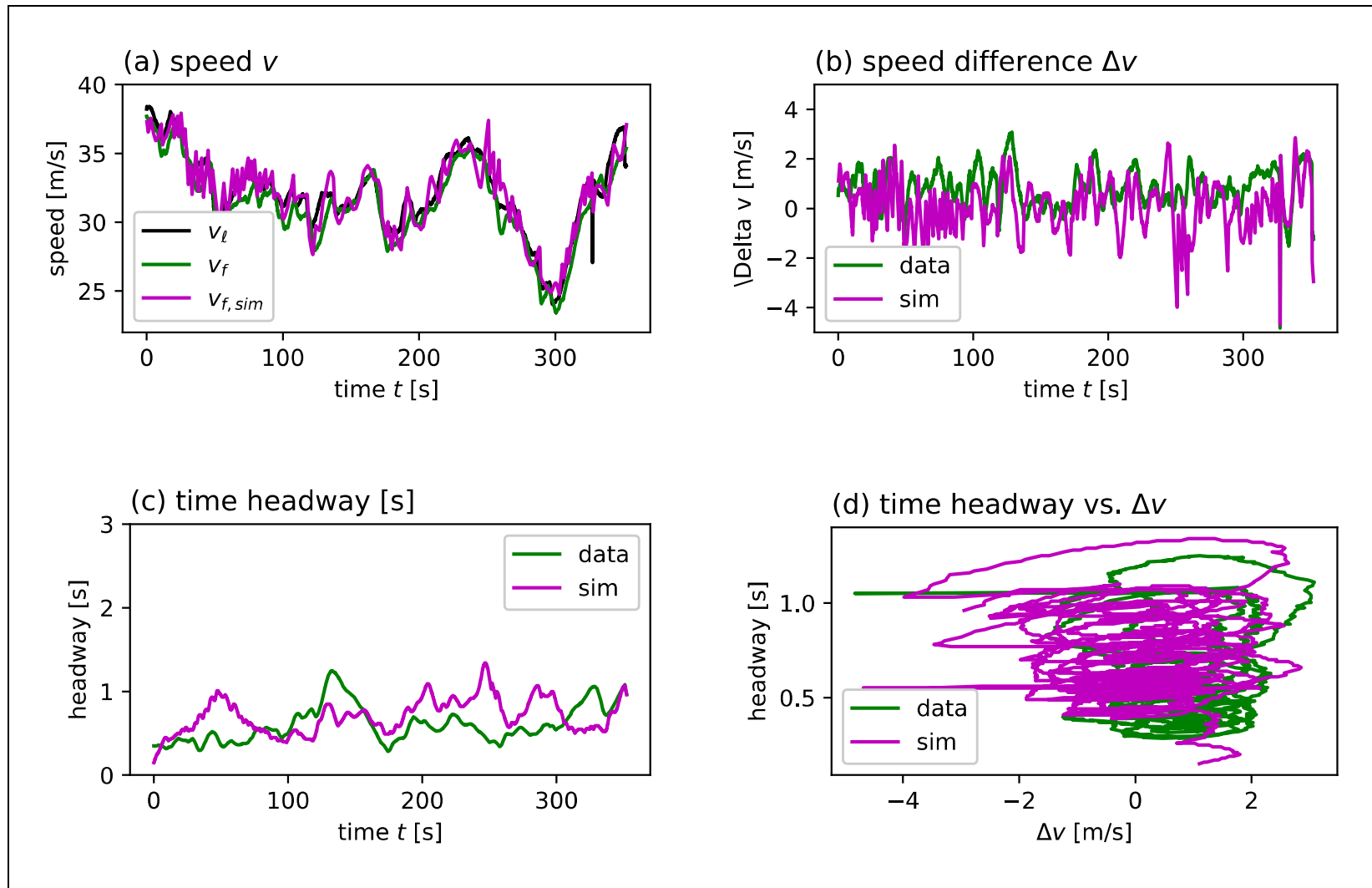


Figure 18. Comparison of a Krauss model with superposed perception errors and real car-following data. The awareness is held constant with a value of $A(t) \equiv 0.1$.

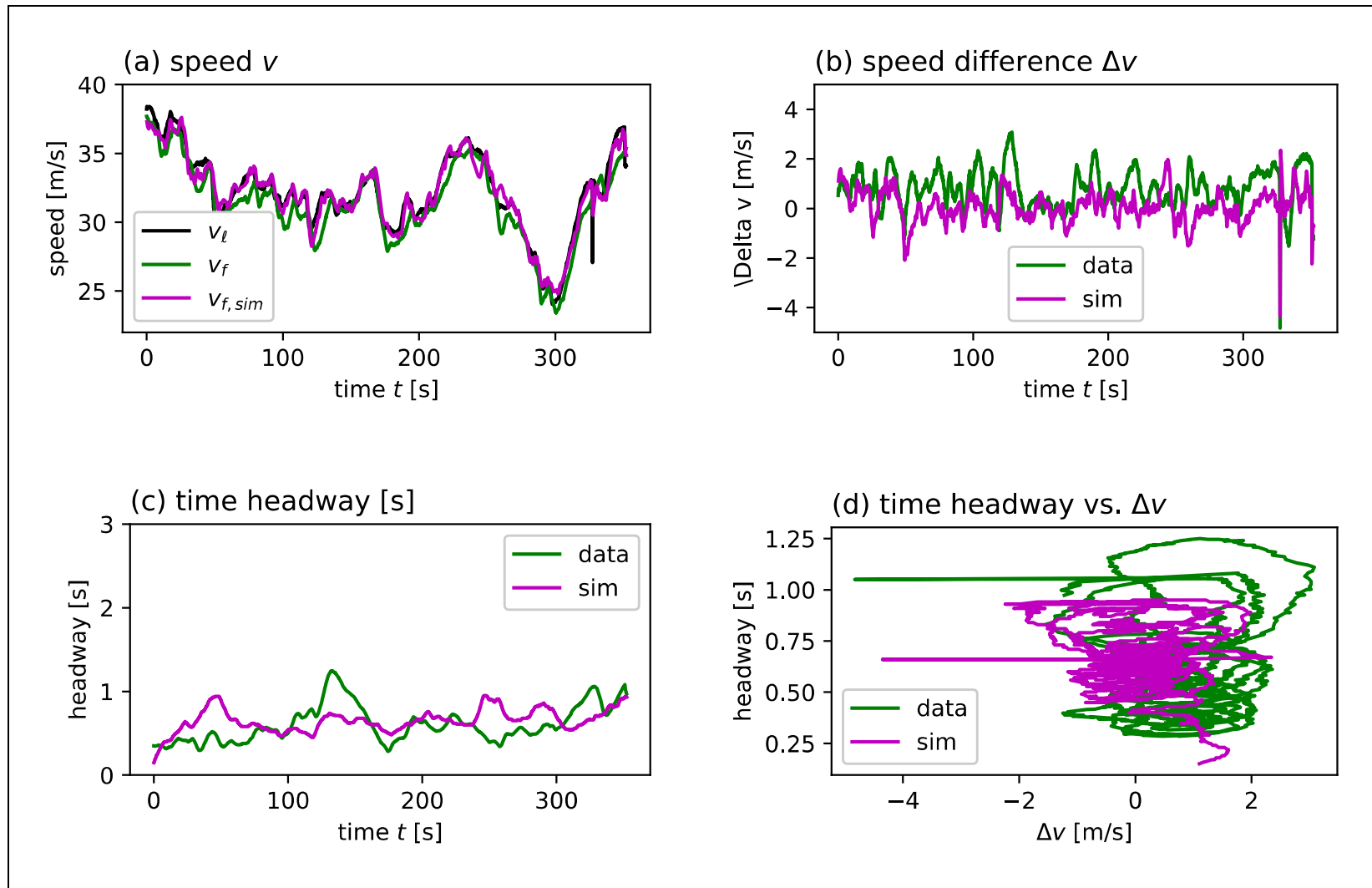


Figure 19. Comparison of a Krauss model with superimposed perception errors and real car-following data. Here, $\theta_x = \theta_v = 0.02$ (other parameters as given above); constant awareness $A(t) \equiv 0.1$.

2.3.4 Implementation of the ToC Model in SUMO

To capture the processes during transitions of control in a simulation, a ToC device and a driver state device were implemented in the open source traffic simulation SUMO. The corresponding code is openly available. The relevant source files are `MSDevice_ToC.h`, `MSDevice_ToC.cpp`, `MSDevice_DriverState.h`, and `MSDevice_DriverState.cpp` in the directory `sumo/src/microsim/devices` of the SUMO repository at <https://github.com/eclipse/sumo>.

The parameters for the ToC model are:

- Manual type: SUMO vehicle type (simulation model) for manual driving mode
- Automated type: SUMO vehicle type (simulation model) for automated driving mode
- Response time: The time the driver needs to react to a ToR
- Initial Awareness: Awareness just after a completed ToC
- Recovery rate: Rate by which the awareness recovers to its maximal value after a ToC
- `mrmDecel`: Value of the constant deceleration rate assumed to be applied during an MRM

To set up a simulated vehicle, which can perform ToCs, the user has to specify at least the two vehicle types, which specify the models for automated and manual driving, as obligatory parameters, see the corresponding [Wiki-page](#)³ for details.

All device parameters are accessible to the user via [TraCI](#) (`traci.vehicle.setParameter()`) and [libsumo](#) (`libsumo::Vehicle::setParameter()`). A special parameter key ‘requestToC’ combined with the value of the ToC lead time after which an MRM will be initiated, can be used to trigger ToCs for the vehicle during the simulation.

Equipping a SUMO vehicle with a ToC-Device automatically adds a driver state device if none was specified previously. This device provides the error states and parameters for the decreased post-ToC driver performance, see Section 2.3.3. If the driver state is automatically generated, default values are used for its parameters, otherwise the user may specify them as described on the corresponding [Wiki-page](#)⁴.

³ http://sumo.dlr.de/wiki/ToC_Device

⁴ http://sumo.dlr.de/wiki/Driver_State

3 Simulation Experiments

3.1 Dimensions of Simulation Experiments

The baseline simulation experiments encompass different traffic demand levels, vehicle mixes, and parameter sets for the (C)AV/CV driver models (ACC, LC2013, ToC/MRM). Whereas Deliverable D2.2 specified traffic demand levels and vehicle mixes for the baseline simulation experiments, we now provide updated vehicle mixes based on a revised definition of actors, considering a more comprehensive set of actual vehicles attributes. Moreover, we here introduce different parametrisation schemes for the (C)AV/CV driver models considering that their behaviour can be aggressive, moderate, or conservative. In addition, the baseline simulation analysis also investigates the effects of a wide range of possible (C)AV/CV behaviours on the Key Performance Indicators (KPIs) defined in D2.1.

3.2 Updated Actors Definition

Deliverable D2.2 categorised actors based on vehicles automation capabilities (longitudinal and/or lateral control), communication capabilities (message types and relevant applications), ToC capabilities (basic or extended), and MRM capabilities (standstill in the ego or the right-most lane).

However, in real life conditions other factors are going to influence the operation of (C)AVs/CVs as well. Early (C)AVs/CVs are expected to be deployed with systems of different automation levels, but system engagement will rely heavily on the driver's discretion. Thus, many (C)AVs/CVs will operate as manual vehicles in several occasions during the first stages of vehicle automation introduction.

Moreover, distracted driving might significantly affect ToCs of Level 1 and 2 AVs. Although drivers of Level 1 and 2 AVs are aware that they should continuously oversee the primary driving tasks when automation is in operation, cases are expected when driver distraction might lead to uncontrolled driving for a short period of time after ToC request (e.g., no acceleration and deceleration until the ego vehicle's distance to leader becomes very short and hard braking must be applied). Finally, there is a possibility that connectivity affects the ToC capabilities of highly automated CAVs (e.g., proactive warning of imminent ToC).

Thus, a revised classification of actors is provided in **Table 6** based on work presented in D2.2 and the newly introduced dimensions with respect to vehicles attributes.

Table 6. Classification of actors (vehicle types).

Class Name	Class Type	Vehicle Capabilities
Class 1	Manual Driving	<ul style="list-style-type: none"> – Legacy Vehicles – (C)AVs/CVs (any level) with deactivated automation systems
Class 2	Partial Automation	<ul style="list-style-type: none"> – AVs/CVs capable of Level 1 and 2 automation – Instant TOC (uncontrolled driving in case of distracted driving) – No MRM capability
Class 3	Conditional Automation	<ul style="list-style-type: none"> – (C)AVs capable of Level 3 automation (level 3 systems activated) – Basic ToC (normal duration) – MRM capability (in the ego lane depending on speed and a predetermined

		desired MRM deceleration level)
		– (C)AVs capable of Level 4 automation (automation activated)
Class 4	High Automation	– Proactive ToC (prolonged duration) – MRM capability (in the right-most lane depending on speed and a predetermined desired MRM deceleration level)

Uncontrolled driving after ToCs of Level 1 and 2 AVs will not be examined during the 1st project iteration. The ToC/MRM model will be adapted to accommodate the latter mentioned corner case during the 2nd project iteration. Currently, the focus lies on the examination of the aforementioned ToC/MRM model that can replicate regular ToCs of Level 3 and 4 (C)AVs. Within the context of the baseline simulation experiments, we assumed that 75% of (C)AVs/CVs will not be able to autonomously handle traffic situations at the TAs presented in D2.2, and will eventually initiate a ToC manoeuvre. We assume connectivity capabilities for specific portions of the latter defined vehicle classes.

Compliance to TransAID infrastructure-assisted traffic management measures is different per vehicle class based on the corresponding vehicle communication capabilities. Non-cooperative vehicles are expected to follow them manually (i.e. by adapting driving because of shown advices on traffic signs, external human-machine interface (HMI), etc.). Compliance rates for non-cooperative vehicles are expected to be significantly lower compared to cooperative ones. Cooperative vehicles of classes 1 and 2 will follow them manually, and those of classes 3 and 4 automatically.

3.3 Traffic Composition

Vehicle mixes for the baseline simulation experiments (1st and 2nd project iteration) are presented in **Tables 7 – 9**, based on the aforementioned vehicle classification. **Table 7** introduces artificial vehicle mixes for the baseline simulation experiments that will be tested during the 1st project iteration. These mixes include explicitly automated vehicles with connectivity capabilities but not non-cooperative vehicles. These latter vehicle classes will be considered during the 2nd project iteration, due to complexities pertaining to conveying TransAID measures to them. Moreover, non-compliant non-cooperative automated vehicles will be disrupting the operations of CAVs when following TransAID measures. Thus, artificial and realistic vehicle mixes encompassing all vehicle classes will be tested during the 2nd project iteration and shown in **Tables 8 – 9**. These mixes will result in more complex but realistic traffic operations. The revised realistic mixes were selected after elaborate discussions within the TransAID consortium considering the work done in D2.2 with respect to projections about future automation and connectivity penetration rates. Please note that TransAID is not linking the penetration rates to specific years, as the key factor is the distribution, not the year.

Table 7. Artificial vehicle mixes for baseline simulations during 1st project iteration.

Vehicle Mix	Class 1	Class 1 (Conn.)	Class 2	Class 2 (Conn.)	Class 3	Class 3 (Conn.)	Class 4	Class 4 (Conn.)
1	60%	10%	-	15%	-	15%	-	-
2	40%	10%	-	25%	-	25%	-	-
3	10%	10%	-	40%	-	40%	-	-

Table 8. Artificial vehicle mixes for baseline simulations during 2nd project iteration.

Vehicle Mix	Class 1	Class 1 (Conn.)	Class 2	Class 2 (Conn.)	Class 3	Class 3 (Conn.)	Class 4	Class 4 (Conn.)
1	60%	10%	5%	5%	5%	5%	5%	5%
2	40%	10%	5%	10%	10%	10%	5%	10%
3	10%	10%	5%	15%	10%	15%	15%	15%

Table 9. Realistic vehicle mixes for baseline simulations during 2nd project iteration.

Vehicle Mix	Class 1	Class 1 (Conn.)	Class 2	Class 2 (Conn.)	Class 3	Class 3 (Conn.)	Class 4	Class 4 (Conn.)
1	60%	3%	5%	4%	9%	8%	6%	5%
2	50%	3%	5%	4%	12%	12%	8%	6%
3	40%	3%	5%	4%	15%	15%	12%	9%

3.4 Traffic Demand Levels

The traffic demand dimension of the baseline simulation experiments was addressed in D2.2. Different traffic demand levels (vehicular flows) corresponding to different Levels of Service (LOS) per facility type (urban, rural, motorway) were selected based on information provided in (HCM, 2010). Vehicular flows were converted to passenger car flows based on the fleet composition section described in D2.2. Thus, baseline simulation scenarios encompass only passenger cars. The corresponding flow rates per hour per lane and LOS that will be considered are shown in **Table 10**.

Table 10. Vehicles/hour/lane for LOS A, B and C in urban, rural, and motorway facilities.

Facility Type	Capacity (veh/h/l)	Level of Service (LOS)		
		A	B	C
Urban (50km/h)	1500 veh/h/l	525	825	1155
Rural (80 km/h)	1900 veh/h/l	665	1045	1463
Motorway (120 km/h)	2100 veh/h/l	735	1155	1617
Intensity / Capacity (IC) ratio		0,35	0,55	0,77

Specifically for Scenario 2.1, the capacity of the merge segment is controlled by the capacity of the exiting section as highlighted in (HCM, 2010):

“The capacity of a merge area is determined primarily by the capacity of the downstream freeway segment. Thus, the total flow arriving on the upstream freeway and the on-ramp cannot exceed the basic freeway segment.”

Therefore, the two-lane motorway capacity is the basic capacity for the simulation network in Scenario 2.1. The vehicle injection rates on the on-ramp entry link and the upstream freeway entry link together should not exceed downstream two-lane motorway service flow rates, which are $600 \times 2 = 1200$ veh/hr/l, $960 \times 2 = 1920$ veh/hr/l, and $1400 \times 2 = 2800$ veh/hr/l based on (HCM, 2010) and show in **Table 11**. The two entry links – upstream motorway and on-ramp – are then injected with approximately 2/3 and 1/3 of these respective rates.

Table 11. Vehicles/hour/lane for Level of Service A, B and C (Scenario 2.1).

Facility Type	Capacity (veh/h/l)	Level of Service (LOS)		
		A	B	C
On-ramp (80km/h)	1650 veh/h/l	462	726	1056
Intensity (demand volume)/Capacity (IC or VC) ratio		0.28	0.44	0.64
Motorway (100 km/h)	2000 veh/h/l	600	960	1400
Intensity (demand volume)/Capacity (IC or VC) ratio		0.3	0.48	0.7

3.5 Driver Models Parametrisation

The parametrisation of the (C)AV/CV driver models integrates the full spectrum of possible (C)AV/CV behaviours into the baseline simulation experiments, and thus, promotes a holistic understanding of their impacts on traffic safety, efficiency, and the environment. (C)AV/CV driver model parameter values are introduced as normal distributions for aggressive, moderate, and conservative (C)AV/CV. **Table 12** presents the adjusted parameters per driver model to reflect the aforementioned behaviours of (C)AVs/CVs.

Table 12. Adjusted driver model parameters to emulate different (C)AV/CV behaviours.

Driver Model	Parameter Name	SUMO Parameter
ACC (Longitudinal Motion)	Desired time headway	<i>tau</i>
Sub-lane (Lateral Motion)	Desired longitudinal gaps	<i>lcAssertive</i>
	Driver response time	<i>responseTime</i>
	Post ToC driver performance	<i>initialAwareness</i>
ToC/MRM		<i>responseTime</i>
	ToC likelihood (internal and external factors)	<i>timeTillMRM</i>

The ACC desired time headway (*tau*) normally spans between 1.2 – 2.2 s (L. Xiao & Gao, 2011). High *tau* values prompt a conservative ACC behaviour, while low values result in aggressive behaviour. The expected effects of different *tau* values on traffic safety and efficiency are assessed in qualitative terms in **Table 13**.

Table 13. Expected impacts of ACC desired headway on safety and efficiency.

Driver Model	Parameter Name	Value	Behaviour	Safety	Efficiency
ACC	Desired time headway (<i>tau</i>)	High	Conservative	Positive (+)	Negative (-)
		Moderate	Moderate	Moderate	Moderate
		Low	Aggressive	Negative (-)	Positive (+)

As explained in Section 2.2.3, the *lcAssertive* calibration parameter was identified as the most significant factor in determining desired ego vehicle gaps for lane-changing relative to surrounding traffic (target follower, target leader, and current leader). Higher *lcAssertive* values dictate a more aggressive vehicle behaviour in accepting shorter gaps, while lower values the opposite. Large desired gaps for lane-changing are expected to have a positive effect on safety and negative on traffic efficiency, and vice versa (**Table 14**).

Table 14. Expected impacts of desired longitudinal gaps for lane-changing on safety and efficiency.

Driver Model	Parameter Name	Value	Behaviour	Safety	Efficiency
Lane Change (LC2013)	Desired longitudinal gaps (<i>lcAssertive</i>)	Large	Conservative	Positive (+)	Negative (-)
		Moderate	Moderate	Moderate	Moderate
		Short	Aggressive	Negative (-)	Positive (+)

The ToC/MRM model parameter *responseTime* determines the driver responsiveness to ToRs by the vehicle automation, while the *initialAwareness* parameter characterises the driver performance after resuming control from the vehicle. Short *responseTime* indicates that the driver can efficiently resume vehicle control in a timely manner, thus positively affecting traffic safety and efficiency (**Table 15**). On the contrary, low *initialAwareness* values imply that a prolonged time horizon is required for drivers to fully recover their driving capabilities after ToC. In these cases, the effects on safety and efficiency will be negative (**Table 16**).

The available time for all drivers to take over control during ToC (*timeTillMRM*) is fixed to 10 s for all vehicle classes and scenarios. Note that the exact value of the *timeTillMRM* has only an effect in relation to the driver's response time and is not as important as in reality, because the models disregard processes preceding the ToC, i.e., in contrast to reality no correlation between the available time and the post-ToC performance of the driver is assumed. The value of 10 s is guided by the time that human drivers usually need to show no significantly reduced performance after a take over in driving simulator experiments, see Section 2.3. When *responseTime* exceeds *timeTillMRM* the ego vehicle will execute MRM for the time difference of the latter parameters. Thus, it is implied that higher *responseTime* results in higher MRM frequency and consequently negative impacts on safety and efficiency (**Table 17**).

Table 15. Expected impacts of driver response time to ToC request on safety and efficiency.

Driver Model	Parameter Name	Value	Behaviour	Safety	Efficiency
TOC/MRM	Driver response time (<i>responseTime</i>)	Long	Conservative	Negative (-)	Negative (-)
		Moderate	Moderate	Moderate	Moderate
		Short	Aggressive	Positive (+)	Positive (+)

Table 16. Expected impacts of post ToC driver performance on safety and efficiency.

Driver Model	Parameter Name	Value	Behaviour	Safety	Efficiency
TOC/MRM	Post TOC driver performance (<i>initialAwareness</i>)	High	Aggressive	Positive (+)	Positive (+)
		Moderate	Moderate	Moderate	Moderate
		Low	Conservative	Negative (-)	Negative (-)

Table 17. Expected impacts of MRM likelihood on safety and efficiency.

Driver Model	Parameter Name	Value	Safety	Efficiency
MRM	MRM likelihood	High	Negative (-)	Negative (-)
		Moderate	Moderate	Moderate
		Low	Positive (+)	Positive (+)

Driver model parameter attributes implying similar (C)AV/CV driving behaviour (aggressive, moderate, and conservative) might exert conflicting or similar effects on traffic safety and efficiency as shown in **Tables 13 – 17**. Namely, large ACC desired time headways (conservative behaviour) impact safety positively but efficiency negatively (**Table 13**), while delayed driver response to ToC requests (conservative behaviour) impacts negatively both safety and efficiency. Thus, driver model parameter attributes are grouped into sets (parametrisation schemes) that yield similar effects to traffic safety or efficiency. The adoption of the latter approach generates five parametrisation schemes for the driver models that represent optimistic, moderate, or pessimistic cases with respect to traffic safety and efficiency impacts (**Table 18**).

Table 18. Driver model parameter attributes per parametrisation scheme.

Parametrization Scheme	ACC	SL2015	ToC/MRM	ToC/MRM	ToC/MRM
	Desired time headway	Desired longitudinal gaps	Driver response time	Post ToC driver performance	MRM likelihood
Pessimistic Safety (PS)	Small	Short	Long	Low	High
Pessimistic Efficiency (PE)	Large	Large	Long	Low	High
Moderate Safety and Efficiency (MSE)	Moderate	Moderate	Moderate	Moderate	Moderate
Optimistic Efficiency (OE)	Small	Short	Short	High	Low
Optimistic Safety (OS)	Large	Large	Short	High	Low

3.5.1 Vehicle Properties

Parameter values for the driver models are specified either in the form of constant values or normal distributions. When normal distributions are used, the distribution mean and standard deviation have to be defined, as well as the lowest and highest values that can be possibly selected from the distribution. Parameter values for LV driver models are uniform for all simulation experiments and were selected based on literature review (Erdmann, 2014; Krauß, 1998) and SUMO developers'

knowledge regarding the underlying driver models acquired through previous work (**Table 19**). Parameter values for (C)AV/CV driver models are provided in **Table 20** considering the aforementioned cases with respect to (C)AV/CV behaviour (aggressive, moderate, and conservative). These values have been selected based on literature review for the ACC and the ToC/MRM model, while parameter values for the lane change model were selected based on the parametrisation analysis of the LC2013 model presented in Chapter 2. CVs have similar parameter values with (C)AVs, except for the *responseTime* parameter which is set equal to zero for CVs (**Table 21**), since drivers of these vehicles are expected to instantly resume vehicle control when a take-over request is issued by the vehicle automation.

Table 19. Driver model parameter values for manual driving (LV).

Parameter Name	Parameter description	Parameter values
<i>sigma</i>	The driver's imperfection (between 0 and 1).	normal(0.2, 0.5); [0.0, 1.0]
<i>tau (s)</i>	The driver's desired (minimum) time headway. For the default Krauss model this is based on the net space between leader back and follower front.	normal(0.6, 0.5); [0.5, 1.6]
<i>decel (m/s²)</i>	The deceleration capability of vehicles.	normal(3.5, 1.0); [2.0, 4.5]
<i>accel (m/s²)</i>	The acceleration capability of vehicles.	normal(2.0, 1.0); [1.0, 3.5]
<i>emergencyDecel (m/s²)</i>	The maximum deceleration capability of vehicles.	9.0
<i>lcAssertive</i>	Willingness to accept lower front and rear gaps on the target lane.	1.3
<i>actionStepLength (s)</i>	The interval length for which a vehicle performs its decision logic (acceleration and lane-changing). The given value is processed to the closest (if possible smaller) positive multiple of the simulation step length.	0.1
<i>speedFactor</i>	The vehicles expected multiplier for lane speed limits.	normal(1.1, 0.2); [0.8, 1.2]

Table 20. Driver Model parameter values for (C)AVs.

Parameter Name	Parameter values/(C)AV Behaviour		
	Aggressive	Moderate	Conservative
<i>tau (s)</i>	normal(1.2,0.1); [1.1,1.3]	normal(1.6,0.2); [1.3,1.8]	normal(2.0,0.2); [1.8,2.0]
<i>decel (m/s²)</i>	normal(3.0,1.0); [2.0,4.0]	normal(3.0,1.0); [2.0,4.0]	normal(3.0,1.0); [2.0,4.0]
<i>accel (m/s²)</i>	normal(1.5,1.0); [0.75,2.0]	normal(1.5,1.0); [0.75,2.0]	normal(1.5,1.0); [0.75,2.0]
<i>emergencyDecel (m/s²)</i>	9.0	9.0	9.0
<i>actionStepLength (s)</i>	0.1	0.1	0.1
<i>lcAssertive</i>	normal(0.9,0.1); [0.8,1.0]	normal(0.7,0.1); [0.6,0.8]	normal(0.5,0.1); [0.4,0.6]
<i>responseTime (s)</i>	normal(7,2.1); [2,60]	normal(7,2.5); [2,60]	normal(7,3); [2,60]
<i>initialAwareness</i>	normal(0.7,0.3); [0.1,1.0]	normal(0.5,0.3); [0.1,1.0]	normal(0.3,0.3); [0.1,1.0]
<i>recoveryRate</i>	normal(0.2,0.1); [0.01,0.5]	normal(0.2,0.1); [0.01,0.5]	normal(0.2,0.1); [0.01,0.5]
<i>mrmDecel (m/s²)</i>	3.0	3.0	3.0

Table 21. Driver Model parameter values for CVs.

Parameter Name	Parameter values/CV Behaviour		
	Aggressive	Moderate	Conservative
<i>tau (s)</i>	normal(1.2,0.1); [1.1,1.3]	normal(1.6,0.2); [1.3,1.8]	normal(2.0,0.2); [1.8,2.0]
<i>decel (m/s²)</i>	normal(3.0,1.0); [2.0,4.0]	normal(3.0,1.0); [2.0,4.0]	normal(3.0,1.0); [2.0,4.0]
<i>accel (m/s²)</i>	normal(1.5,1.0); [0.75,2.0]	normal(1.5,1.0); [0.75,2.0]	normal(1.5,1.0); [0.75,2.0]
<i>emergencyDecel (m/s²)</i>	9.0	9.0	9.0

<i>actionStepLength (s)</i>	0.1	0.1	0.1
<i>lcAssertive</i>	normal(0.9,0.1); [0.8,1.0]	normal(0.7,0.1); [0.6,0.8]	normal(0.5,0.1); [0.4,0.6]
<i>responseTime (s)</i>	0	0	0
<i>initialAwareness</i>	normal(0.7,0.3); [0.1,1.0]	normal(0.5,0.3); [0.1,1.0]	normal(0.3,0.3); [0.1,1.0]
<i>recoveryRate</i>	normal(0.2,0.1); [0.01,0.5]	normal(0.2,0.1); [0.01,0.5]	normal(0.2,0.1); [0.01,0.5]
<i>mrmDecel (m/s²)</i>	3.0	3.0	3.0

3.6 Simulation Runs

Baseline simulation experiments are ran for three different vehicle mixes, three different traffic demand levels, and five different driver model parameter sets per scenario. Thus, 270 simulation runs have to be executed for the six scenarios considered during the 1st project iteration, without accounting for the statistical significance of the simulation output. To ensure that simulation results are statistically significant, we estimated the required number of runs per simulation experiment. Initially, five runs were performed per TransAID scenario and aggregate network-wide performance measurements were collected. Average network speed was selected as the mean statistic to estimate the required number of runs based on the following equation (Ott & Longecker, 2004):

$$n = \frac{(z_{\alpha/2})^2 (s_d)^2}{E} \quad (\dots)$$

where n is the number of required runs, $z_{\alpha/2}$ is the critical normal distribution value for significance level $(1 - \alpha)$, s_d is the standard deviation, and E is the allowable error. The significance level was set at 95%, the tolerable error equal to 0.5 km/h, and the standard deviation was computed based on the simulation output collected during the first five simulation runs executed per scenario. The required number of runs was estimated to be 10 for each simulation scenario. The simulation timeline per simulation run spans to 1 h.

3.7 Simulation Output

KPIs were introduced in D2.1 for the assessment of traffic efficiency, safety, environmental impacts, and traffic dynamics at TAs before (baseline scenarios) and after (TransAID measures) the implementation of infrastructure-assisted traffic management schemes at TAs. A set of KPIs for the evaluation of the baseline simulation experiments is chosen from the comprehensive list of KPIs defined in D2.1 (**Table 22**). These KPIs can be directly estimated and exported by SUMO as simulation output.

Table 22 List of KPIs for the evaluation of baseline simulation experiments.

KPI Name	KPI Description
Average network speed	Average space-mean speed of the vehicular fleet on a specific road network.
Space-mean speed/Edge	Mean speed estimated based on travel time along or road segment.
Total Number of Lane Changes	Number of lane changes performed in the whole network.
Time-to-collision (TTC)	The time required for two vehicles (or a vehicle and an object) to collide if they continue at their present speed and on the same path. Measures a longitudinal margin to lead vehicles or objects.
CO₂ emissions (gr)/km	Total CO ₂ emitted per km travelled on the road network during the analysis period.

Traffic efficiency is interpreted through the following aggregated (network-wide) and disaggregated (local) statistics: (i) average network speeds and (ii) space-mean speed per network edge. Traffic dynamics at TAs is investigated in terms of total number of lane changes executed. Total number of lane changes is expected to show the disruption introduced due to lane change manoeuvres per traffic mix and relevant driver behaviour induced by different vehicle types. Since the objective of TransAID is to manage connected and automated vehicles in the presence of mixed traffic along TAs so as to prevent, manage, or distribute ToC/MRM, the estimation of the the total number of lane changes will be useful for parallel comparison after TransAID measures encompassing lane change advice are examined.

Traffic safety can be only indirectly assessed in microscopic traffic simulations by means of surrogate safety measures⁵ (SSMs). SSMs were selected based on results published in literature and are correlated with crash rates when not enough accident data is available in simulation studies. We chose time-to-collision (TTC) to indicate the probability of safety critical situations for the baseline simulation experiments. There, TTCs are measured under the following conditions: (i) follower has a higher speed than leader, (ii) they travel along the same path, and (iii) the follower's space headway is less than 50 m. We assume that events with TTC lower than three seconds are safety critical conflicts based on SUMO's default threshold for TTC and literature findings (Horst & Hogema, 1993).

Finally, environmental impacts are quantified in terms of CO₂ emissions per km travelled, which are estimated with the use of the PHEMlite model that is incorporated in SUMO. PHEMlite, is a simplified version of PHEM, which is an instantaneous vehicle emission model developed by the TU Graz, and is based on an extensive European set of vehicle measurements and covers passenger

⁵ As traffic safety itself cannot be directly observed, it is relied on other 'proxy' measures such as the space gaps and speed differences between vehicles. These measures are called 'surrogate safety measures' (SSM), and – based on results published in literature – they give an indication of a safe, unsafe, or accident situation. The SSMs can then be analysed to determine the accident risk, and in case of an accident the injury risk. As such, the type of information which should be measured in order to guarantee safety of vehicles in the context of a Transition Areas is known.

cars, light duty vehicles and heavy duty vehicles from city buses up to 40 ton semi-trailers (Hausberger et al., 2011).

4 Baseline Simulation Scenarios

4.1 Scenario 1.1 Provide path around road works via bus lane

4.1.1 Scenario Description

In the case of road works, the existence of a bus lane serves as an alternative route to circumvent lane closures. However, (C)AVs/CVs might not be able to understand that driving on the bus lane is permitted in the given situation (unable to detect correct road lane markings), and therefore ToCs become mandatory. Especially in urban situations, such lane markings may not always be available (in every country). If the road side infrastructure (RSI) provides an explicit path around the road works, (C)AVs/CVs can drive without disrupting their AD mode (preventing ToCs). Thus, it is clear where the (C)AV/CV can break the traffic rules and drive across the bus lane.

In this scenario, road works are carried out on a two-lane urban road adjacent to a bus lane (**Figure 20**). The RSI has planned a path and distributes it; thus, when (C)AVs/CVs approach the road works, they receive the path information from the RSI which allows them to drive around the road works.

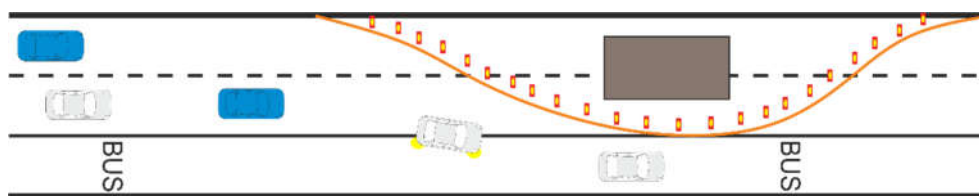



Figure 20. Schematic overview of Scenario 1.1.

More details about the simulation network of Scenario 1.1 can be found in **Table 23**.

Table 23. Network configuration details for Scenario 1.1.

Scenario 1.1	Settings	Notes
Road section length	1.85 km	
Road priority	3	
Allowed road speed	13.89 m/s	• 50 km/h
Number of nodes	11	• n0 – n10
Number of edges	10	
Number of O-D relations	1	• from n0 to n8
Number of lanes	3	• 2 normal lanes; 1 bus lane (the rightmost lane)
Work zone location	from n5 to n6	• 250 m
Closed edges ^{1, 2} (defined in the file closeLanes.add.xml)	workzone	• 2 normal lanes
	safetyzone1_1	• the leftmost lane
	safetyzone1_2	• 2 normal lanes
	safetyzone2_1	• 2 normal lanes
	safetyzone2_2	• the leftmost lane
Disallowed vehicle classes	• normal lanes: pedestrians, tram, rail_urban, rail, rail_electric, ship	• from n0 to n10
	• bus lane: all expect buses, coaches and emergency vehicles	• from n0 to n2 • from n9 to n10

	<ul style="list-style-type: none"> bus lane: same as the normal lanes with custom_1 	<ul style="list-style-type: none"> from n2 to n9 custom_1: AVs without providing information
Filenames	<ul style="list-style-type: none"> network: UC1_1.net.xml lane closure: closeLanes.add.xml traffic signs: shapes.add.xml 	
<p>Intended control of lane usage</p> <p>Around the construction site, the bus lane’s <i>vClass</i> permissions are altered to allow all classes but the class ‘custom1’ which is assigned to automated vehicles, which were not informed about the possible circumvention along the bus lane. As soon as they are informed, their <i>vClass</i> should be switched to the default class (“passenger”), which in turn allows them to use the bus lane in the specified region.</p>		
<p>Network layout</p> 		
<p>Road segments</p> <p>n0→n1: Insertion and backlog area (300 m) n0→n2: Bus only on bus lane (650 m) n2→n9: all <i>vClasses</i> but uninformed automated allowed (class “custom1”) on bus lane (800 m) n3→n4: the leftmost lane closed (safety zone 1_1) (25 m) n4→n5: the second leftmost lane closed as well (safety zone 1_2 (25 m)) n5→n6: the second leftmost lane closed as well (work site (250 m)) n6→n7: the second leftmost lane closed as well (safety zone 2_1 (25 m)) n7→n8: the leftmost lane closed (safety zone 2_2 (25 m)) n9→n10: Bus only on bus lane (400 m)</p>		

¹ Required minimum safety distance according to the German Technical Rules for Workplaces ASR A5.2: 10 m with allowed maximum speed 30 km/h; 50 m with allowed maximum speed 50 km/h; 100 m with allowed maximum speed 100 km/h. Each safety area is divided into two parts: one is with one-lane closure and the other one is with two-lane closure for smoother transition; ² The placement of the traffic signs is based on the German Guidelines for road job security (RSA).

4.1.2 Results

4.1.2.1 Impacts on Traffic Efficiency

Network-wide Impacts

Figure 21 shows the average network speed in the different scenarios. The two columns of the figure show the same data in a distinct grouping to allow an easier visual assessment with respect to the different traffic mixes (left column) and the different levels of service (right column).

For the first column we observe that regardless of the level of service and the parameter scheme, the average speed is decreasing with an increased share of automated vehicles. This capacity loss by the introduction of automated vehicles in the absence of special measures is caused by different factors, which affect the dynamics of automated vehicle models: (i) the required headway is estimated larger for automated vehicles, (ii) their acceleration rate is lower (the downstream end of jams dissolves slower), (iii) driver performance decreases after ToC, and (iv) MRMs may occur.

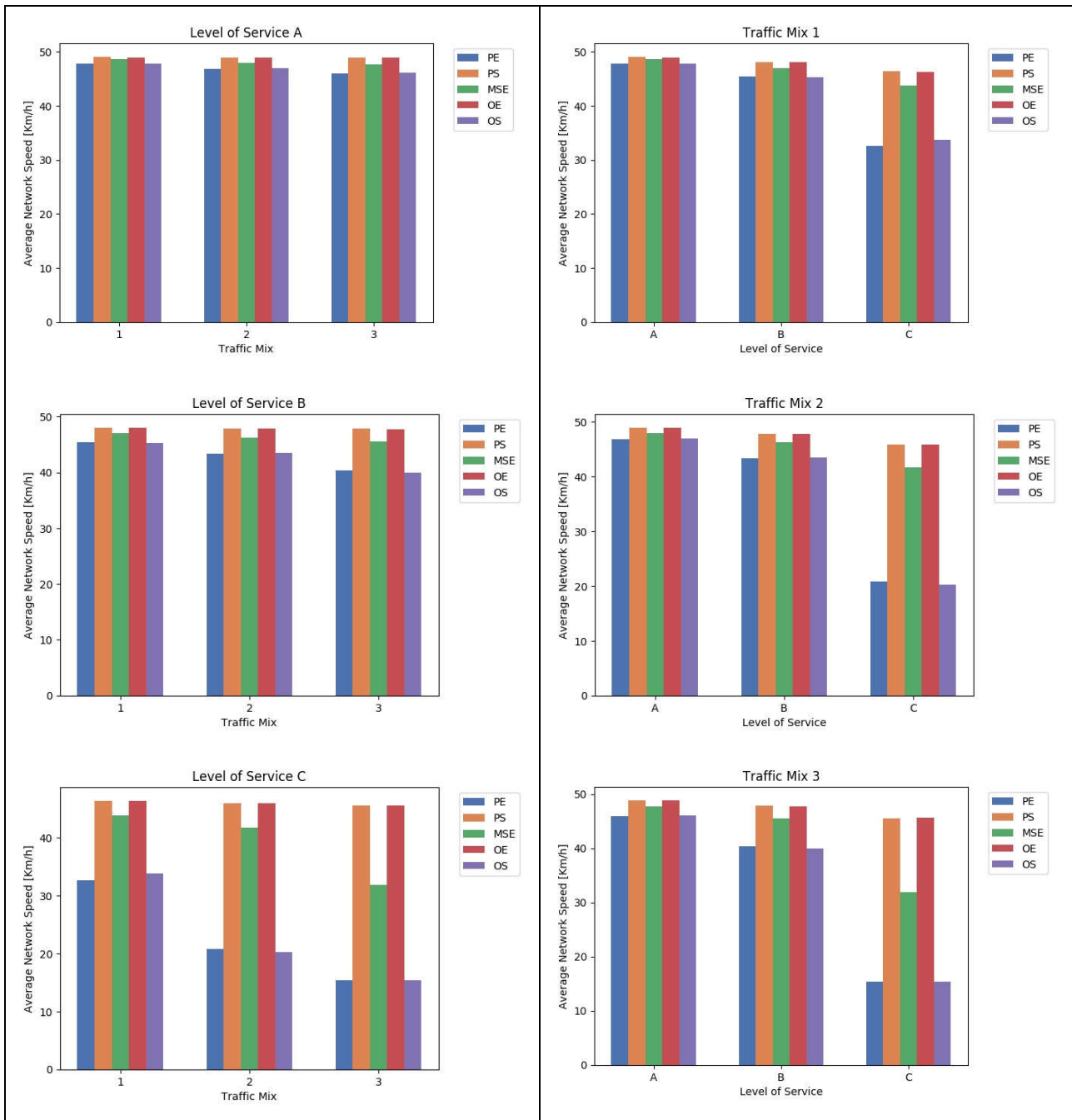


Figure 21. Average network speed for Scenario 1.1 baseline simulation experiments (varying parameter scheme, LOS, and traffic mix). Different bar colours correspond to different parameter schemes. The left column groups results by LOS, the right column by traffic mix.

The right column shows, that accordingly the average speed decrease from LOS A to LOS B is more dramatic in the presence of a larger number of CAVs/CVs, as these decrease the capacity and consequently the region of free flow.

Local Impacts

Figure 22 shows the average speed (taken over 5 minutes) on the edge ‘approach_2’, which is located just before the bottleneck induced by the subsequent lane drops at the beginning of the construction site, see **Figure 23**. The left column shows the results for different shares of AVs for LOS C and the right column for different LOS levels for traffic mix 3. The average speed drops for

the parameter schemes OS and PE already at LOS B to some intermediate state, and completely deteriorates at LOS C indicating heavy merging problems at the beginning of the construction side. Level MSE also show a tendency for passing the point to the congestion-induced capacity drop as can be suspected from the long term transient for the combination LOS C / Mix 3.

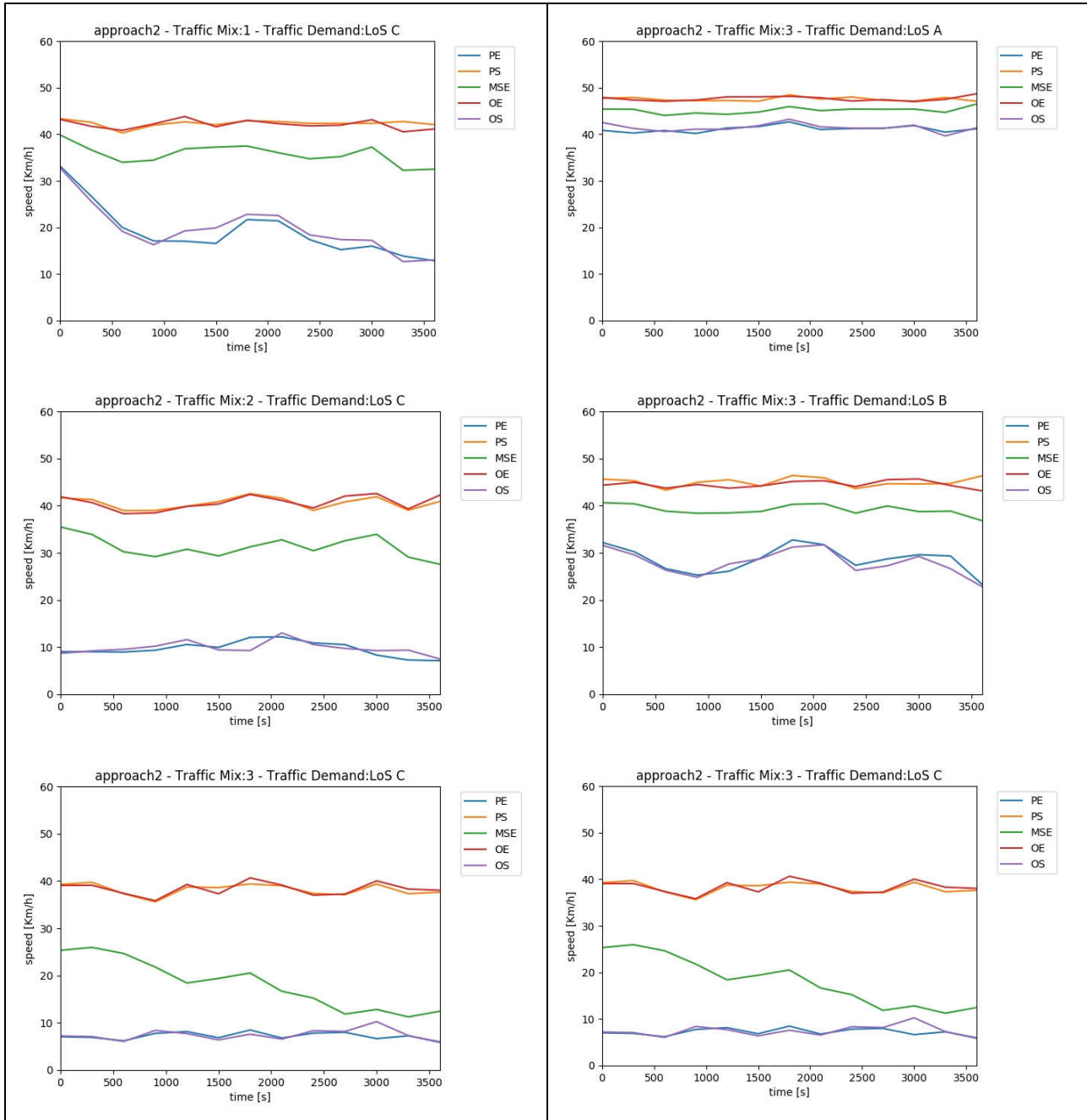


Figure 22. Average speed at the edge ‘approach_2’ for the different parameter sets. Left column: varying traffic mix at LOS C; right column: varying demand level at traffic mix 3.

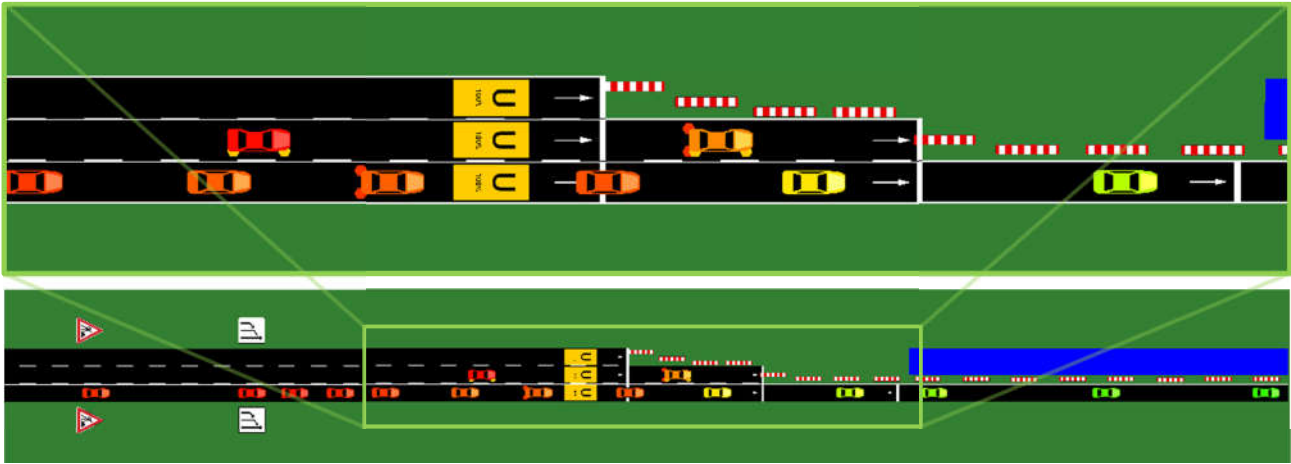
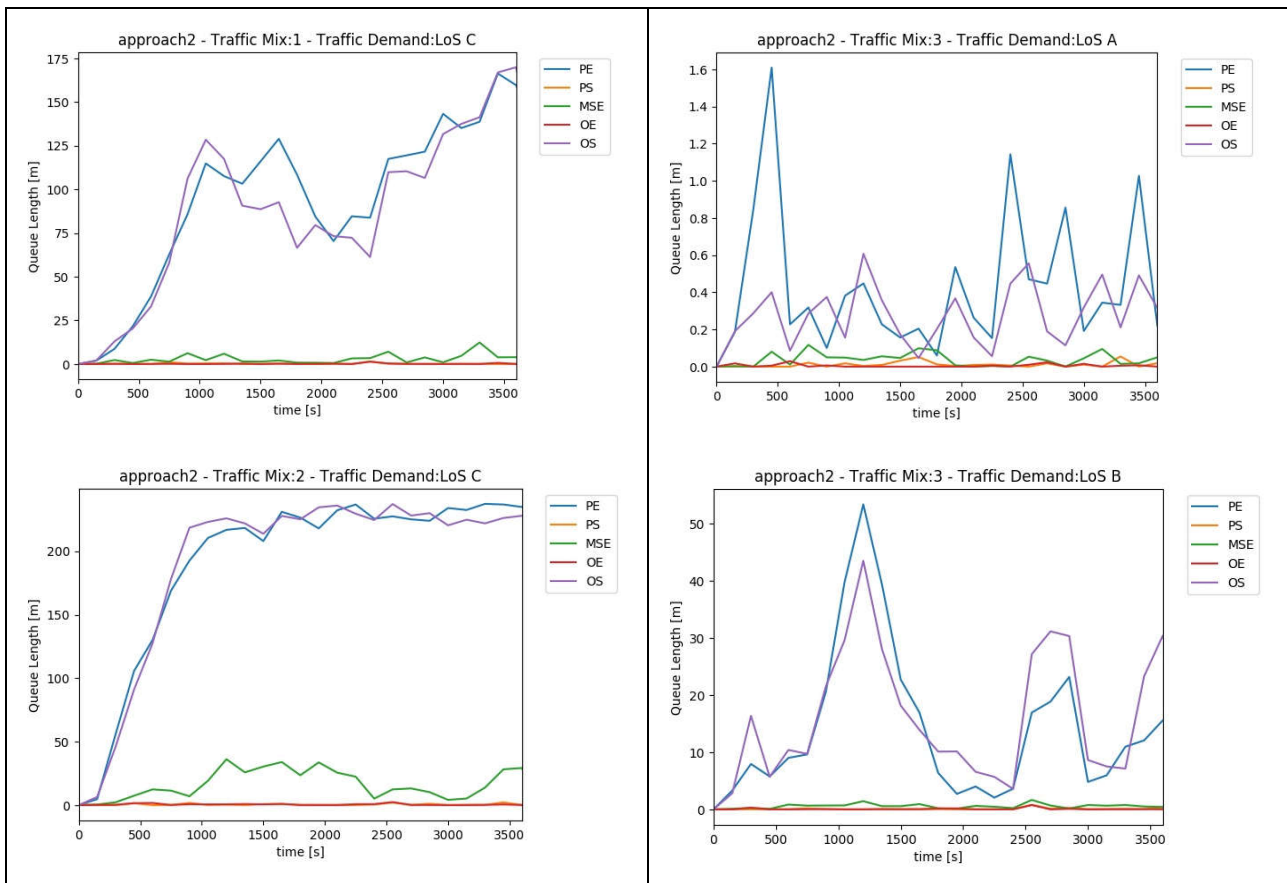


Figure 23. Queuing situation at the merge point, where two lanes are closed. Vehicles are coloured according to their current speed, with red corresponding to speeds close to 0 km/h and green to 50 km/h.

In **Figure 24** we show the average lengths of the queues (during the last 150 seconds) building up on the edge ‘approach_2’ during the simulation. The queue length is defined as the back position of the last vehicle on the edge, which is slower than 5 km/h.

For congested scenarios a constant queue of length ~250 m builds up on the edge ‘approach_2’ (the edge’s length is 350 m), while in other scenarios (Mix 1/LOS C and Mix 3/LOS B) the queue length strongly fluctuates during alternating episodes of relatively smooth flow and disruptions arising from merging problems. Note the inhomogeneous length-scale on the ordinate.



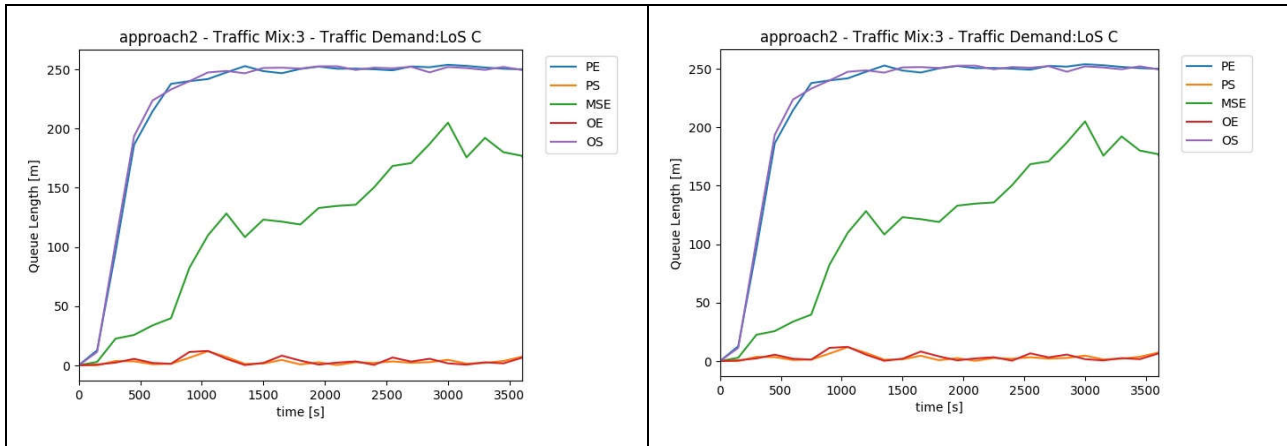
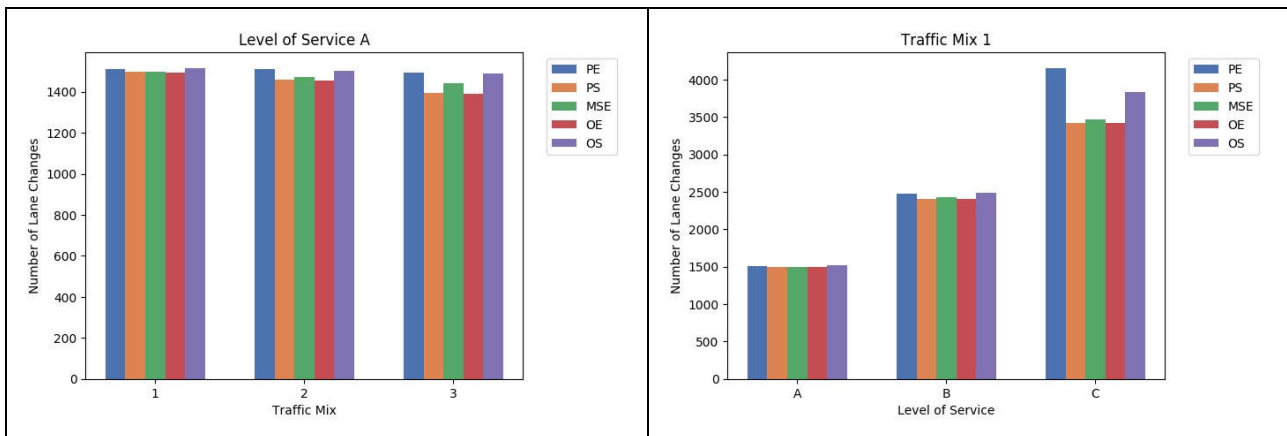


Figure 24. Average queue length at the edge ‘approach_2’ for the different parameter sets. Left column: varying traffic mix at LOS C; right column: varying demand level at traffic mix 3.

4.1.2.2 Impacts on Traffic Dynamics

Figure 25 shows the total number of lane changes for each simulated scenario (accumulated over the ten executed runs). For mainly uncongested scenarios (LOS A and B, and LOS C for parameter schemes OE/PS) the number varies only slightly and is roughly proportional to the number of vehicles with a constant factor of approximately three lane changes per vehicle, indicating homogeneous flow conditions.

For congested conditions, the number of lane changes per vehicle increases, cf. LOS C simulations for parameter schemes PE/OS, and to some also scheme MSE for traffic mix 3. Interestingly, the number does not seem to be a monotonic function of the share of CAVs/CVs, respectively the congestion level, as one can observe a decrease from mix 2 to mix 3 for LOS C.



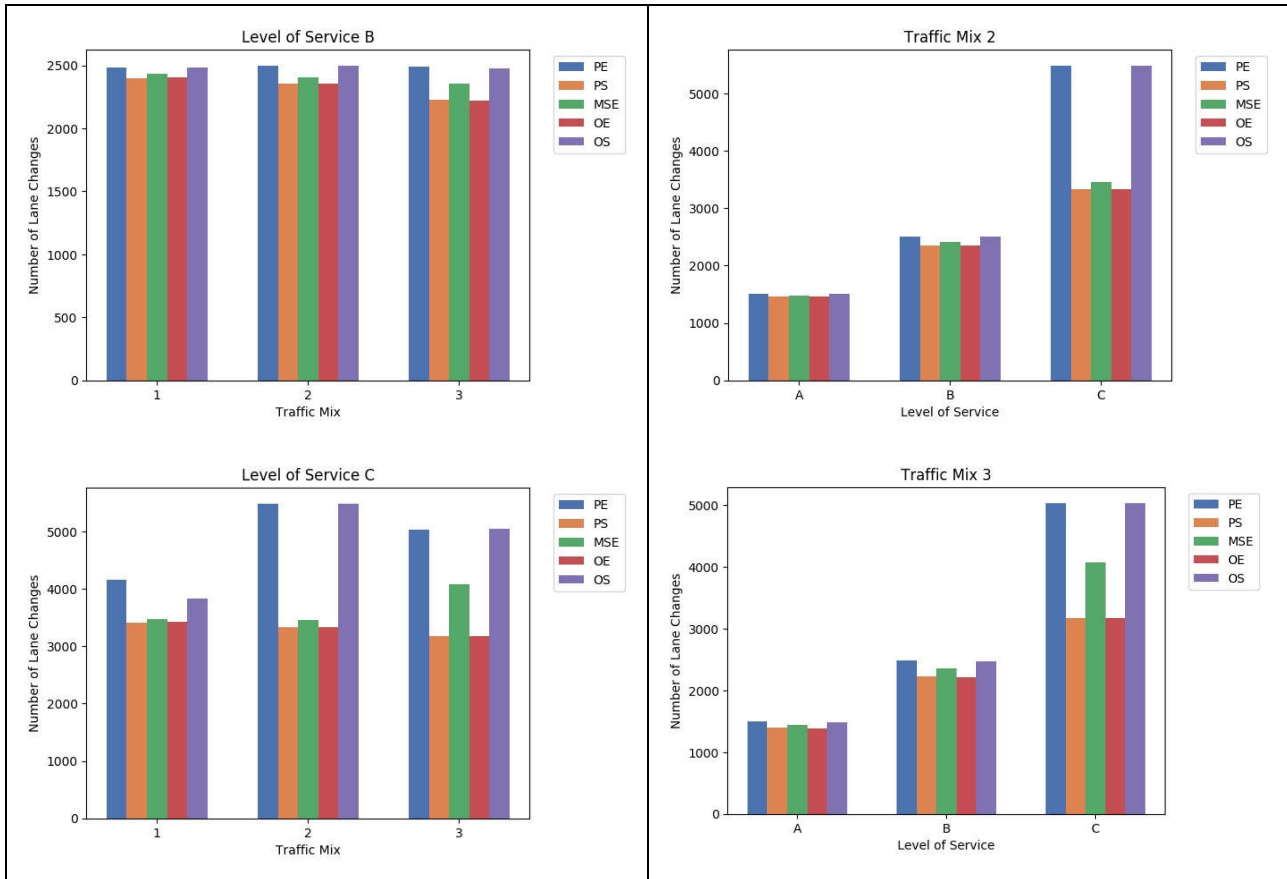


Figure 25. Number of lane changes for Scenario 1.1 baseline simulation experiments (varying parameter scheme, LOS, and traffic mix). Different bar colours correspond to different parameter schemes. The left column groups results by LOS, the right column by traffic mix.

4.1.2.3 Impacts on Traffic Safety

Figure 26 shows the average number of events with TTC below three seconds (termed ‘critical’ below). The dependence on the LOS is monotonic by and large, giving an increasing number of critical events for increasing demand. In dependence of the traffic mix the number of TTCs seems to have a more complex form for several parameter schemes and LOSs.

Most notable there seems to be a positive influence of efficiency on safety in the scenario (in terms of TTC frequency) as higher values for the efficiency indicators (See Section 4.1.2.1) correlate with a lower number of TTCs below three seconds. This effect even overrules the direct injection of parameter values, which seem favourable for the traffic safety (e.g., larger desired gaps and decreased perception errors), but may have an adverse effect on the efficiency.

The main reason for critical situations observed in the simulations is the reduction of the number of lanes. Indeed, the situations, where the increased TTCs are recorded almost always correspond to rear end conflicts involving vehicles, which have to reduce their speed significantly because they could not find a merging gap on their right before the end of a lane in time, see Sections 4.4.2.1.3 and 4.4.2.2.3 for similar phenomena.

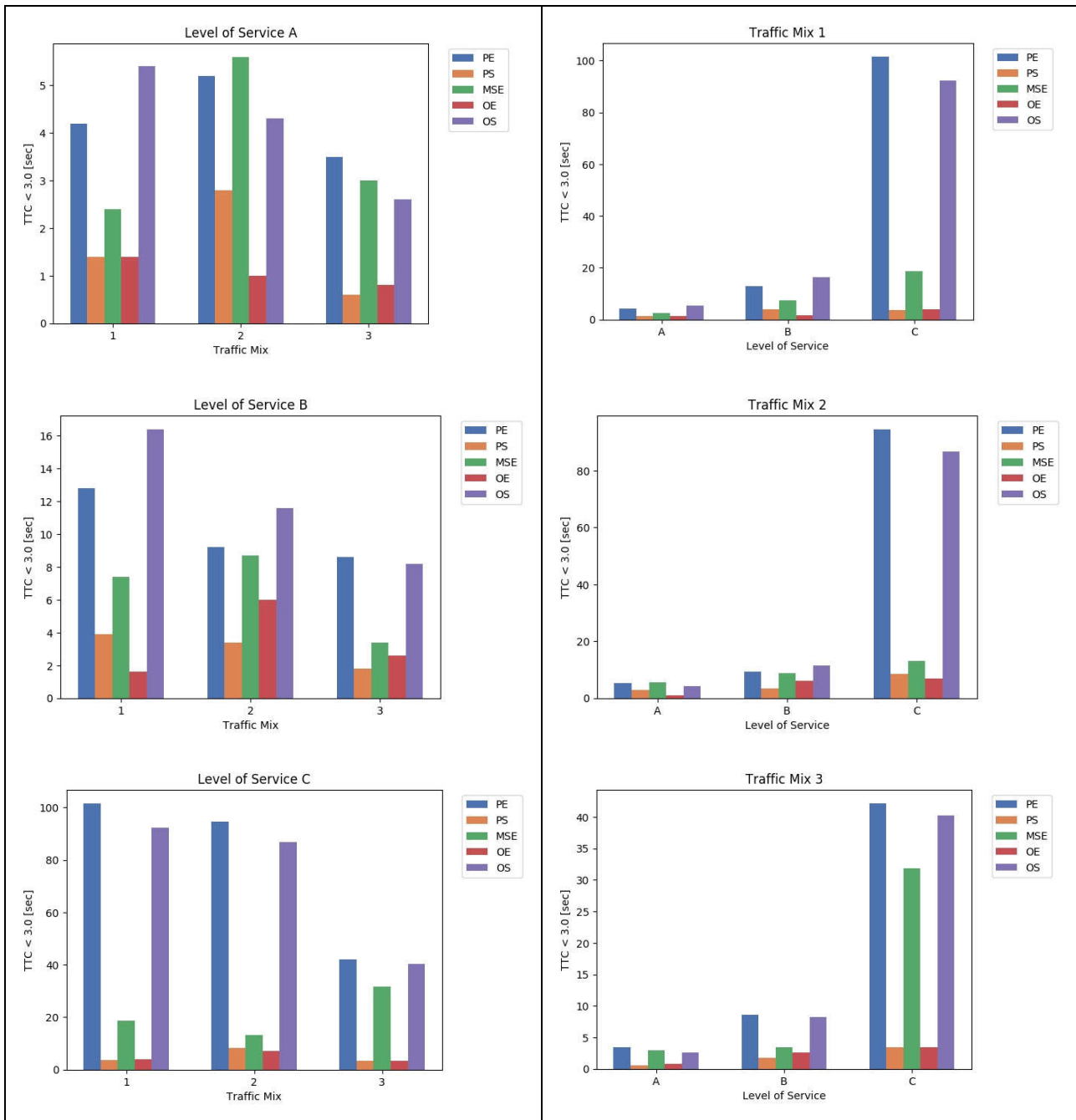


Figure 26 Average number of events with TTCs below 3.0 seconds for Scenario 1.1 baseline simulation experiments (varying parameter scheme, LOS, and traffic mix). Different bar colours correspond to different parameter schemes. The left column groups results by LOS, the right column by traffic mix.

4.1.2.4 Environmental Impacts

Figure 27 shows the average CO₂ emissions per travelled kilometre. We observe that increased emission levels are directly related to increased congestion, see **Figure 21**. The highest values (> 200 g CO₂/km) are observed for LOS C, where also the average speed is below 35 km/h. Again, indirect benefits following from efficiency benefits override assumingly favourable microscopic parameters which seem to promote a more homogeneous driving style, e.g., moderate desired acceleration and deceleration rates and larger desired headways.

Another interesting implication of the results is that more CO₂ emissions are observed in the presence of a larger number of CAVs/CVs. This can be seen by comparing the essentially constant emission levels of uncongested scenarios (parameter schemes PS and OE in the right column of **Figure 27**) when the traffic mix is fixed with the increasing emission levels for uncongested scenarios when the share of CAVs/CVs is increased. This may be due to the disturbances caused by ToCs and MRMs, which would also explain the distribution between the different parameter schemes.

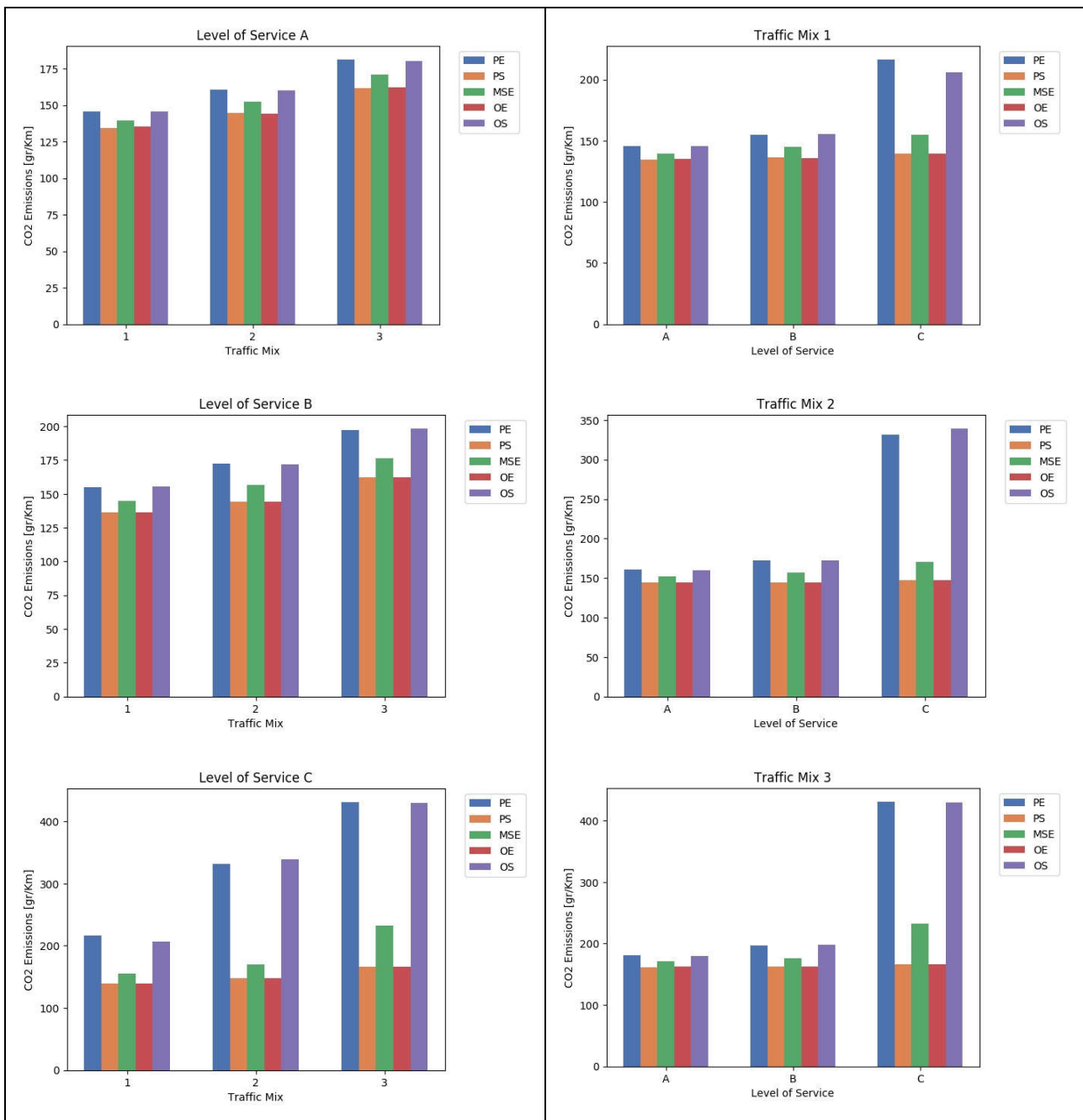


Figure 27. Average CO₂ emissions per km travelled for Scenario 1.1 baseline simulation experiments (varying parameter scheme, LOS, and traffic mix). Different bar colours correspond to different parameter schemes. The left column groups results by LOS, the right column by traffic mix.

4.2 Scenario 2.1 Prevent ToC/MRM by providing speed, headway and/or lane advice

4.2.1 Scenario Description

The simulation network of Scenario 2.1 is a typical one-lane on-ramp joining a one-direction two-lane motorway segment (**Figure 28**). Scenario 2.1 (baseline experiments) encompasses CAVs, CVs, and LVs traveling along a motorway merge segment or entering the mainline motorway lanes through an on-ramp. While LVs on the mainline can speed up, slow down, or perform cooperative lane changes to the left, in order to create bigger gaps for the merging vehicles, CAVs on the mainline may not break up platoons or create bigger gaps with temporary acceleration/deceleration for merging vehicles encountering limited space to merge. Due to the complexity of driver behaviour, which is induced by the multiple vehicle types and mixes, it is essential for the RSI to oversee and monitor traffic operations along the motorway, especially at TAs.

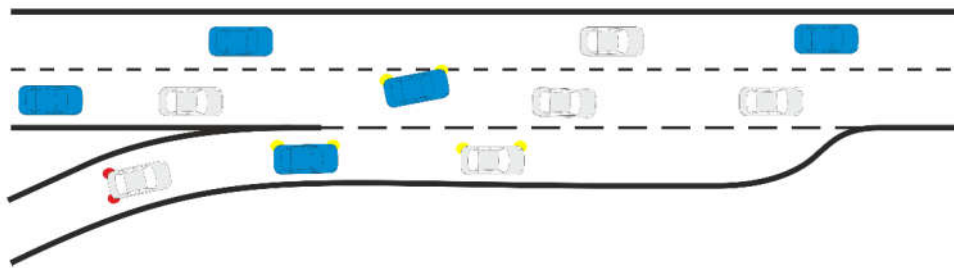


Figure 28. Schematic overview of Scenario 2.1.

The infrastructure detects the available gaps on the right-most mainline lane to estimate speed and lane advice for CAVs/CVs entering the mainline motorway from the on-ramp. We also assume that CAVs/CVs constantly update (near real-time) their speed and lane information to the RSI. The RSI integrates this information with measurements collected by the available road-side sensors. The speeds and locations of LVs can be estimated based on the information gathered via the road-side sensors and on the location (and available sensing information) of CAVs/CVs. With this information, the infrastructure has the option to advise vehicles on the network, for example, lane advice including position and time of the lane change, speed advice, headway advice, or lane change advice on the mainline motorway.

Without the aforementioned infrastructure-assisted measures, vehicles might be impeded or involved in certain safety critical situations under specific traffic conditions (e.g., incidents) or automated driving operations (e.g., platooning at motorway merge/diverge segments). Under these circumstances, CAVs/CVs might request ToCs or execute consequently MRMs at TAs for safety reasons.

The network configuration details are described in **Table 24**. To have a clear view of the merging area (beginning from the on-ramp and ending at the mainline motorway), which is part of the transition area, a more detailed network schematic is added under the SUMO network layout.

The general scenario description in this section showed that a typical on-ramp to motorway merging scenario can be complex due to various driver behaviours generated by different vehicle types and their interactions. The actions and interactions of vehicles (actors) on the network will take place mainly at TAs, and so will the ToCs or MRMs.

Table 24. Network configuration details for Scenario 2.1.

UC2_1	Settings	Notes
Road section length	<ul style="list-style-type: none"> Highway: 1.5 km On-ramp: 0.5 km 	
Road priority	3	
Allowed road speed	<ul style="list-style-type: none"> Highway: 27.78 m/s On-ramp: 22.22 m/s 	<ul style="list-style-type: none"> Highway: 100 km/h On-ramp: 80 km/h
Number of nodes	7	<ul style="list-style-type: none"> jun1 - jun7 priority nodes
Number of edges	6	
Number of O-D relations (routes)	2	<ul style="list-style-type: none"> from jun1 to jun7 from jun3 to jun7
Number of lanes	1-2-3-2	<ul style="list-style-type: none"> 1 lane on-ramp 2 normal lanes on highway 3 lanes at merging zone (from jun4 to jun5, including acceleration lane) 2 lanes downstream of the merging zone. Thus, a lane drop from 3 to 2 lanes at the end of merging zone.
Filenames	<ul style="list-style-type: none"> network: UC2_1.net.xml 	
Network layout		
<p>The diagram shows a network layout on a green background. Nodes are labeled: jun1, jun2, jun3, jun4, jun5, jun6, jun7. Edges are labeled: longEdge1 (between jun2 and jun4), longEdge2 (between jun4 and jun5), longEdge3 (between jun5 and jun7). An on-ramp connects jun3 to jun4. jun1 is labeled 'entry' and jun6 is labeled 'exit'.</p>		
Network Schematic		
<p>The schematic shows lane configurations across three edge segments. Top row: longEdge1_lane1, longEdge2_lane2, longEdge3_lane1. Middle row: longEdge1_lane0, longEdge2_lane1, longEdge3_lane0. Bottom row: longEdge2_lane0. An on-ramp is shown merging into the highway. An acceleration lane of 500m is indicated between jun4 and jun5.</p>		
Road segments		

jun1 → jun2: Insertion and backlog area (100 m, 2 lanes)
 jun2 → jun4: mainline motorway (500 m, 2 lanes)
 jun3 → jun4: on-ramp (500 m, 1 lane)
 jun4 → jun5: mainline motorway with acceleration lane (500 m, 3 lanes)
 jun5 → jun6: mainline motorway (300 m, 2 lanes)
 jun6 → jun7: exit (100 m, 2 lanes)

In Section 3.2 we introduced an updated actors' definition, in which three classes of actors (vehicle types) are proposed: manual driving, partial automation, and conditional automation. In the baseline simulation, actors are interpreted into three types of artificial vehicles: LVs, CVs, and CAVs. LVs are modelled to perform motorway merging as human driven vehicles in the real world. On the contrary, CAVs and CVs might request ToCs or consequently execute MRMs at TAs.

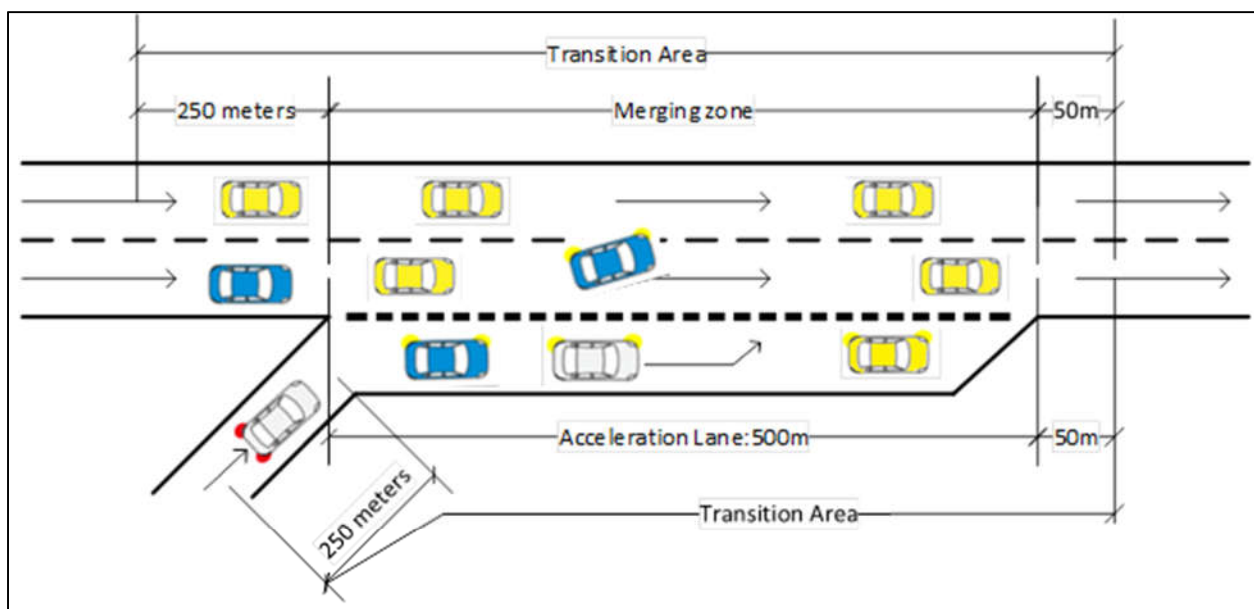


Figure 29. Merging zone schematic of UC2_1 network.

The merging zone is 500 m in length and is composed of one acceleration lane (right-most lane) and two mainline motorway lanes (**Figure 29**). At the end of the merging zone, a merging bottleneck is formed due to the lane drop. In the merging zone, mandatory lane changes (from the acceleration lane to main motorway lanes) frequently take place, which lead to downwards ToCs of CAVs and CVs upstream of the merging zone. In the baseline simulation experiments, a take-over request is issued 250 m (both in main motorway and on-ramp lanes) upstream of the merging zone.

As introduced in the timeline of a downward transition in **Figure 13**, if the driver response time exceeds the available lead time ($timeTillMRM$ in the simulation), the requested ToC fails and the execution of MRM begins, which is performed as a constant deceleration of 3 m/s^2 on the ego-lane for CAVs and CVs in baseline simulation. The duration of MRMs is explained in Section 2.3.2.

4.2.2 Results

4.2.2.1 Impacts on Traffic Efficiency

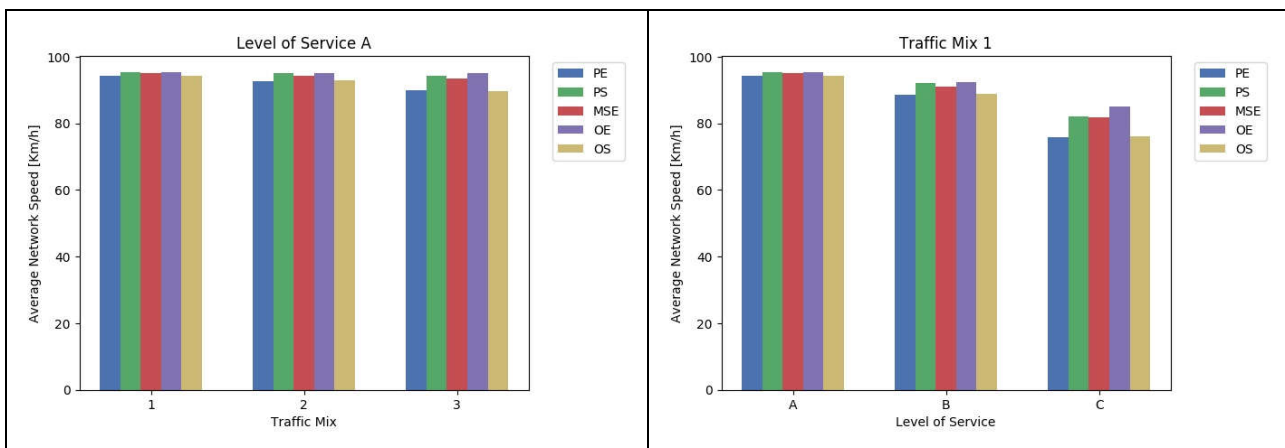
Network-wide impacts

The average network speed is presented in the form of bar charts for three LOSs and three traffic mixes (six plots in **Figure 30**). The left three plots depict average network speed for traffic mix 1, 2 and 3, under LOS A, B and C; the right plots depict average network speed for LOS A, B and C, under traffic mix 1, 2 and 3. For each plot, average network speed is shown for each of the five parametrisation schemes: PE, PS, MSE, OE, and OS.

Starting from the upper left plot, we observe that parametrisation schemes PS and OE exhibit the highest average network speed, followed by the MSE scheme, and finally by the PE and OS schemes. As traffic intensity increases (from LOS A to C in the left plots), the average network speed decreases for all five schemes. For higher traffic intensity, the differences between five schemes are more significant. The highest decrease in average network speed (approximately 47%) occurs for schemes PE and OS for traffic mix 3, from LOS B to LOS C.

The above trend is normal and can be explained by the fundamental diagram of traffic flow theory. Increasing traffic flow prior to the point of critical density (capacity drop point) causes speeds to drop slightly, which is the case for the transition from LOS A to LOS B; when the critical density of the network is reached, increasing traffic flow incurs significant speed drop. This is the case for schemes PE and OS for the transition from LOS B to LOS C under mix 3 that encompasses the highest CAVs/CVs penetration rate, where high ToC and MRM occurrences are causing more variation in speed and flow perturbation.

Schemes PS and OE exhibit the best performance in terms of average network speed and this can be explained given the driver model parameter attributes per parametrisation scheme in **Tables 19, 20, and 21**. For scheme PS, the desired time headways for car-following and desired longitudinal gaps for lane-changing are short, which results in increased traffic efficiency. Additionally, the driver response time to ToC is also short for scheme OE, which further contributes to increased traffic efficiency.



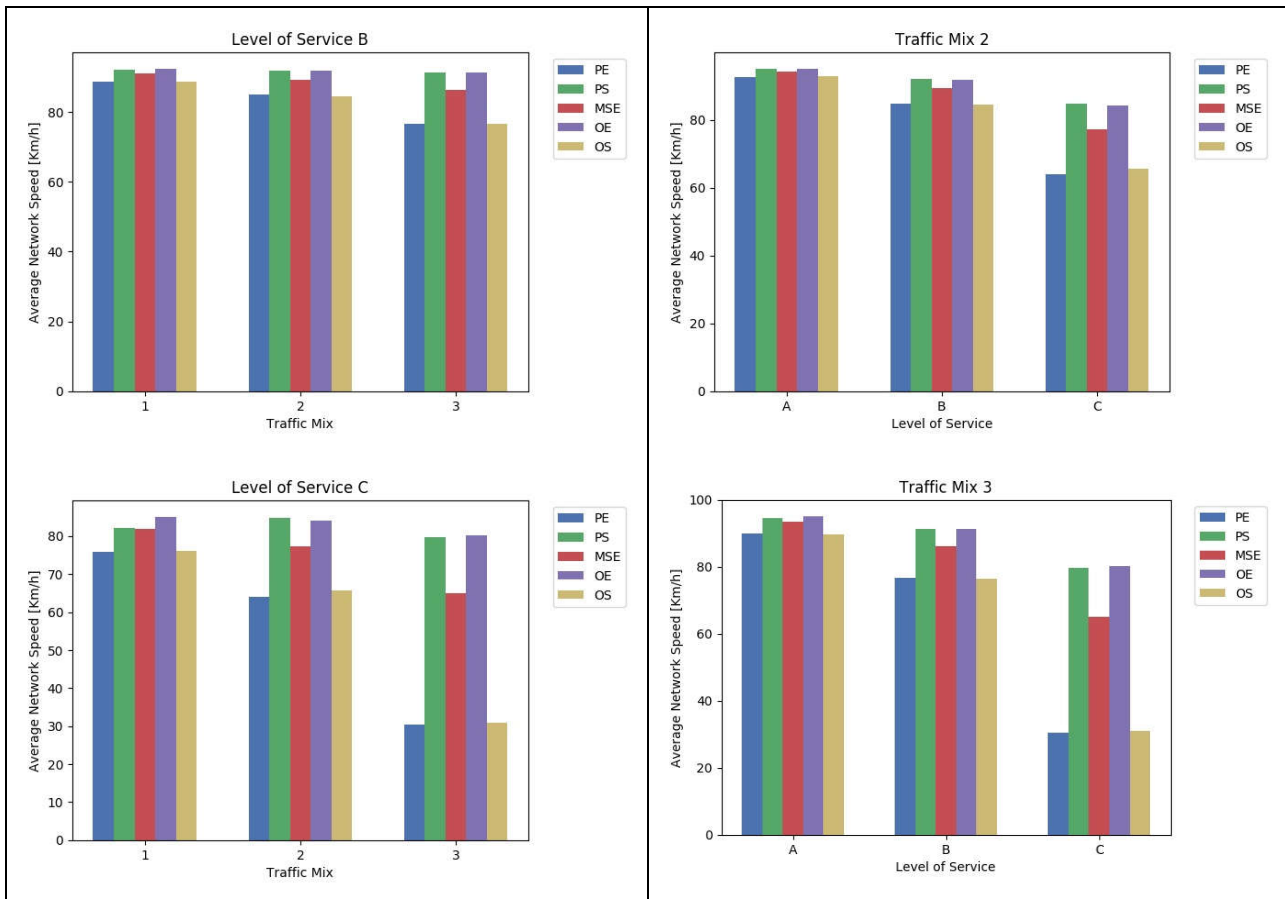
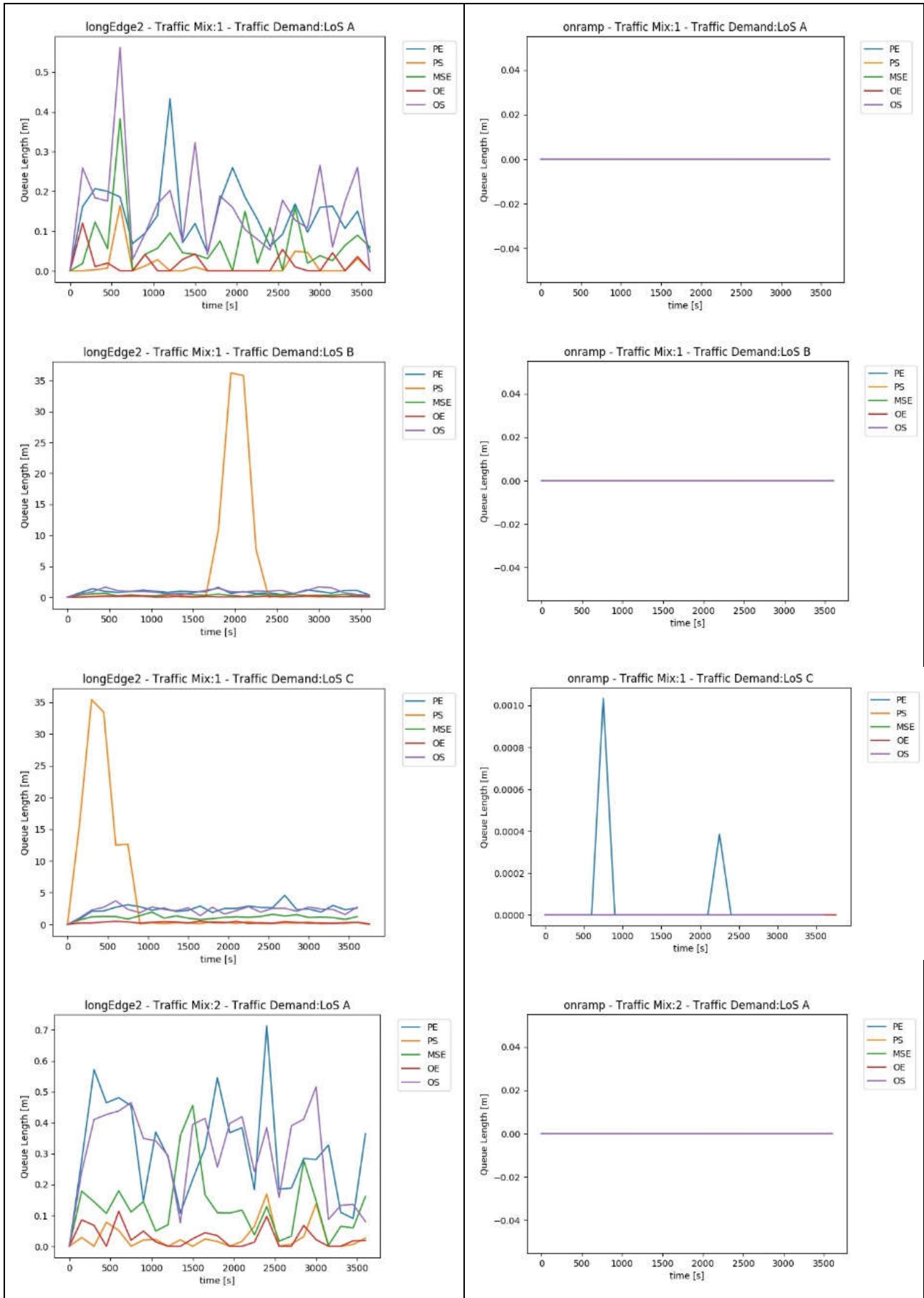


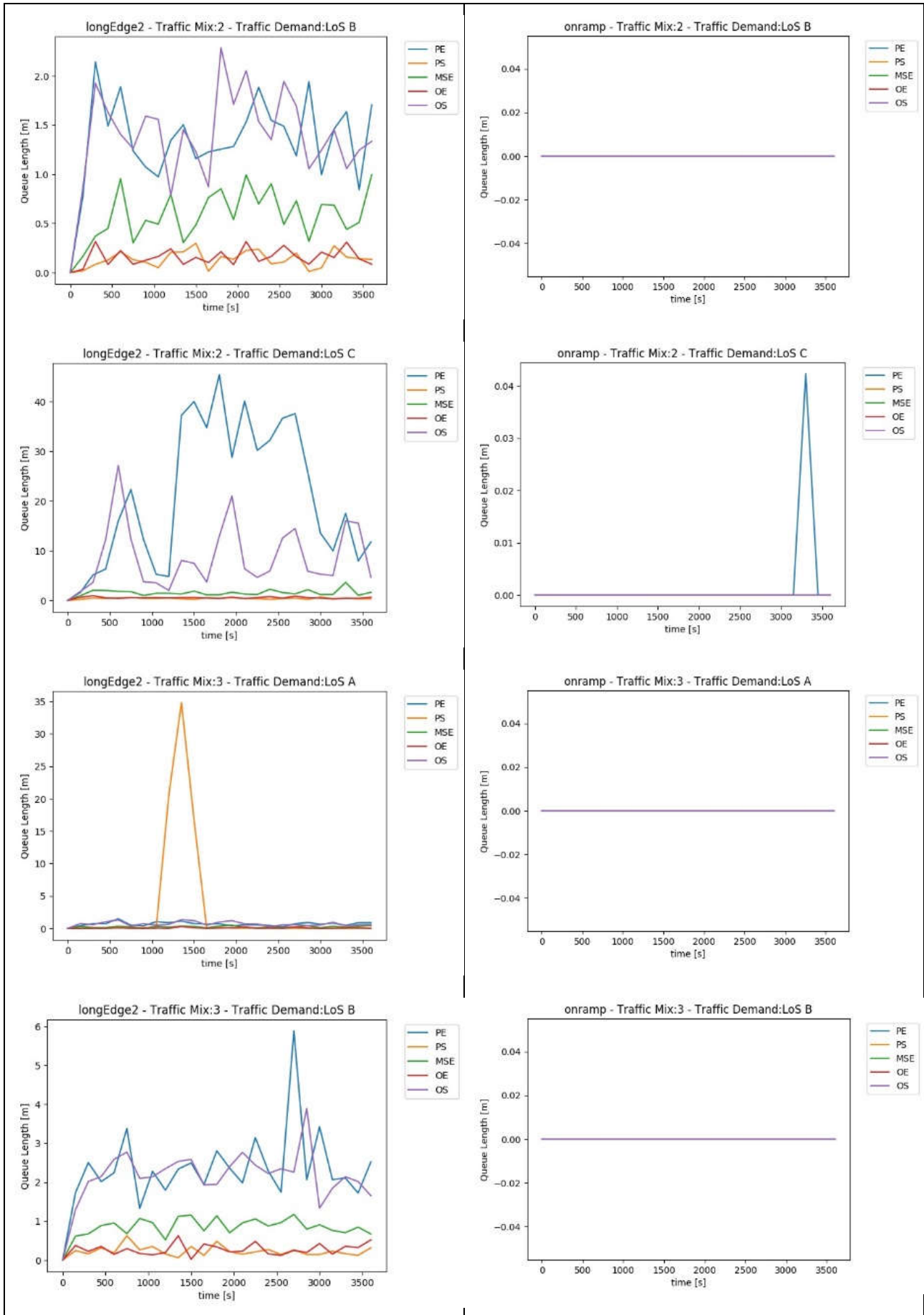
Figure 30. Average network speed for Scenario 2.1 baseline simulation experiments (varying parameter scheme, LOS, and traffic mix). Different bar colours correspond to different parameter schemes. The left column groups results by LOS, the right column by traffic mix.

The right three plots show that the average network speed decreases generally for schemes PE and OS when the CAVs/CVs penetration in traffic mix increases, but not in the cases for schemes PS and OE. For scheme PE, it is self-explanatory because all five attributes in this set are not optimal. It is interesting to point out that scheme OS is equally underperforming as PE. They shared the same attributes regarding desired time headway and desired longitudinal gaps. It can also be observed (**Figure 33**) that the total number of lane changes does not increase with higher CAVs/CVs penetration rates. Therefore, a preliminary conclusion is that large desired time headway and longitudinal gaps of CAVs/CVs affect average network speed adversely.

Local impacts

To investigate the local impacts on traffic efficiency, the queue length of the merging zone edge and the on-ramp edge, as well as the space-mean speed of the merging zone edge, are presented in **Figure 31** and **Figure 32**.





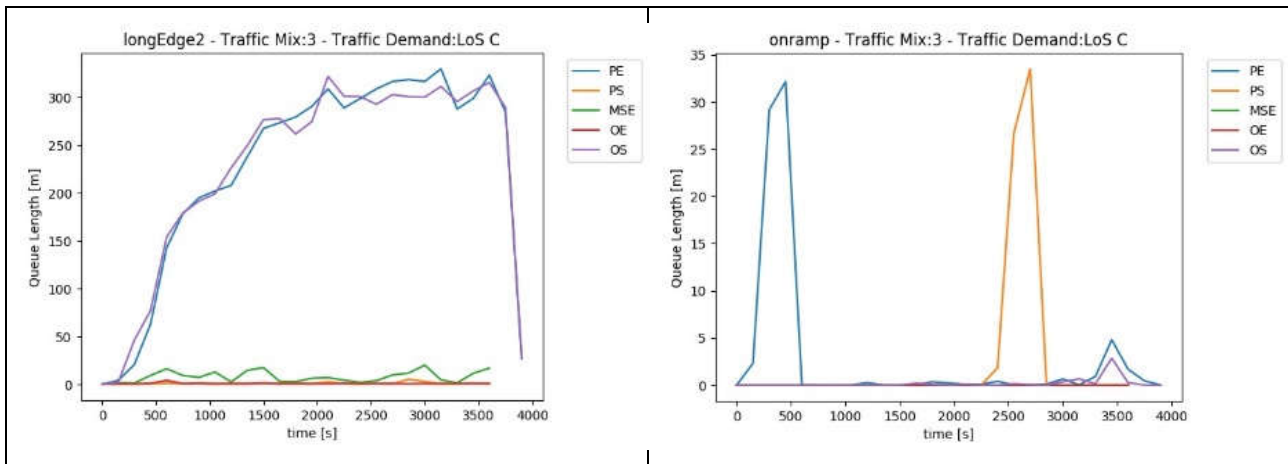


Figure 31. Queue lengths on longEdge2 and on-ramp for Scenario 2.1 baseline simulation experiments.

The left nine plots (**Figure 31**) show the queue length on longEdge2 (see the network schematic of **Table 24** for position reference), under three LOSs and then over three traffic mixes. For each traffic mix, the queue length increases with increasing traffic demand as expected. A few spikes of approximate 35 m queue can be spotted on all LOSs, which could be caused by the following reasons:

1. Several continuous unsuccessful merging cases that lead to vehicles stuck at the end of acceleration lane. This will result in high-risk merging situation that induces a spillback queue upstream to the beginning of the edge in general.
2. Some vehicles are still in the process of MRM (ToC begins on halfway on-ramp) in the beginning of acceleration lane; or some vehicles are in recovery after MRM. Both situations have negative effect (slow speed, large speed deviation) on traffic efficiency regarding queue length.

We also observe that, for schemes PE and OS, noticeable long queues were formed gradually on the merging zone under traffic mix 3 and LOS C, which is again due to the “non-optimal” driver model attributes of large desired time headways for car-following and large desired longitudinal gaps for lane-changing. Meanwhile, the queue length on the on-ramp is mostly stable with a few small spikes (under traffic mix 3 and traffic demand LOS C) that could be caused by vehicles that performed ToCs and consequently longer than normal MRMs, which in turn could result in queue to the beginning of the on-ramp.

The average space-mean speed of longEdge2 is shown in **Figure 32**, under three traffic mixes and three LOSs. As the LOS increases, the average speed decreases, especially for schemes PE and OS which show a higher decrease in average speed. This result corresponds to the inefficiency of these two schemes regarding their driver model attributes.

Looking at the nine plots horizontally and vertically, on the one hand, the five schemes are more “spread-out” in speed range when LOS or CAVs/CVs penetration rate increases. On the other hand, the negative effect of “non-optimal” schemes PE and OS are showing the same patterns and they are more pronounced under worsened traffic conditions, such as higher traffic intensity or higher ToCs and MRM events, which is generated by higher CAVs/CVs penetration rate. The phenomenon agree with the preliminary conclusions on traffic efficiency, traffic dynamic, and environmental impacts.

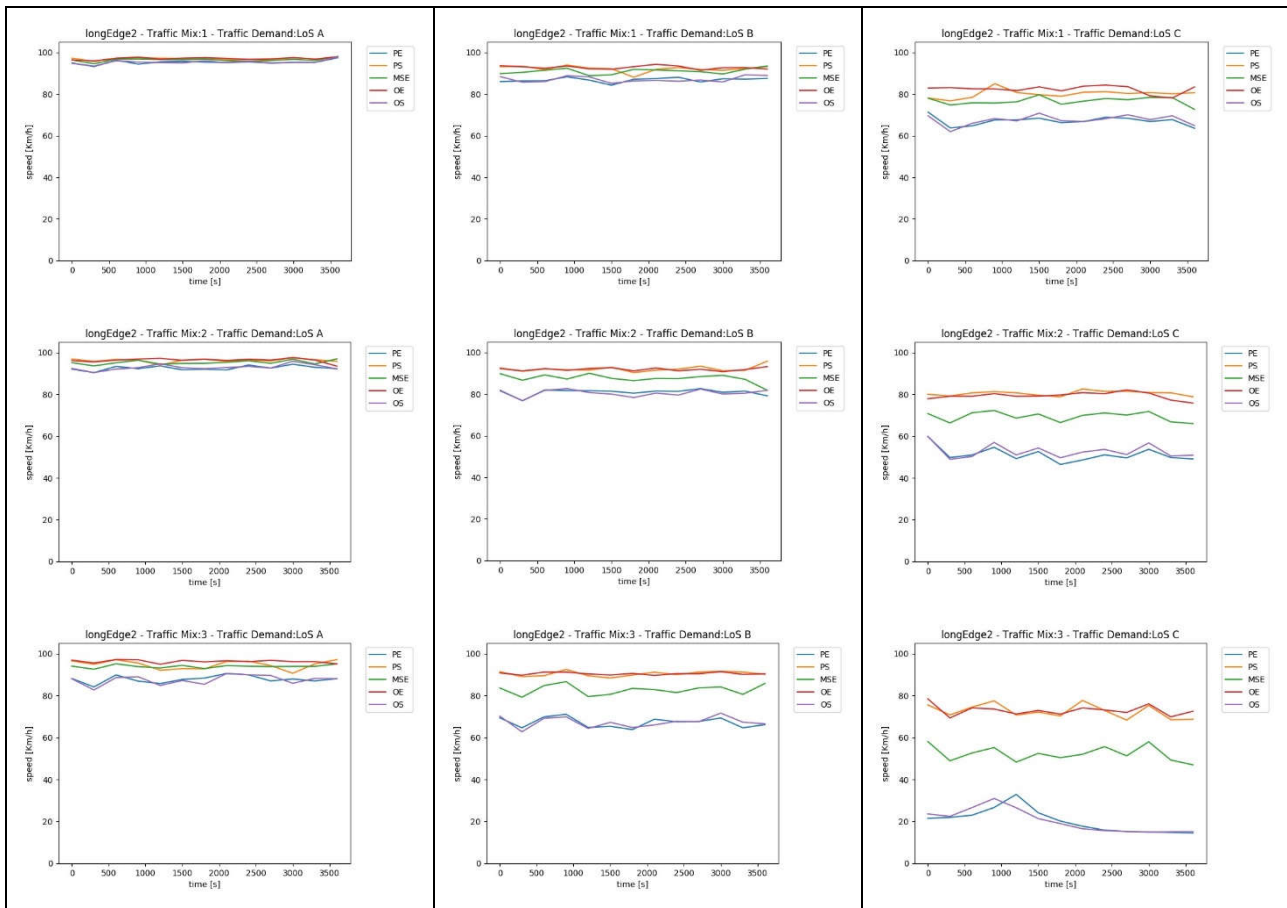


Figure 32. Average speed on longEdge2 for Scenario 2.1 baseline simulation experiments.

4.2.2.2 Impacts on Traffic Dynamics

The total number of lane changes is reported to show the disruption caused in the traffic flow by lane change manoeuvres per traffic composition, in which different vehicle types embody different driver behaviours. Results are depicted in **Figure 33** below.

The left three plots indicate that the total number of lane changes for all five schemes generally increase at the same rate as traffic intensity. Thus, the increased rates of traffic intensity did not affect lane changes of mixed traffic significantly under baseline scenario. The right plots show that the total number of lane changes decrease for all five schemes when the penetration rate of CAVs/CVs increases due to relatively higher accepted lane change gaps for CAVs/CVs.

The seemingly more “optimal” scheme OE in terms of traffic efficiency exhibits the lowest total number of lane changes, while less “optimal” schemes PE, OS show a higher total number of lane changes.

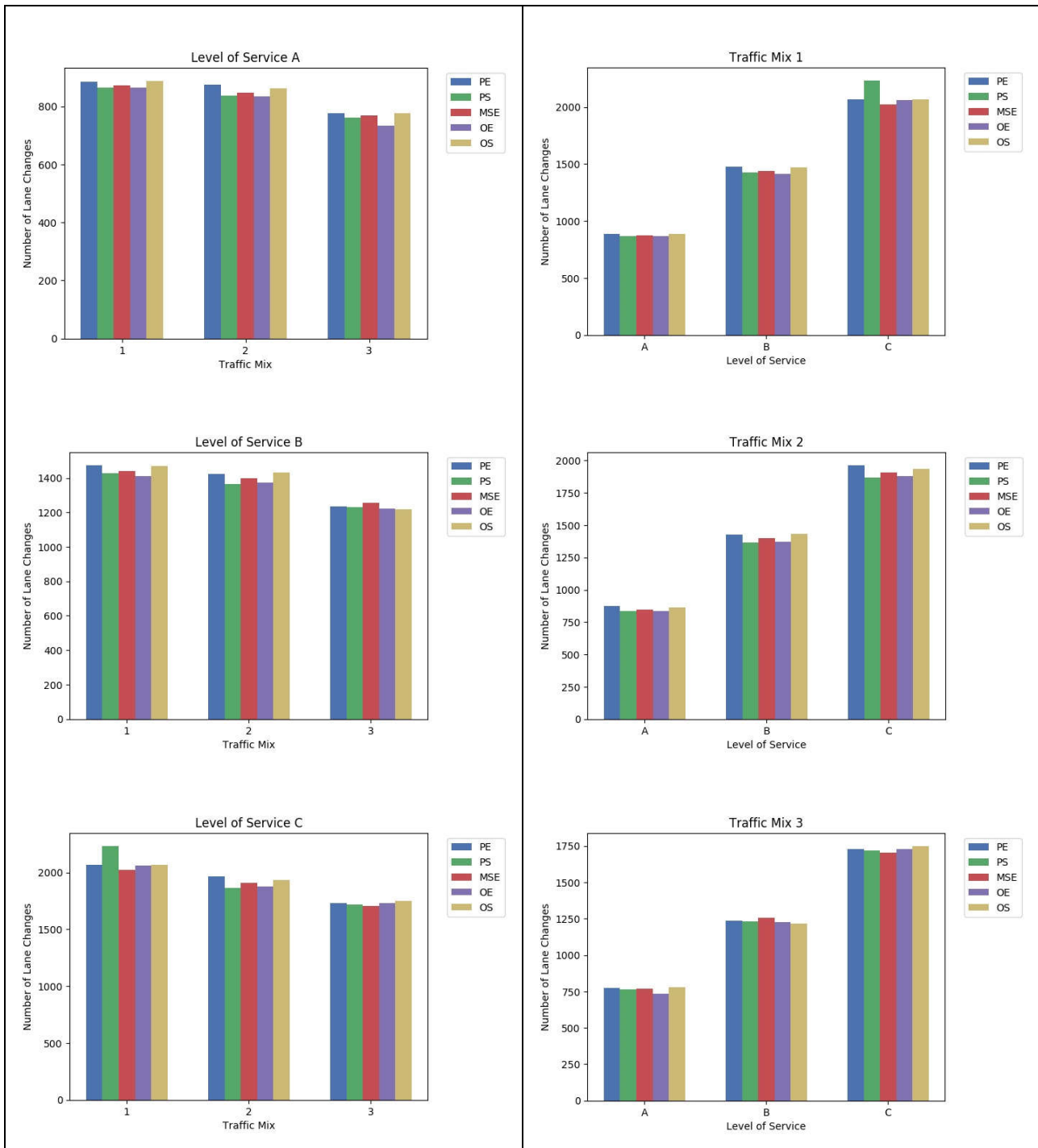


Figure 33. Number of lane changes for Scenario 2.1 baseline simulation experiments (varying parameter scheme, LOS, and traffic mix). Different bar colours correspond to different parameter schemes. The left column groups results by LOS, the right column by traffic mix.

4.2.2.3 Impacts on Traffic Safety

As explained in Section 3.7, time-to-collision (TTC) measures a longitudinal margin to lead vehicles or objects, and is a proxy for traffic safety. **Figure 34** includes six plots that depict the number of conflicts corresponding to $TTC < 3.0$ s (threshold value indicating safety critical events) for the different LOSs, traffic mixes, and parametrisation schemes.

The left three plots show number of conflicts per scheme as LOS increases. Schemes PE and OS yield most of the safety critical events. Looking at the driver model parameter attributes of these two schemes in **Table 17**, it appears that both of them correspond to large desired time headways for car-following and large desired longitudinal gaps for lane-changing, thus inducing more conflicts at the lane drop location.

The right three plots also show a mixed behaviour among different traffic mixes. It seems that conflicts for all five schemes increase from traffic mix 1 to 3, where CAVs/CVs penetration increases from 30% to 50%, and finally to 80% . We also observe that conflicts for all five schemes (with a few exceptions) increase when traffic intensity increases, under the same traffic mix.

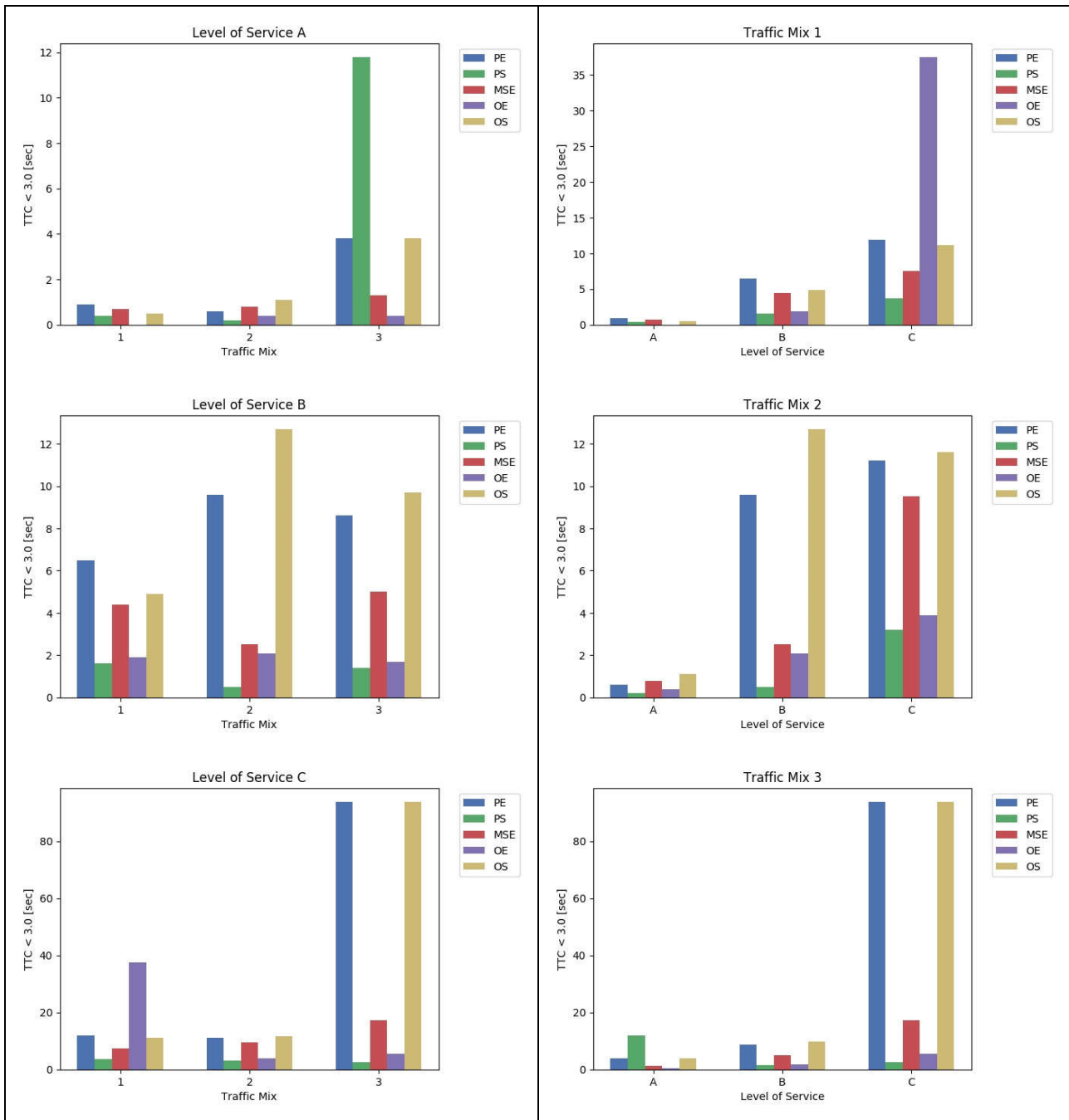


Figure 34. Number of conflicts ($TTC < 3$ s) for Scenario 2.1 baseline simulation experiments (varying parameter scheme, LOS, and traffic mix). Different bar colours correspond to different parameter schemes. The left column groups results by LOS, the right column by traffic mix.

4.2.2.4 Environmental Impacts

The total CO₂ emissions for all vehicle types are shown in the six plots of **Figure 35**. The left three plots indicate that the total CO₂ emissions for all five schemes increase when the LOS increases. The increase rate for all schemes is comparable to the increase rate of traffic demand, except for schemes PE and OS under traffic mix 3 and LOS C. For these two schemes, the total CO₂ emissions values are almost one and a half times the values under LOS B. This result complies with average network speed for the same schemes, traffic mix, and LOS. These two schemes are less optimal in terms of traffic efficiency, thus causing stop and go traffic, where the CO₂ emissions increase significantly.

The right three plots show that under the same traffic intensity, the CO₂ emissions of all five schemes slightly increase when the traffic mix changes from 1 to 3. This is rather emphasised for schemes PE and OS under higher traffic intensity (LOS C). It can be explained by the higher number of ToC and MRM occurring in the merging area, which generate more changes in speed, and in return, increased CO₂ emissions.

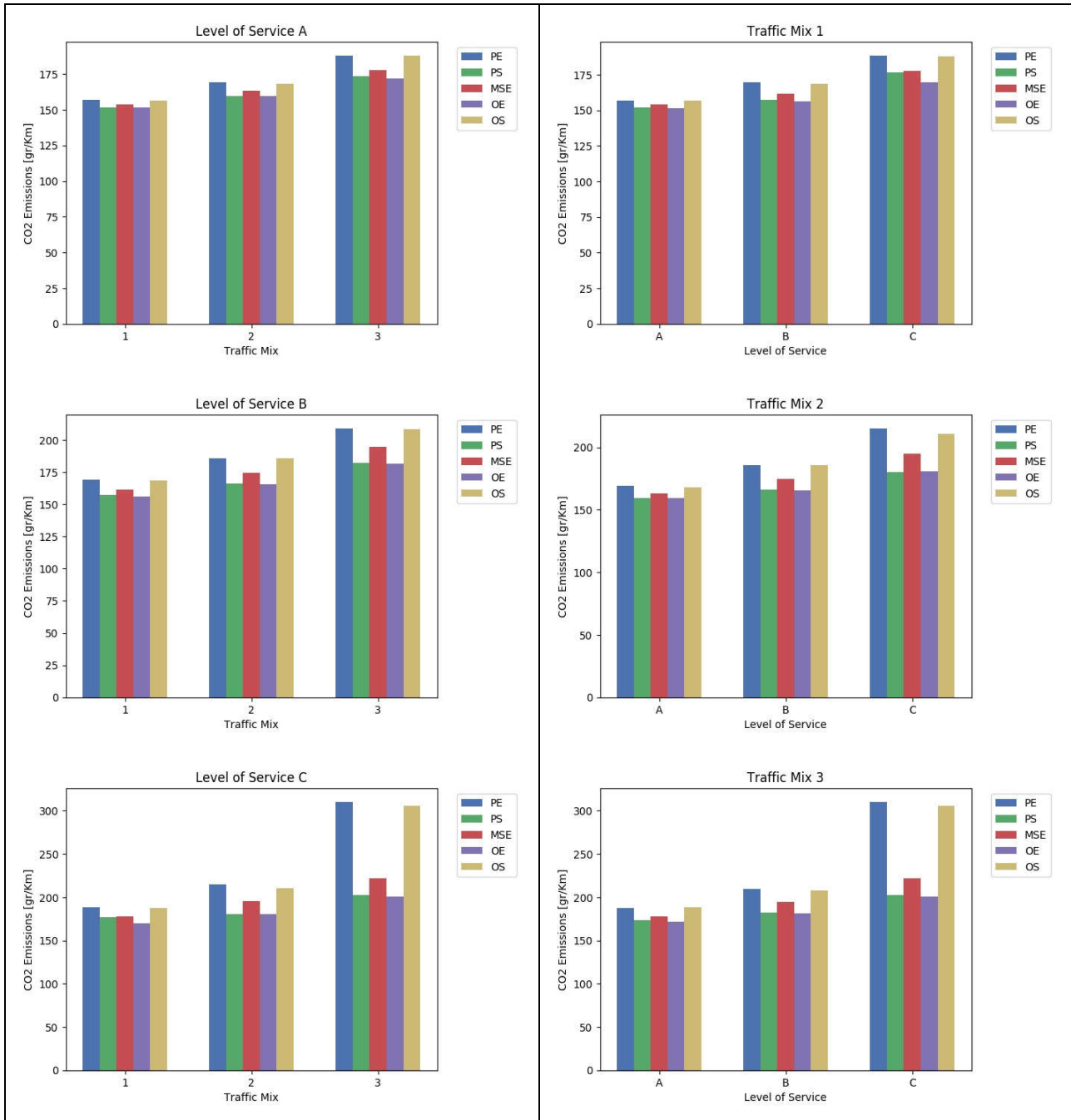


Figure 35. Total CO₂ emissions for Scenario 2.1 baseline simulation experiments (varying parameter scheme, LOS, and traffic mix). Different bar colours correspond to different parameter schemes. The left column groups results by LOS, the right column by traffic mix.

4.3 Scenario 3.1 Apply traffic separation before motorway merging/diverging

4.3.1 Scenario Description

In Scenario 3.1 (C)AVs, CVs and LVs drive along two two-lane motorways merging into a four-lane motorway (**Figure 36**). RSI monitors traffic composition upstream of the merge area through collective perception but also via Cooperative Awareness Message (CAM) receptions, and infrared sensors.

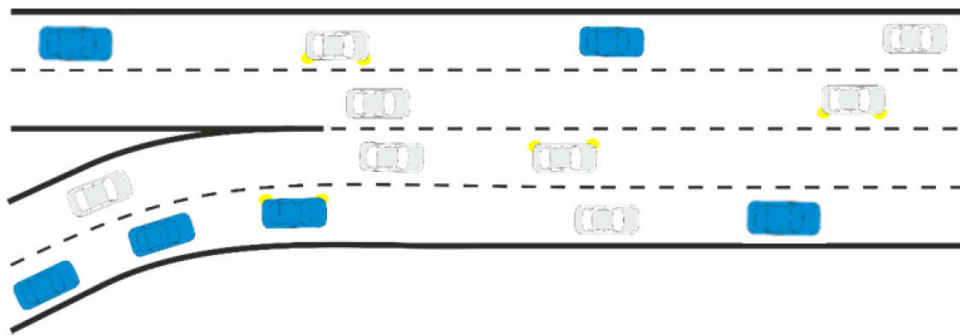


Figure 36. Schematic overview of Scenario 3.1.

(C)AVs/CVs move to the left lane on the left two-lane motorway and to the right on the right two-lane motorway at some point upstream of the merging area according to the selected traffic separation policy. LVs move to the other lanes not allocated to (C)AVs/CVs. Thus, (C)AVs/CVs enter the four-lane section on the outer lanes, giving space to manually driven vehicles (LVs) to occupy the central lanes (in many of these situations human driving still may generate risky and dangerous traffic conditions).

The proposed traffic separation policy is expected to significantly mitigate the total number of risky situations occurring in the merge area, thus resulting in lesser ToCs issued in this area. At some point downstream of the merging area, traffic separation is disabled, and all vehicles can gradually start changing lanes to reach their target destination.

More details about the simulation network of Scenario 3.1 can be found in **Table 25**

Table 25. Network configuration details for Scenario 3.1.

Scenario 3.1	Settings	Notes
Road section length	2.3 km	• for each motorway
Road priority	9	
Allowed road speed	36.11 m/s	130 km/h
Number of nodes	5	• n0 – n5
Number of edges	4	
Number of start nodes	2	• n0, n4
Number of end nodes	1	• n3
Number of O-D relations	2	• From n0 to n3 • From n4 to n3
Number of lanes upstream of the merging area	2	
Number of lanes upstream	4	• from n1 to n2

of the merging area		
Merging area length	1.3 km	
Filename	• network: UC3_1.net.xml	
Intended control of lane usage		
<p>There is no control on lane usage. In the sub-scenario 1, Based on the RSI provided traffic separation policy, CAVs and CAV Platoons move to the left lane of the left 2-lane motorway and to the right on the right 2-lane motorway some point upstream of the merging point. CVs move to other lanes than the CAVs and CAV Platoons. CAVs and CAV Platoons thus enter the 4-lane section on the outer lanes, giving space to other vehicle types to merge.</p>		
Network layout		
<p>The diagram shows a network layout on a green background. It features five nodes: n0, n1, n2, n3, and n4. Node n4 is at the bottom left, with two orange lines labeled 'start_south' and 'start_north' leading to node n1. From node n1, a horizontal line goes to node n2, labeled 'merge_area'. From node n2, another horizontal line goes to node n3, labeled 'leave_area'. A scale bar in the bottom left corner indicates 0 to 100m.</p>		
Road segments		
<p>n0→n1: Insertion and backlog area (500 m) n4→n1: Insertion and backlog area (500 m) n1→n2: Merging area (1300 m) n2→n3: Leaving area (500 m)</p>		

4.3.2 Results

4.3.2.1 Impacts on Traffic Efficiency

Network-wide Impacts

Figure 37 depicts the average network speed for all baseline simulation experiments of Scenario 4.2 (urban network) encompassing the different demand levels, traffic mixes, and parametrisation schemes. The two columns present the same data in a different format to facilitate the visual assessment with respect to the different traffic mixes (left column), and the different traffic demand levels (right column).

All plots indicate that traffic conditions are uncongested irrespective of the demand level, traffic mix, and parametrisation scheme. This implies that no major breakdown occurs at the merge area of the two motorways. Increasing penetration rate of CAVs/CVs does not affect traffic efficiency for LOS A. On the contrary, average network speed is slightly reduced when CAVs/CVs increase for LOS B due to the higher number of vehicles executing ToCs (and possibly MRM) upstream and along the merge area. An interesting finding is that the latter trend is reversed for LOS C. In this case, it seems that denser traffic urges LVs to make more tactical lane changes for speed gain reasons thus inducing turbulence to the traffic flow. Results suggest that the effect of lane-changing on average network speed is more significant compared to that of ToC/MRM.

Plots in the right column show that average network speed decreases with increasing demand. We observe that the latter speed reduction is more significant for parametrisation schemes PE and OS, where driving behaviour was assumed to be more conservative.

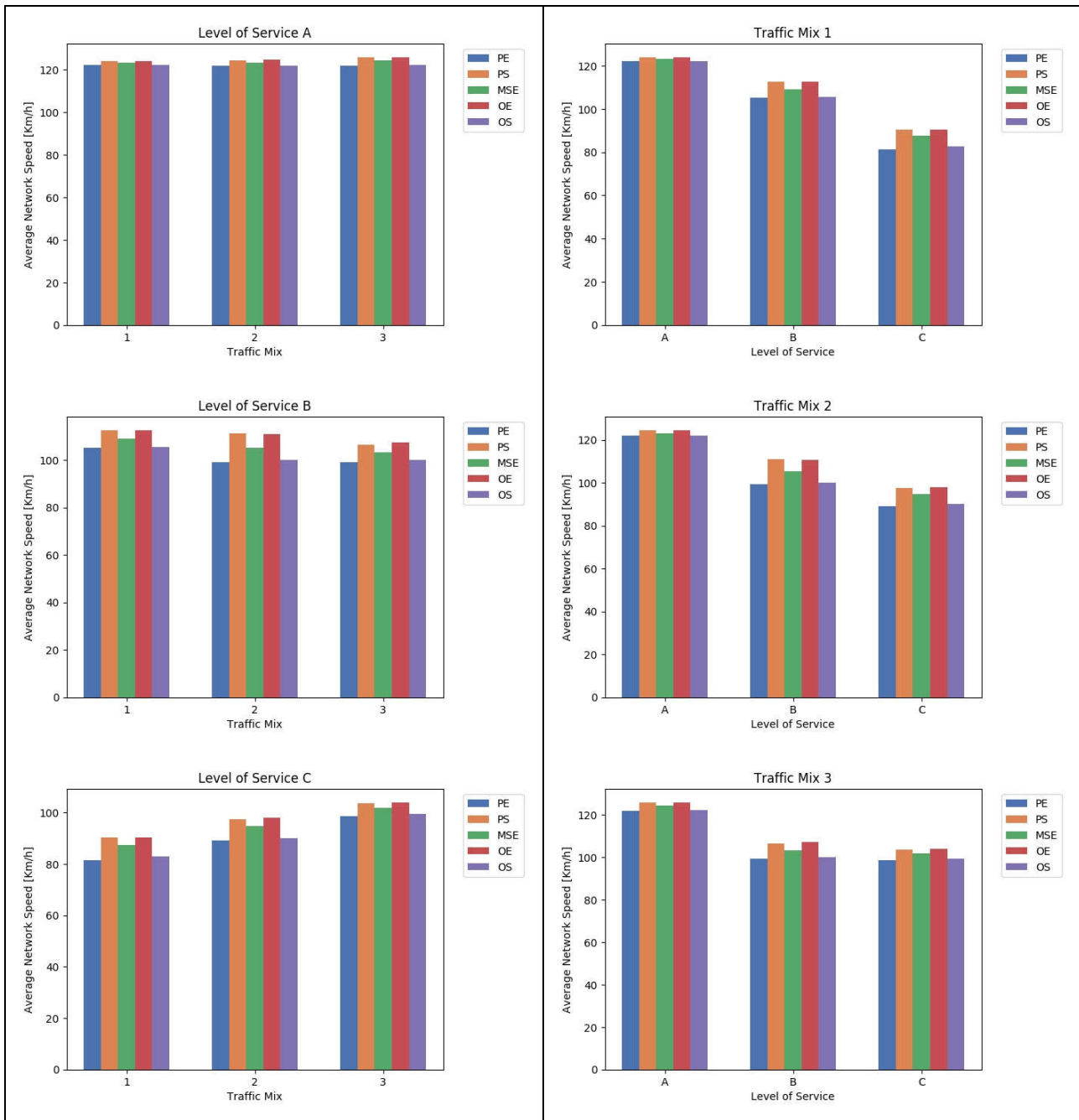


Figure 37. Average network speed for Scenario 3.1 baseline simulation experiments (varying parameter scheme, LOS, and traffic mix). Different bar colours correspond to different parameter schemes.

Local Impacts

Figure 38 shows the average speed (taken over five minutes) on the edge ‘start_north’, which is located just upstream of the merging area (see network schematic in **Table 25**). The left-most column indicates that free flow traffic operations prevail on the edge for any traffic mix and LOS A. Space-mean speed is reduced for parametrisation schemes PE and OS for higher share of CAVs/CVs (traffic mix 3) due to their conservative behaviour in terms of car-following and lane-changing. When demand increases (LOS B in middle column), the distinct effects of parametrisation schemes become clear in the presence of more dense traffic. Finally, as traffic

density further increases these distinct effects fade out for LOS C, and average edge speed slightly fluctuates around 65 km/h.

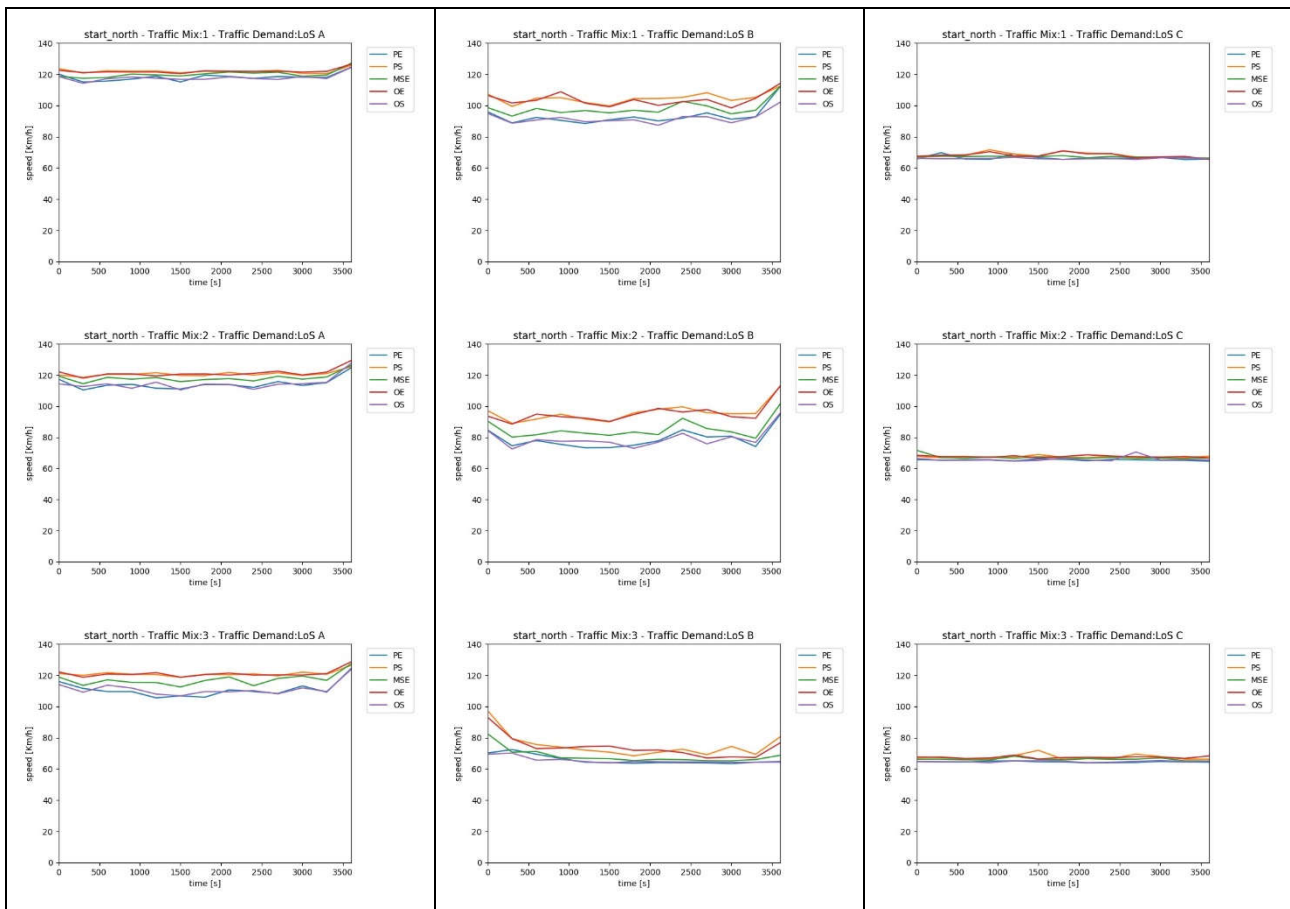
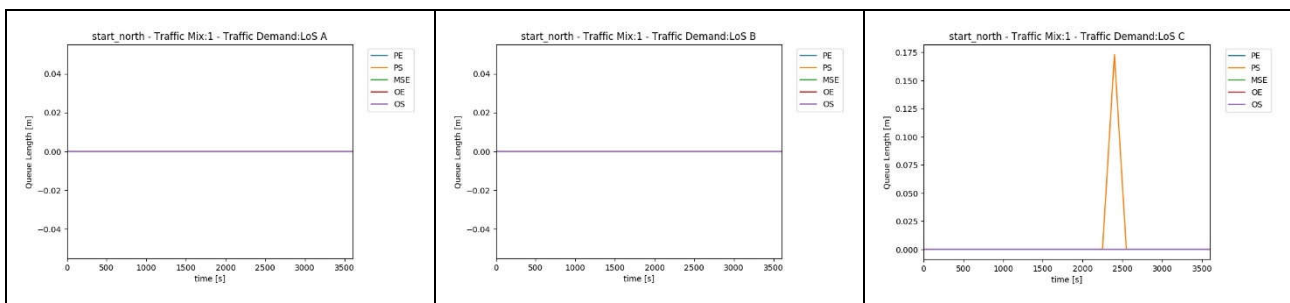


Figure 38. Average speed at the edge ‘start_north’ for the different parameter sets. First row: varying LOS at traffic mix 1; second row: varying LOS at traffic mix 2; third row: varying LOS at traffic mix 3.

Figure 39 shows the average queue lengths (during the last 150 seconds) building up on the edge ‘start_north’ during the simulation. The queue length is defined as the back position of the last vehicle on the edge, which is slower than 5 km/h.

It can be observed that traffic operations remain uncongested along the edge irrespective of the traffic mix, demand level, and parametrisations scheme, since no queue spillback is formed on the edge.



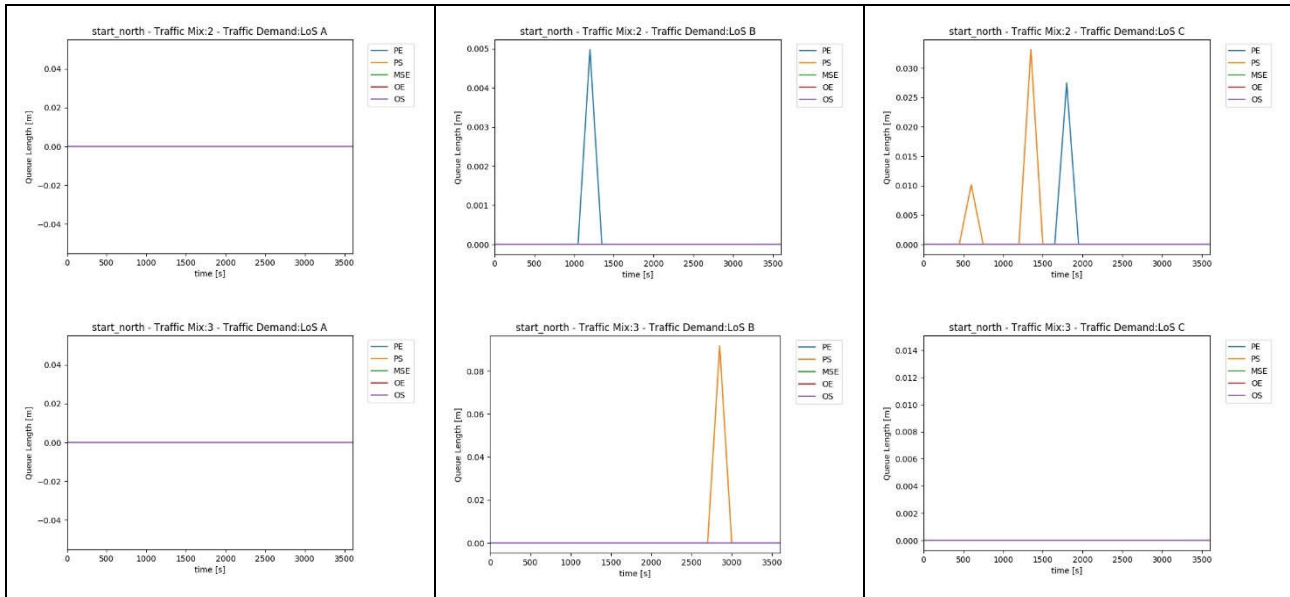
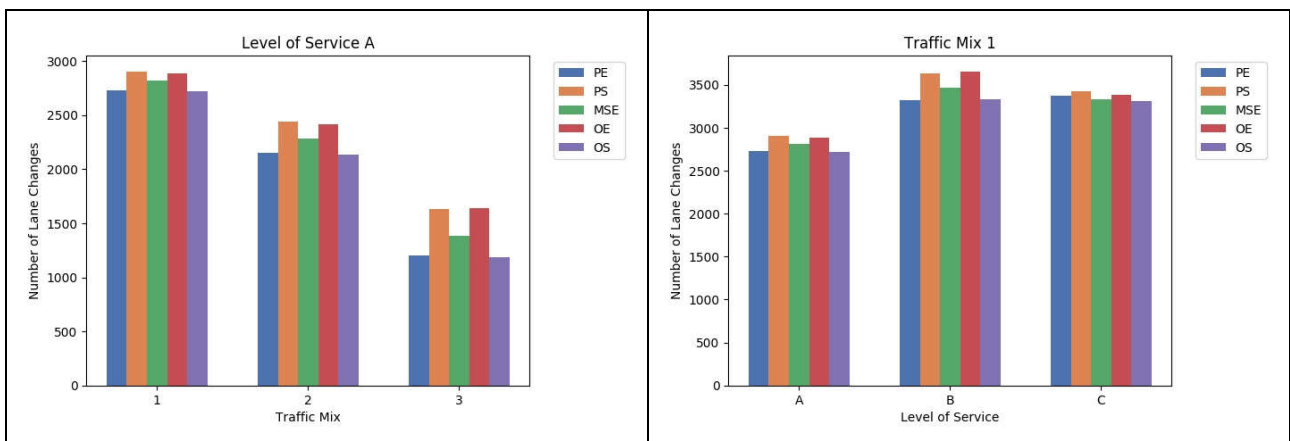


Figure 39. Average queue length at the edge ‘approach_2’ for the different parameter sets. First row: varying LOS at traffic mix 1; second row: varying LOS at traffic mix 2; third row: varying LOS at traffic mix 3.

4.3.2.2 Impacts on Traffic Dynamics

Figure 40 shows the total number of lane changes per simulated scenario. Lane change intensity decreases for higher shares of CAVs/CVs. This is expected since the *lcAssertive* parameter (i.e. the willingness to accept lower front and rear gaps on the target lane) is in general higher for LVs compared to CAVs/CVs. The latter effect is more pronounced for parametrisation schemes PE and OS, where CAVs/CVs exhibit the most conservative behaviour in terms of lane-changing. Additionally, it is shown that the total number of lane changes increases with increasing demand. However, it is noteworthy that for Scenario 3.1, less than 1 lane change per vehicle correspond to each simulated scenario. Thus limited turbulence is induced to the traffic due to lane changing, since several vehicles can follow their desired routes without changing lanes.



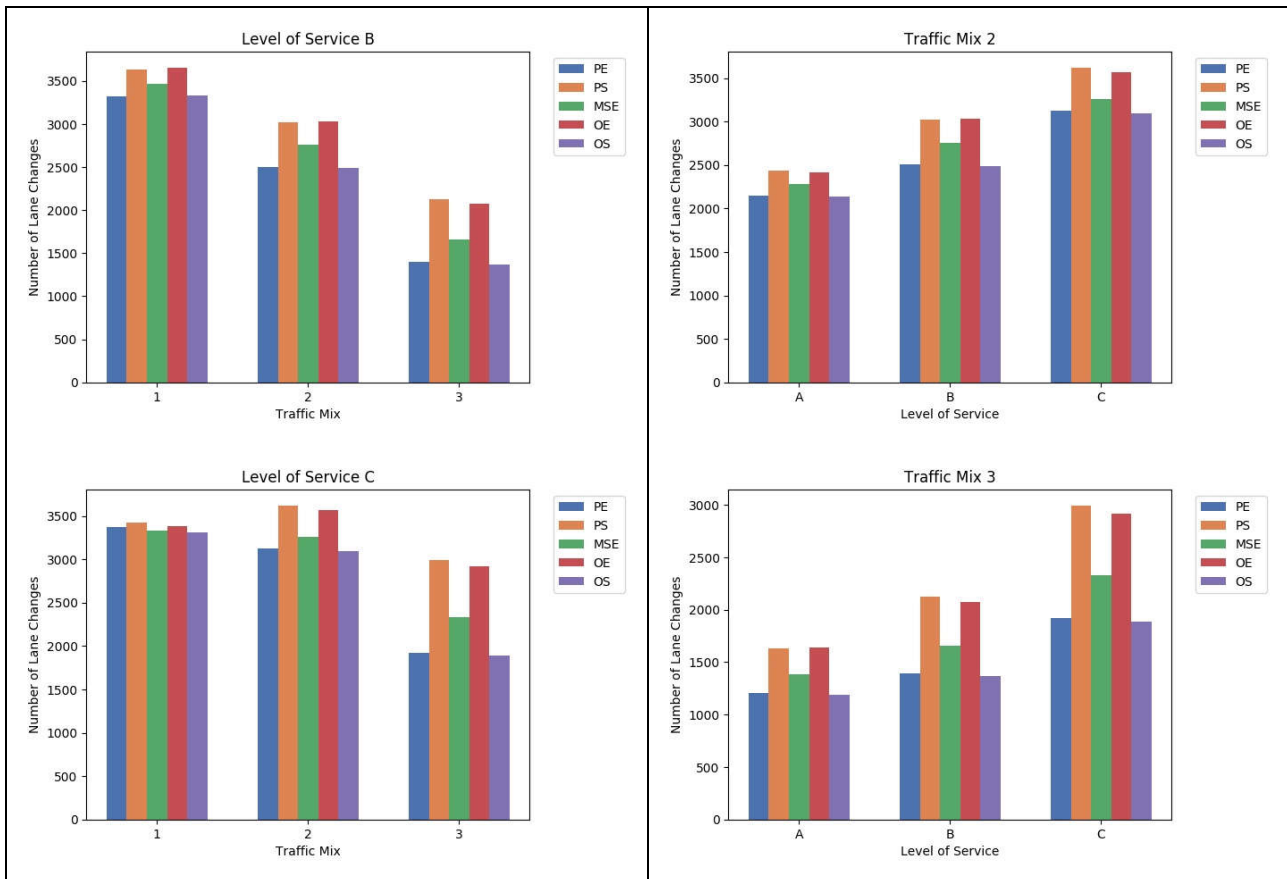


Figure 40. Number of lane changes for Scenario 3.1 baseline simulation experiments (varying parameter scheme, LOS, and traffic mix). Different bar colours correspond to different parameter schemes. The left column groups results by LOS, the right column by traffic mix.

4.3.2.3 Impacts on Traffic Safety

Figure 41 presents the average number of events with $TTC < 3.0$ s (termed ‘critical’ below). It is evident that almost no conflicts take place per simulated scenario. Simulation scenarios corresponding to LOS A exhibit no safety critical events (plots not included for this reason). Similar conditions can be observed for other cases (traffic mix 2 and 3 for LOS B, traffic mix 3 for LOS C). The very few existing events with $TTC < 3.0$ s correspond to parametrisation scheme PE, where reduced driver performance during ToC generates rear-end conflicts with following vehicles.

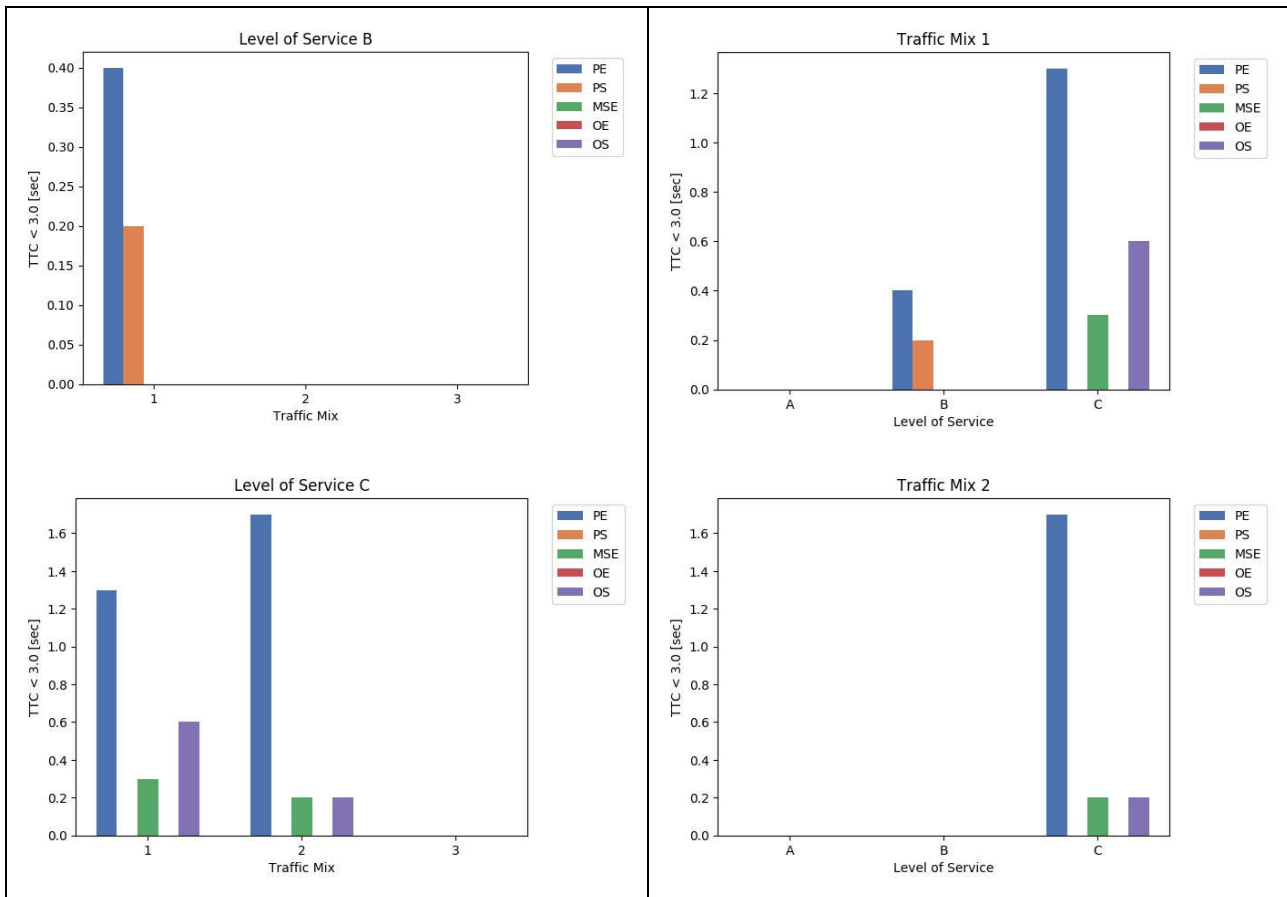


Figure 41. Average number of events with TTCs below 3.0 seconds for Scenario 3.1 baseline simulation experiments (varying parameter scheme, LOS, and traffic mix). Different bar colours correspond to different parameter schemes. The left column groups results by LOS, the right column by traffic mix.

4.3.2.4 Environmental Impacts

Figure 42 depicts average CO₂ emissions per kilometre travelled. It can be seen that CO₂/km increases with increasing demand (plots in the right column). However, it was shown in Section 4.3.2.1 that as demand increases average network speed decreases from 120 km/h (LOS A) to approximately 85 km/h (LOS C). For steady-state traffic flow (in the uncongested traffic flow regime) it would be expected that CO₂ emissions per kilometre travelled would decrease for the aforementioned speed drop. Thus, the observed increase of the emissions levels can be only explained by the disturbance introduced in the traffic stream by MRMs. This disturbance is increasing with increasing penetration rate of CAVs/CVs, thus yielding higher emissions levels.

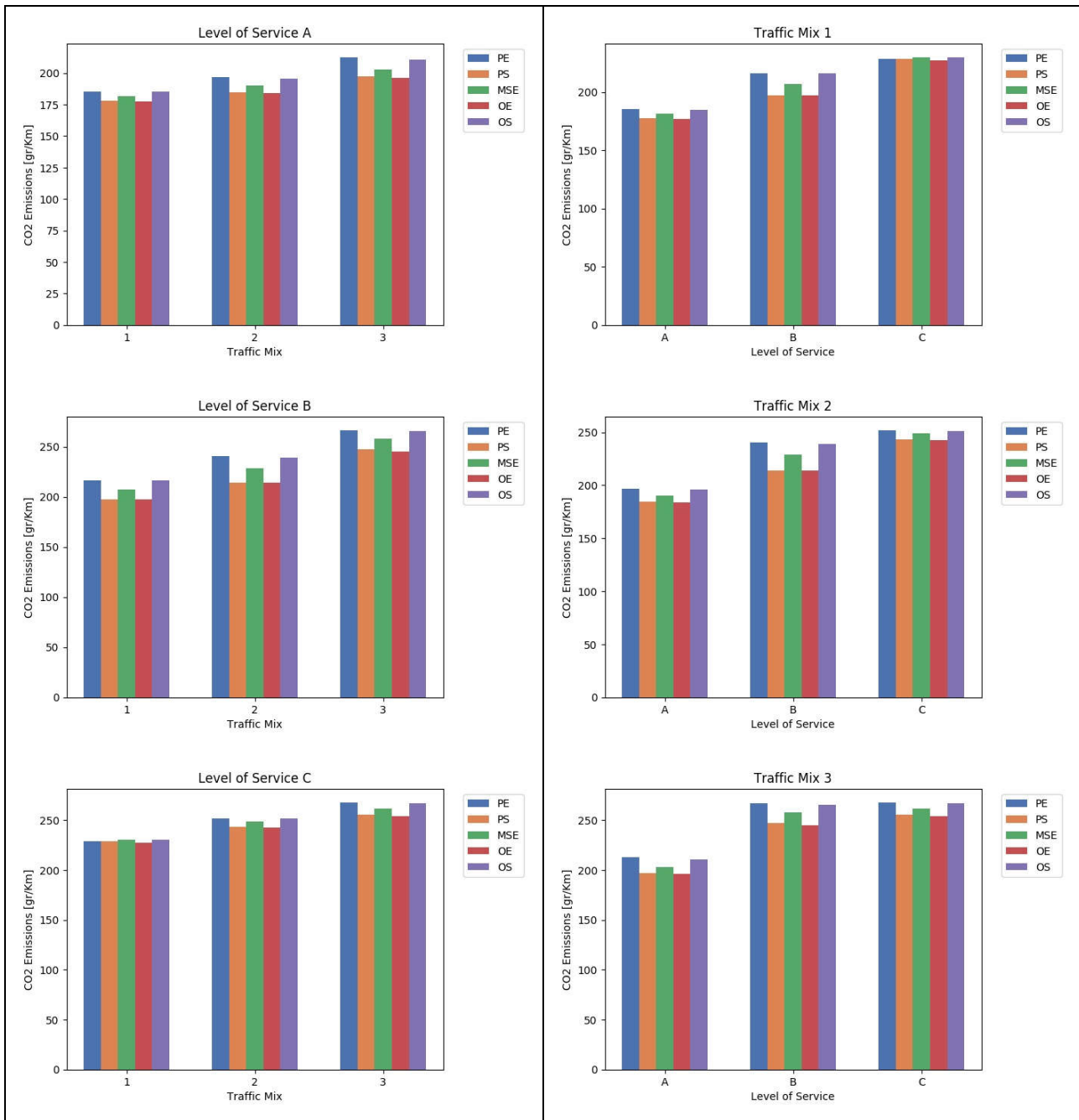


Figure 42. Average CO₂ emissions per km travelled for Scenario 3.1 baseline simulation experiments (varying parameter scheme, LOS, and traffic mix). Different bar colours correspond to different parameter schemes. The left column groups results by LOS, the right column by traffic mix.

4.4 Scenario 4.2: Safe spot in lane of blockage

4.4.1 Scenario Description

A construction site occupies the left lane of a two-lane road in Scenario 4.2 (urban and motorway cases considered) (Figure 42). The RSI is informed about the construction site and the surrounding environment, and shares the relevant information with the approaching CAVs/CVs.

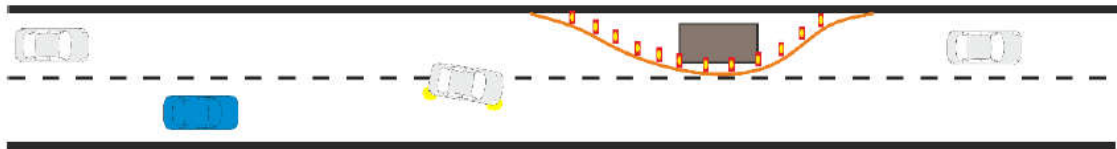


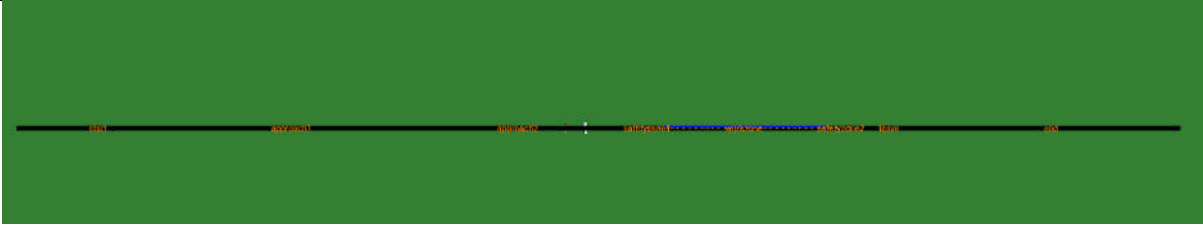
Figure 42. Schematic overview of Scenario 4.2.

However, there are CAVs that cannot drive along the construction site without additional guidance. Therefore, they need to perform a ToC; in case that a ToC is unsuccessful, the corresponding CAV must perform an MRM. Without additional measures the CAV would brake and come to a full stop in the ego lane, thus disrupting the traffic flow when that happens in the right lane. To prevent the latter case, the RSI also monitors the area just in front of the construction site and provides this place as a safe stop to the vehicle, if it is not occupied. The CAV uses the safe spot information to come to a smooth and safe stop in case of an MRM.

More details about the simulation networks (urban and motorway cases) of Scenario 4.2 can be found in Table 26 & 27.

Table 26. Network configuration details for Scenario 4.2 (urban).

Scenario 4.2_urban	Settings	Notes
Road section length	1.85 km	
Road priority	3	
Allowed road speed	13.89 m/s	• 50 km/h
Number of nodes	9	• n0 – n8
Number of edges	8	
Number of O-D relations	1	• from n0 to n8
Number of lanes	2	
Work zone location	from n4 to n5	• 250 m
Closed edge ^{1,2} (defined in the file: closeLanes.add.xml)	workzone	• the leftmost lane (250 m)
	safetyzone1	• the leftmost lane (50 m)
	Safetyzone2	• the leftmost lane (50 m)
Filenames	<ul style="list-style-type: none"> • network: UC4_2_urban.net.xml • lane closure: closeLanes.add.xml • traffic signs: shapes.add.xml 	
Intended control of lane usage	There is no control on lane usage. The RSI knows about it and provides this information to the approaching CAVs. Some CAVs are not able to pass the construction site and perform a ToC. Some of the ToCs are unsuccessful, so the respective CAV must perform a MRM. It uses the safe spot information just in front of the construction site to come to a safe stop.	
Network layout		



Road segments
 n0→n1: Insertion and backlog area (300 m)
 n1→n3: Approaching area (700 m)
 n3→n4: Safety area (50 m)
 n4→n5: Work zone (250 m)
 n5→n6: Safety area (50 m)
 n6→n8: Leaving area (500 m)

¹ The placement of the traffic signs is based on the German Guidelines for road job security (RSA).

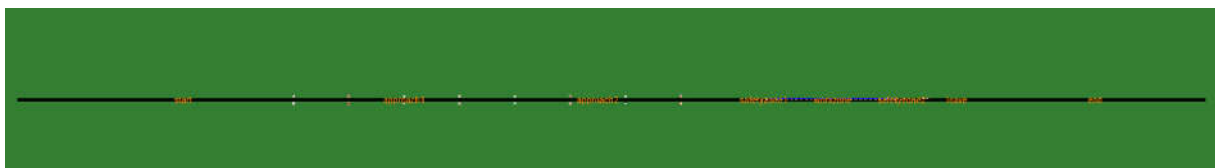
² Required minimum safety distance according to the German Technical Rules for Workplaces ASR A5.2: 10m with allowed maximum speed 30 km/h; 50 m with allowed maximum speed 50 km/h; 100 m with allowed maximum speed 100 km/h.

Table 27. Network configuration details for Scenario 4.2 (motorway).

UC4.2 motorway	Settings	Notes
Road section length	2.15 km	
Road priority	3	
Allowed road speed	<ul style="list-style-type: none"> • 36.11 m/s • 27.78 m/s (700 m in front of the safety zone before entering the work zone area) • 22.22 m/s around the work zone 	<ul style="list-style-type: none"> • 130 km/h • 100 km/h • 80 km/h
Number of nodes	9	• n0 – n8
Number of edges	8	
Number of O-D relations	1	• from n0 to n8
Number of lanes	2	
Construction location	from n4 to n5	• 150 m
Closed edge ^{3,4} (defined in the file: closeLanes.add.xml)	workzone	• the leftmost lane (150 m)
	safetyzone1	• the leftmost lane (100 m)
	safetyzone2	• the leftmost lane (100 m)
Filenames	<ul style="list-style-type: none"> • network: UC4_2_urban.net.xml • lane closure: closeLanes.add.xml • traffic signs: shapes.add.xml 	

Intended control of lane usage
 There is no control on lane usage. This situation is the same as the situation in an urban area, but on motorways. Speeds are higher, and more space and time are needed to execute the measures of this service.

Network layout



Road segments
 n0→n1: Insertion and backlog area (600 m)
 n1→n3: Approaching area (700 m)

n3→n4: Safety area (100 m)
 n4→n5: Work zone (150 m)
 n5→n6: Safety area (100 m)
 n6→n8: Leaving area (500 m)

³ The placement of the traffic signs is based on the German Guidelines for road job security (RSA).

⁴ Required minimum safety distance according to the German Technical Rules for Workplaces ASR A5.2: 10m with allowed maximum speed 30 km/h; 50 m with allowed maximum speed 50 km/h; 100 m with allowed maximum speed 100 km/h.

4.4.2 Results

4.4.2.1 Urban Network

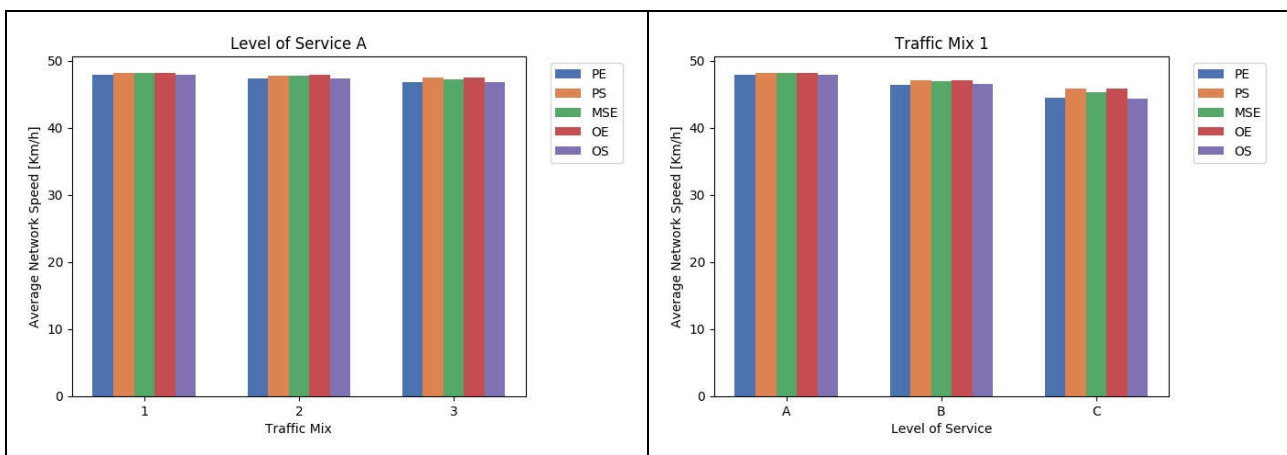
4.4.2.1.1 Impacts on Traffic Efficiency

Network-wide Impacts

Figure 43 depicts the average network speed for all Scenario 4.2 (urban network) baseline simulation experiments encompassing the different demand levels, traffic mixes, and parametrisation schemes. The two columns present the same data in a different format to facilitate the visual assessment with respect to the different traffic mixes (left column), and the different traffic demand levels (right column).

All plots indicate that average network speed does not decrease below 40 km/h despite the presence of the work zone (lane drop) and irrespective of the demand level, traffic mix, and parametrisation scheme. This implies that no major breakdown occurs due to the lane drop bottleneck.

Plots in the left column show that average network speed slightly decreases with increasing penetration rate of CAVs/CVs. As suggested in Section 4.1.2.1, this speed drop can be attributed to different factors, which affect the dynamics of automated vehicle models: (i) the required headway is estimated larger for automated vehicles, (ii) their acceleration rate is lower (i.e. the downstream end of jams dissolves slower), (iii) driver performance is decreased after a ToC, and (iv) MRMs may occur.



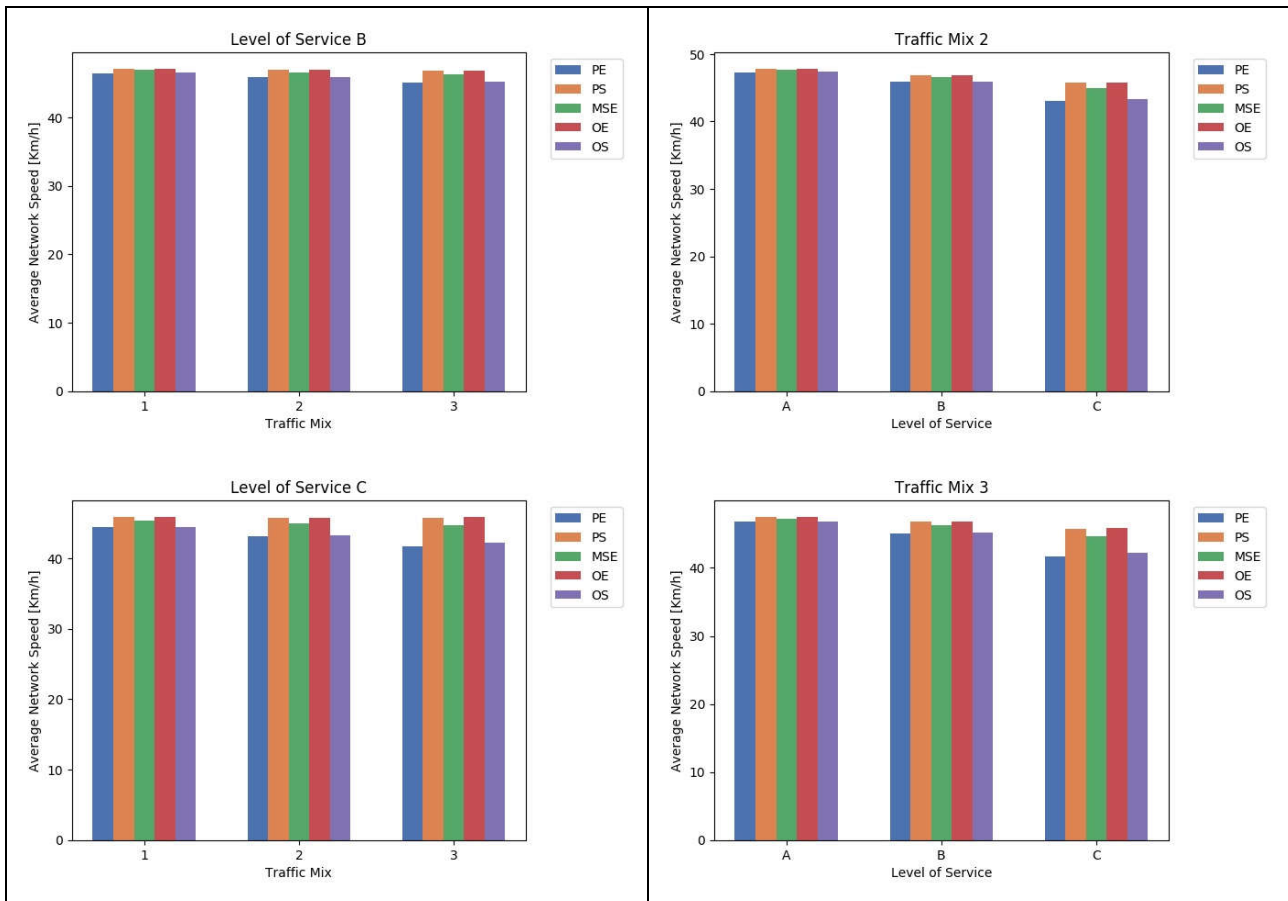


Figure 43. Average network speed for Scenario 4.2 (urban network) baseline simulation experiments (varying parameter scheme, LOS, and traffic mix). Different bar colours correspond to different parameter schemes.

We observe that the latter speed reduction is more significant for parametrisation schemes PE and OS, where driving behaviour was assumed more conservative. Finally, plots in the right column show that speed reduction is constant from LOS A to LOS B, and LOS B to LOS C for increasing penetration rate of CAVs/CVs.

Local Impacts

Figure 44 shows the average speed (taken over 5 minutes) on the edge ‘approach_2’, which is located just upstream of the subsequent lane drop at the beginning of the work zone (see network schematic in **Table 26**). The first row shows the results for different traffic demands (from LOS A to LOS C) and traffic mix 1. The average speed decreases for the parameter schemes OS and PE already at LOS B to some intermediate state, and drops slightly below 40 km/h at LOS C. Thus, we infer that merging operations remain smooth enough for traffic mix 1 irrespective of traffic demand. The latter picture deteriorates for higher traffic demands (lesser for LOS B, and more for LOS C) under traffic mixes 2 and 3. It is clear that traffic operations in the merging area upstream of the work zone become less efficient when both traffic demand (LOS C) and the penetration rate of CAVs/CVs are high. Observations regarding the local impacts coincide with the aforementioned network-wide ones.

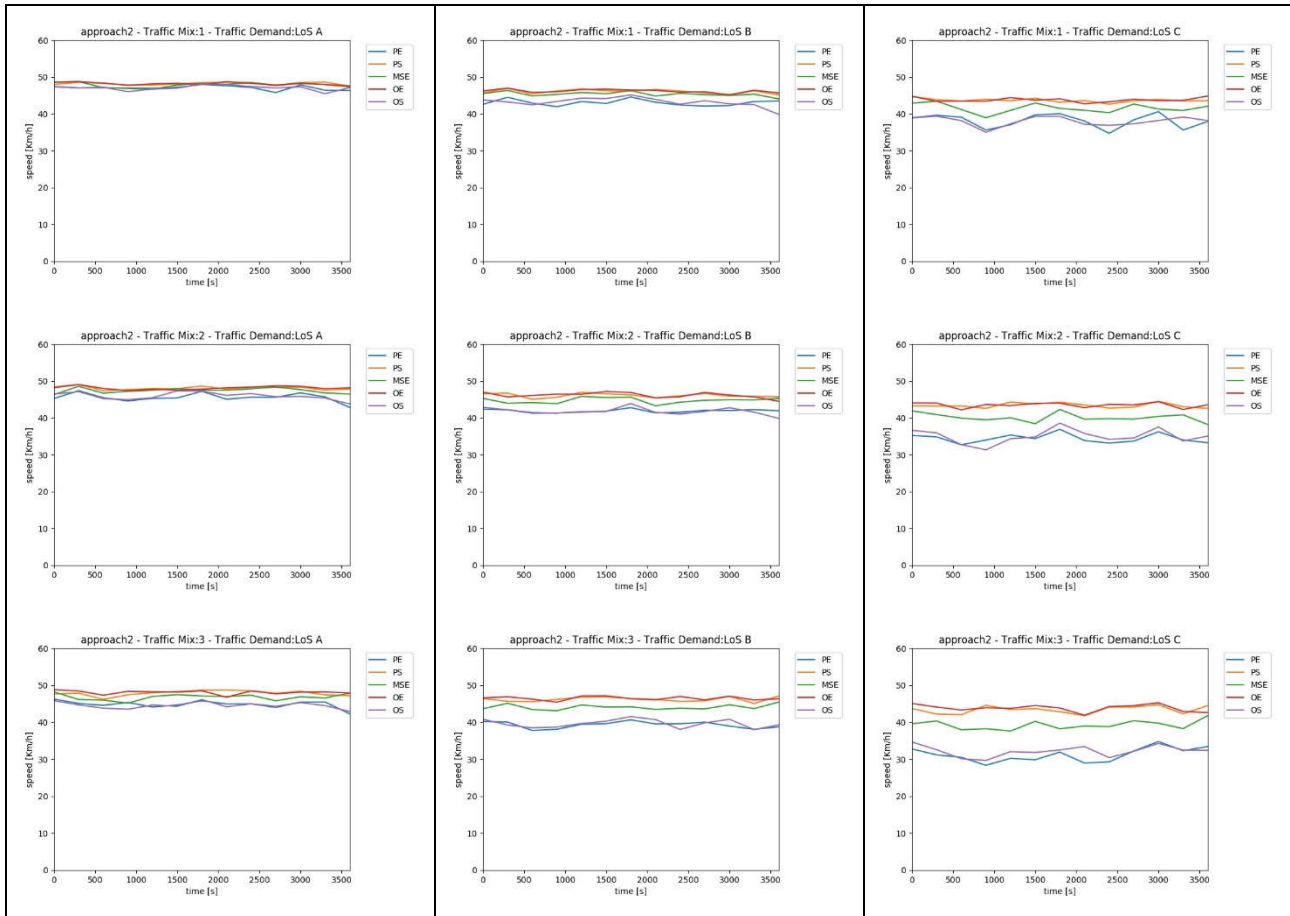
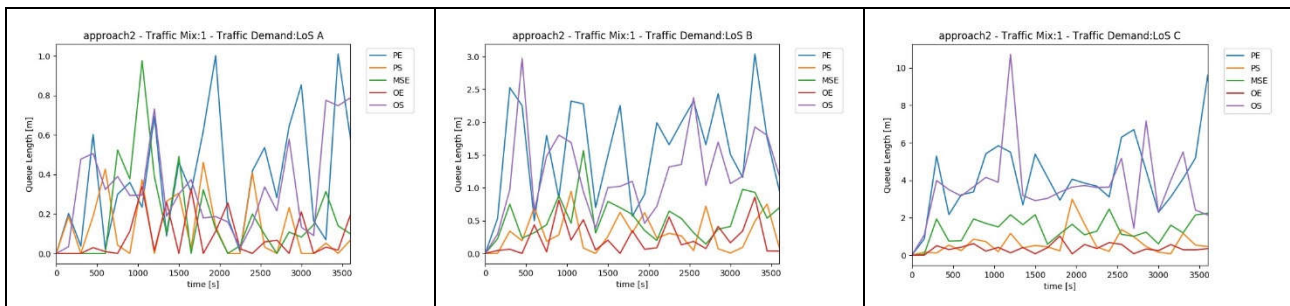


Figure 44. Average speed at the edge ‘approach_2’ for the different parameter sets. First row: varying LOS at traffic mix 1; second row: varying LOS at traffic mix 2; third row: varying LOS at traffic mix 3.

Moreover, no significant spillbacks are formed along edge ‘approach_2’ irrespective of the traffic mix, traffic demand level, and parametrisation scheme (**Figure 45**). An average queue length of 20 m is observed in the worst case scenario (traffic mix 3, LOS c and parametrisation scheme PE), which is typical for lane drop locations due to construction site. Therefore, queue length statistics also demonstrate that merging operations at the lane drop are smooth for the examine scenarios.



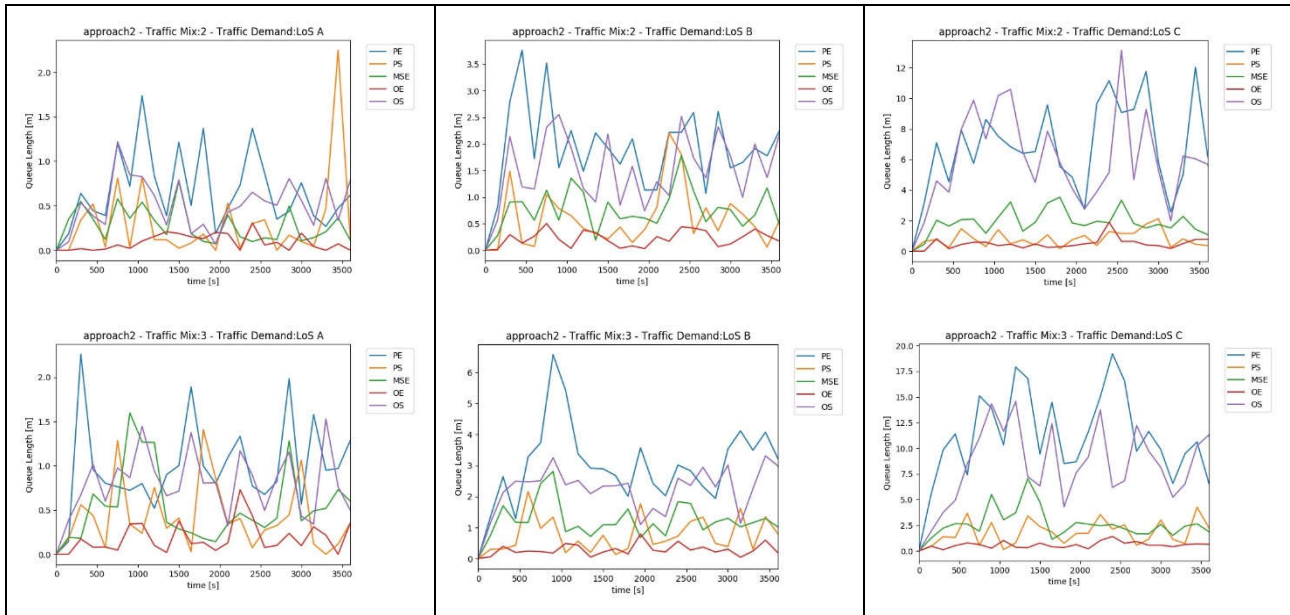
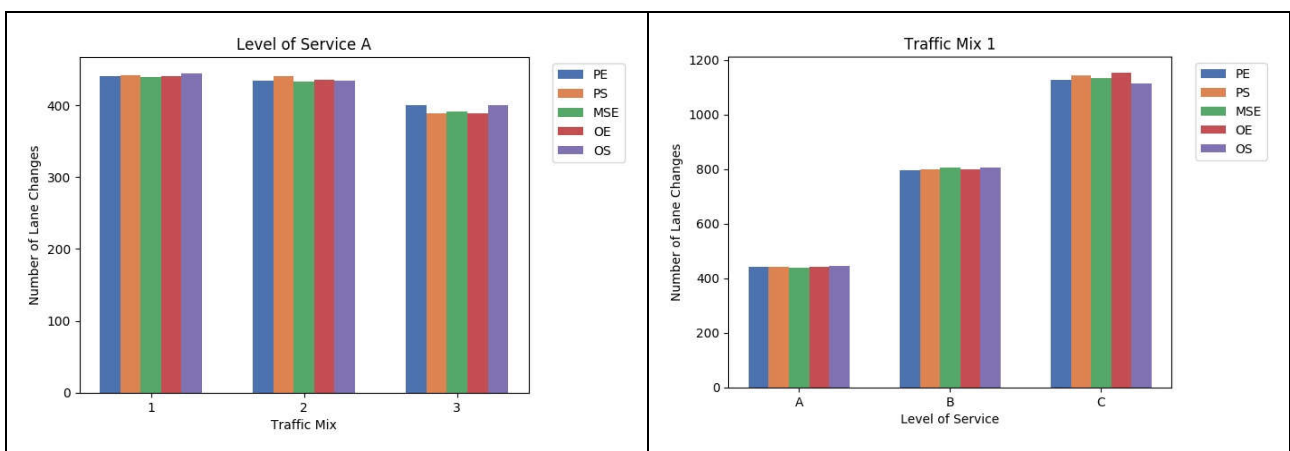


Figure 45. Average queue length at the edge ‘approach_2’ for the different parameter sets. First row: varying LOS at traffic mix 1; second row: varying LOS at traffic mix 2; third row: varying LOS at traffic mix 3.

4.4.2.1.2 Impacts on Traffic Dynamics

Figure 46 shows the total number of lane changes per simulated scenario. For traffic mix 1 the number of lane changes is proportional to the number of injected vehicles in the simulation network with a constant factor of approximately one lane change per vehicle (irrespective of LOS). As the share of CAVs/CVs increases, it can be observed that the number of lane changes per vehicle decreases (especially for traffic mix 3 and LOS B and C). This phenomenon is expected since the *lcAssertive* parameter (i.e. the willingness to accept lower front and rear gaps on the target lane) is in general higher for LVs compared to CAVs/CVs. Moreover, for high share of CAVs/CVs (traffic mix 3) and traffic demand (LOS) it appears that parametrisation schemes corresponding to more congested conditions (MSE, PE and OS) result in more lane changes per vehicle compared to less congested ones (OE and PS). This observation complies similar findings in Section 4.1.2.2.



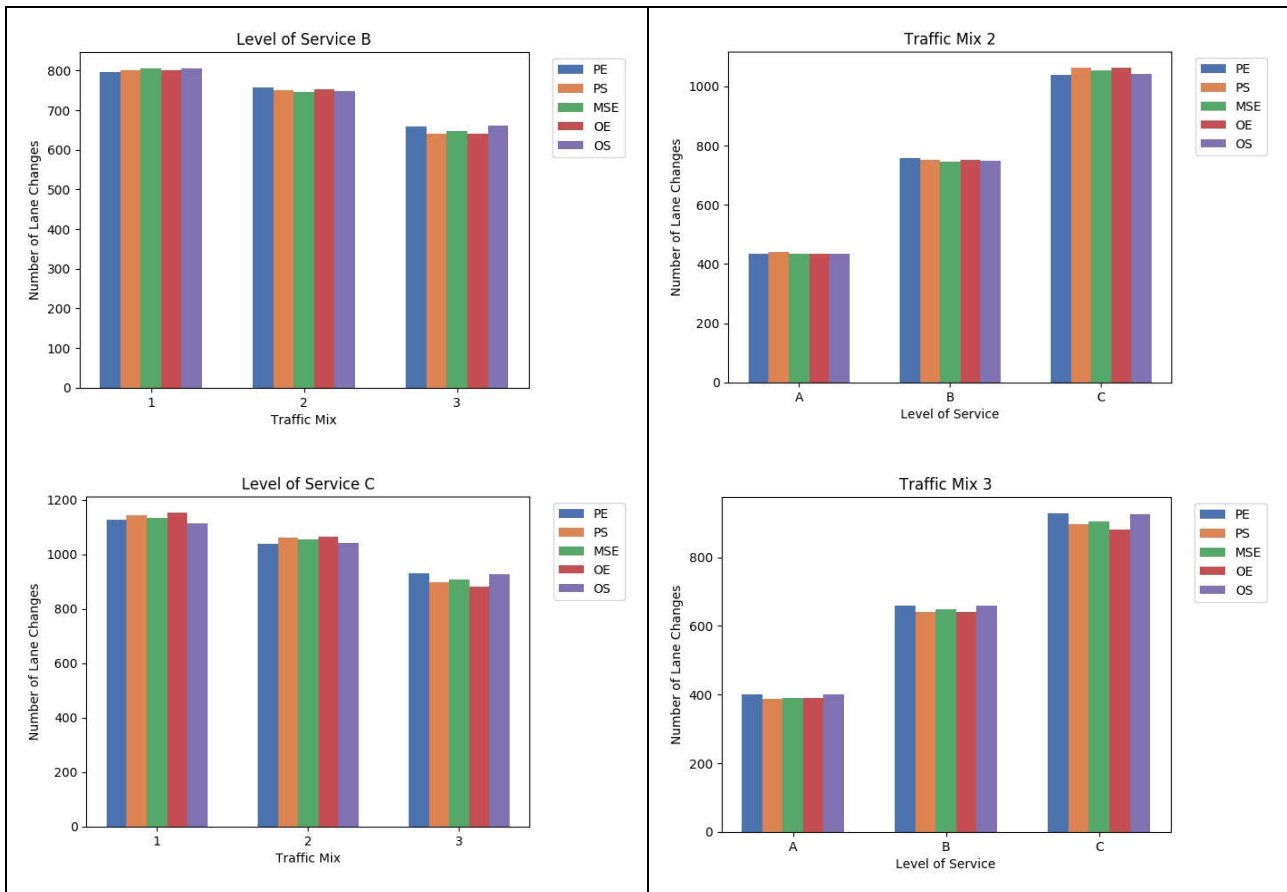


Figure 46. Number of lane changes for Scenario 4.2 (urban network) baseline simulation experiments (varying parameter scheme, LOS, and traffic mix). Different bar colours correspond to different parameter schemes. The left column groups results by LOS, the right column by traffic mix.

4.4.2.1.3 Impacts on Traffic Safety

Figure 47 presents the average number of events with $TTC < 3.0$ s (termed ‘critical’ below). Plots in the left column indicate that the number of critical events increases with increasing traffic demand. However, it has to be noted that this increase becomes more distinct for scenarios corresponding to lower average network speed (PE and OS schemes). An increase in the number of critical events is also observed for increasing penetration rate of CAVs/CVs.

As discussed in Section 4.4.2.1.2, CAVs/CVs accept larger gaps for lane-changing compared to LVs in baseline simulation experiments. Thus, the likelihood of finding a gap to merge early on the right-most lane (open lane) is lower and finally they have to come to a full stop (emergency braking) in front of the closed lane more frequently. This phenomenon causes several rear-end conflicts which are safety critical. This tendency is more pronounced for schemes PE and OS where CAVs/CVs become more unwilling to accept short gaps for lane-changing due to the corresponding driver model parameter values. However, it has to be stressed that based on this finding (which is counter-intuitive), schemes that were expected to favour efficiency explicitly, also generate safety benefits which would be expected when driving behaviour is more conservative in general.

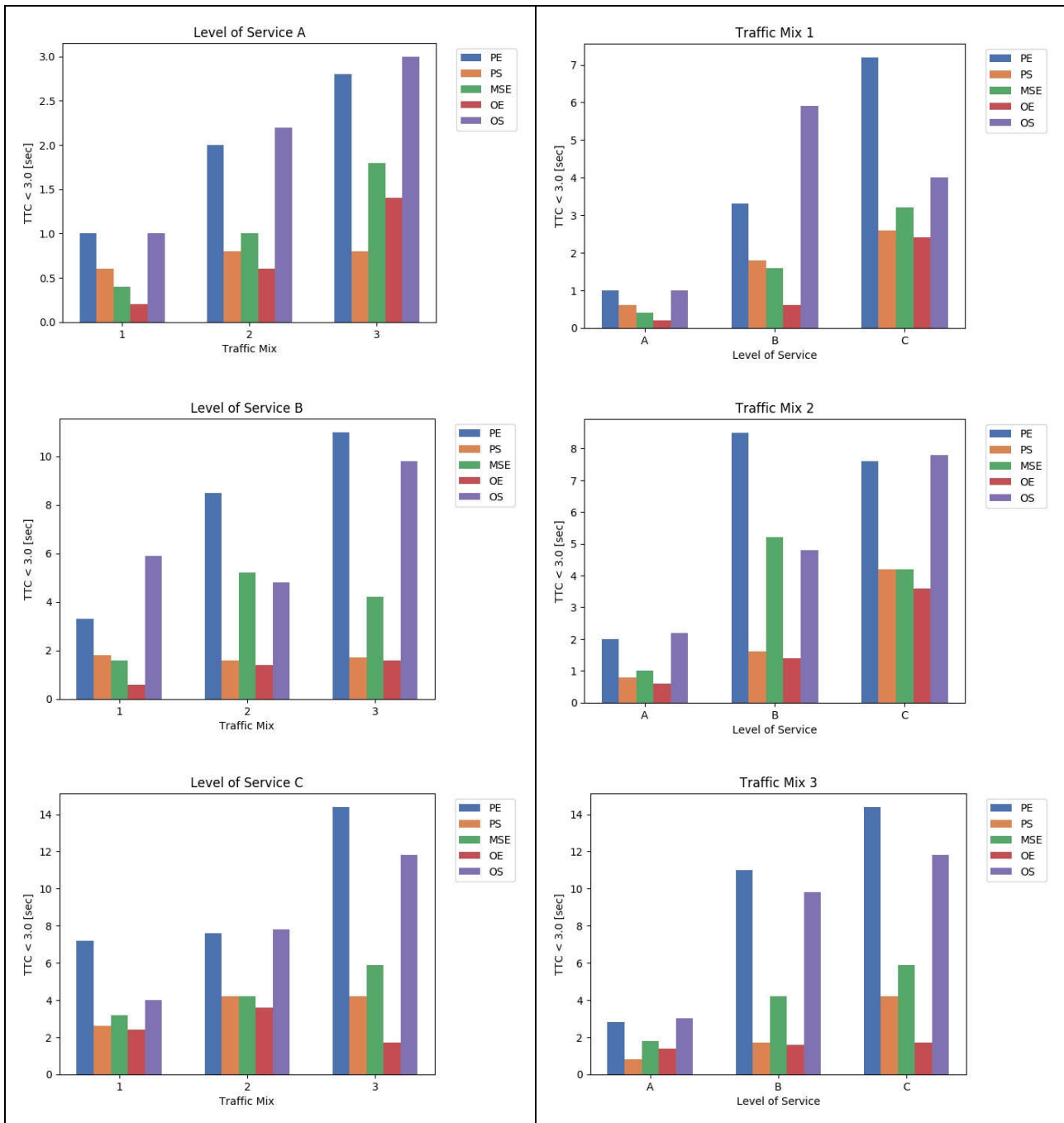


Figure 47. Average number of events with TTCs below 3.0 seconds for Scenario 4.2 (urban network) baseline simulation experiments (varying parameter scheme, LOS, and traffic mix). Different bar colours correspond to different parameter schemes. The left column groups results by LOS, the right column by traffic mix.

4.4.2.1.4 Environmental Impacts

Figure 48 depicts average CO₂ emissions per kilometre travelled. It can be seen that CO₂/km increases as traffic efficiency decreases (**Figure 43**). Even for the same LOS and traffic mix, parametrisation schemes that favour efficiency exhibit reduced emissions levels compared to those favouring safety. This trend is uniform irrespective of the traffic demand level and traffic mix.

Moreover, it is shown that as the share of CAVs/CVs increases in the traffic mix, CO₂/km increases irrespective of the traffic demand level. The increased emission rates in the case CAVs/CVs are

more in the traffic mix can be ascribed to the fact that 75% of them execute ToCs (a few leading to MRMs) at TAs, thus disturbing traffic operations at TAs as mentioned in Section 4.1.2.4. This phenomenon is more prominent for parametrisation scheme PE where driver awareness at the onset of ToC is reduced. Another reason is the fact that traffic composition is more homogeneous for traffic mix 1.

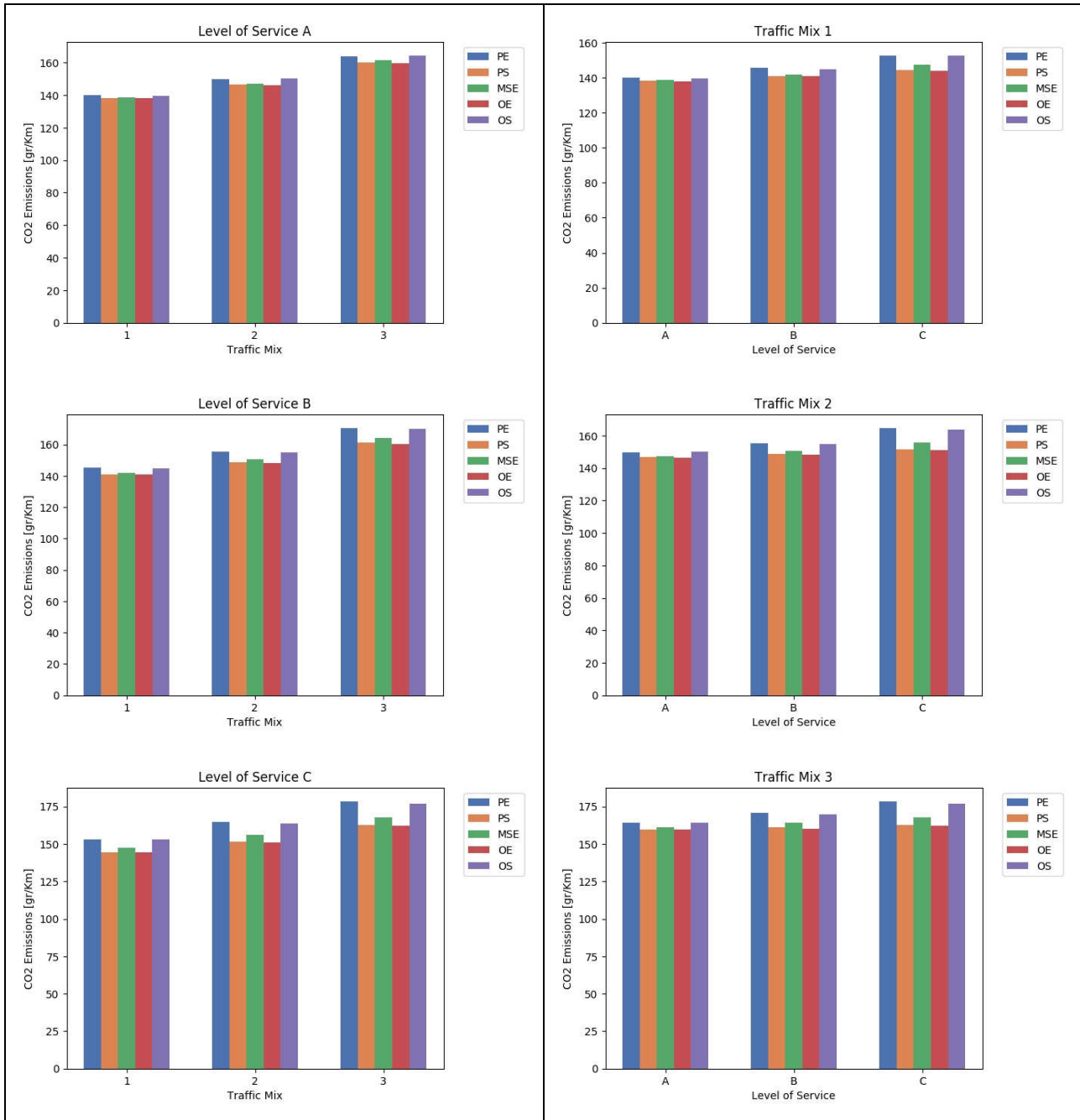


Figure 48. Average CO₂ emissions per km travelled for Scenario 4.2 (urban network) baseline simulation experiments (varying parameter scheme, LOS, and traffic mix). Different bar colours correspond to different parameter schemes. The left column groups results by LOS, the right column by traffic mix.

4.4.2.2 Motorway Network

4.4.2.2.1 Impacts on Traffic Efficiency

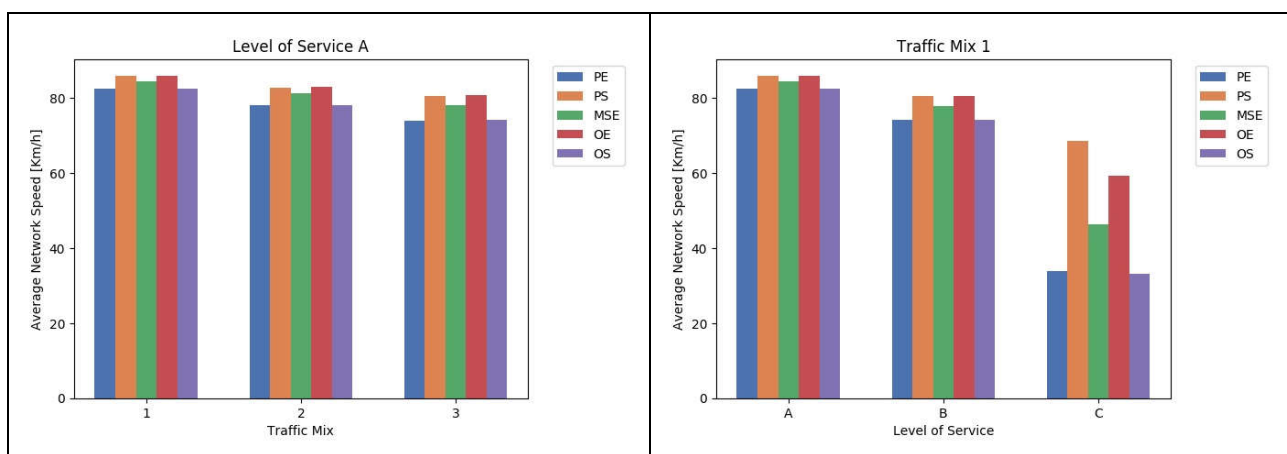
Network-wide Impacts

Figure 49 depicts the average network speed for all Scenario 4.2 (motorway network) baseline simulation experiments encompassing the different demand levels, traffic mixes, and parametrisation schemes. The two columns present the same data in a different format to facilitate the visual assessment with respect to the different traffic mixes (left column), and the different traffic demand levels (right column).

Plots in the left column indicate that average network speed decreases with increasing CAVs/CVs penetration rate. This effect becomes more significant as traffic demand increases. Moreover, it is shown that the influence of the different parametrisation schemes on average network speed exhibits the same trend irrespective of the traffic mix. Schemes PS and OE impact traffic efficiency positively (even in LOS C traffic conditions), while schemes PE and OS result in reduced levels of traffic efficiency.

Plots in the right column show that traffic efficiency is significantly decreased for LOS C. Parametrisation schemes MSE, PE and OS yield congested conditions (stop-and-go traffic) in this case, while schemes OE and PS result in less dense traffic. Free-flow traffic does not prevail even for LOS A, since merging at the lane drop area cannot be smooth due to the high injection rate of vehicles in the motorway network. The injection rate is higher compared to the urban case as shown in Section 3.4, because the capacity of a motorway lane is higher compared to an urban one. Thus, the differences in the operation of the urban and the motorway network can be explained.

As mentioned in previous sections, an important factor affecting merging operations upstream of the work zone is the desired longitudinal gaps by vehicles to change lane. For vehicle types that demand larger gaps, merging on the right-most open lane is less likely to occur upstream of the lane drop, thus resulting in full vehicle stops just upstream of the work zone. Therefore, stop-and-go traffic for LOS C and parametrisation schemes PE and OS is reasonable.



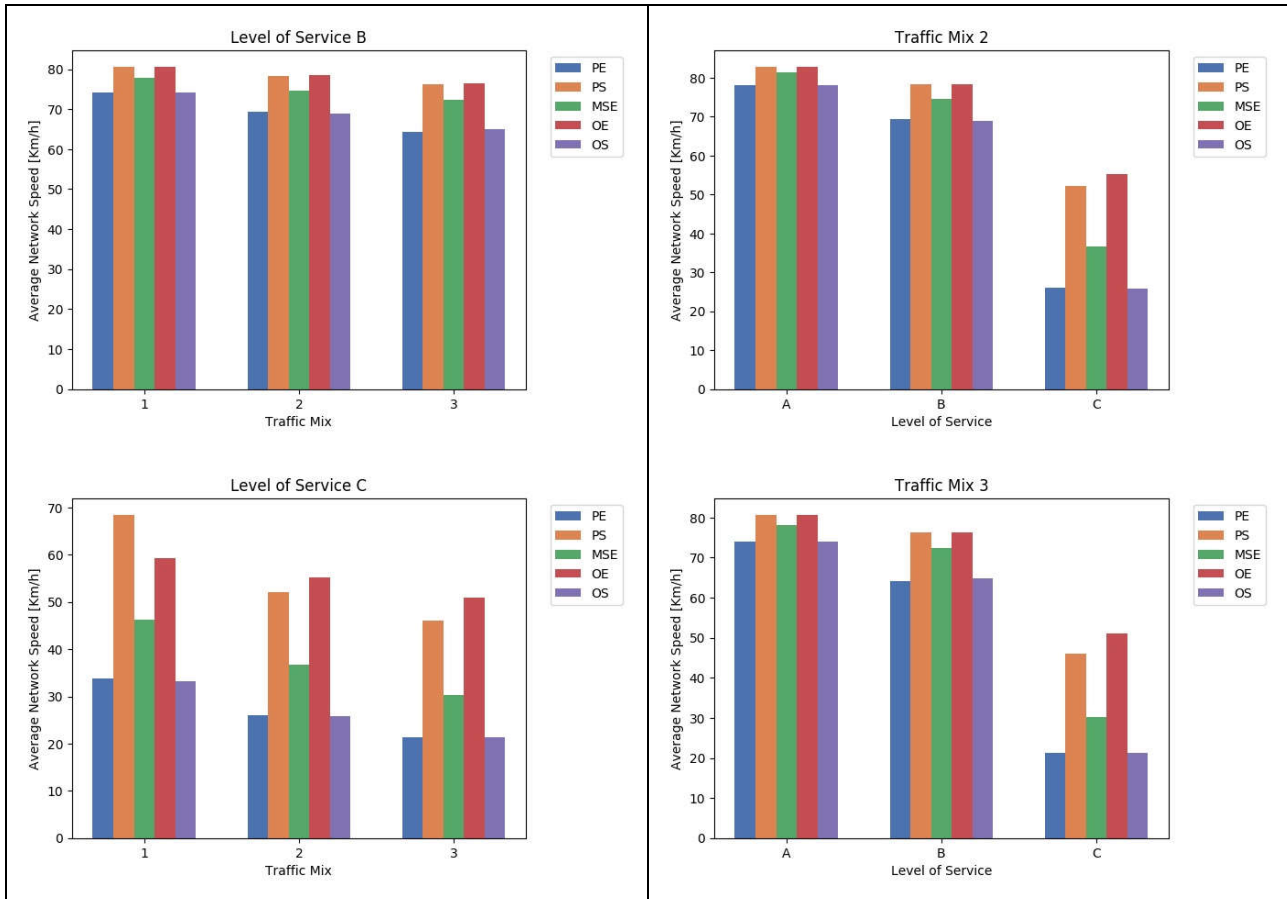
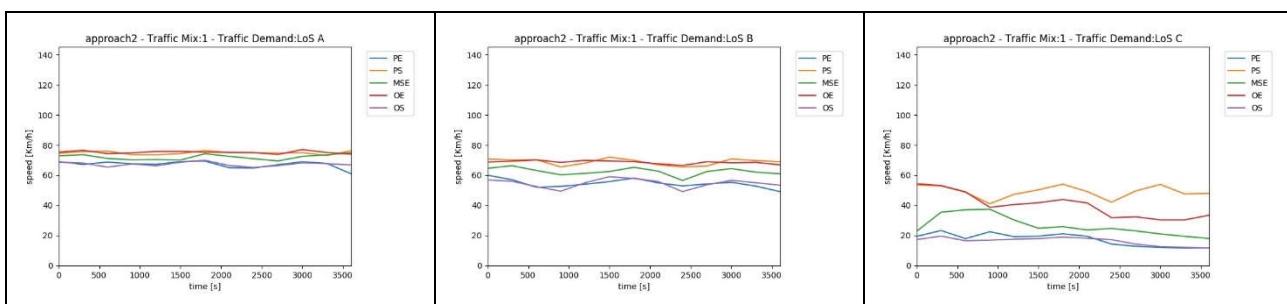


Figure 49. Average network speed for Scenario 4.2 (motorway network) baseline simulation experiments (varying parameter scheme, LOS, and traffic mix). Different bar colours correspond to different parameter schemes.

Local Impacts

Figure 50 shows the average speed (taken over 5 minutes) on the edge ‘approach_2’, which is located just upstream of the subsequent lane drop at the beginning of the work zone (see network schematic in **Table 27**). The first row shows the results for different traffic demands (from LOS A to LOS C) and traffic mix 1. As traffic increases, the efficiency of merging operations deteriorates until breakdown occurs for LOS C. The effect of the different parametrisation schemes becomes more distinct with the increase of traffic demand as well. Schemes PE and OS generate stop-and-go traffic due to conservative lane-changing. The latter distinction is more pronounced for higher penetration rate of CAVs/CVs, since these vehicles were modelled to accept larger gaps for lane-changing compared to LVs. Observations regarding the local impacts coincide with the aforementioned regarding the network-wide ones.



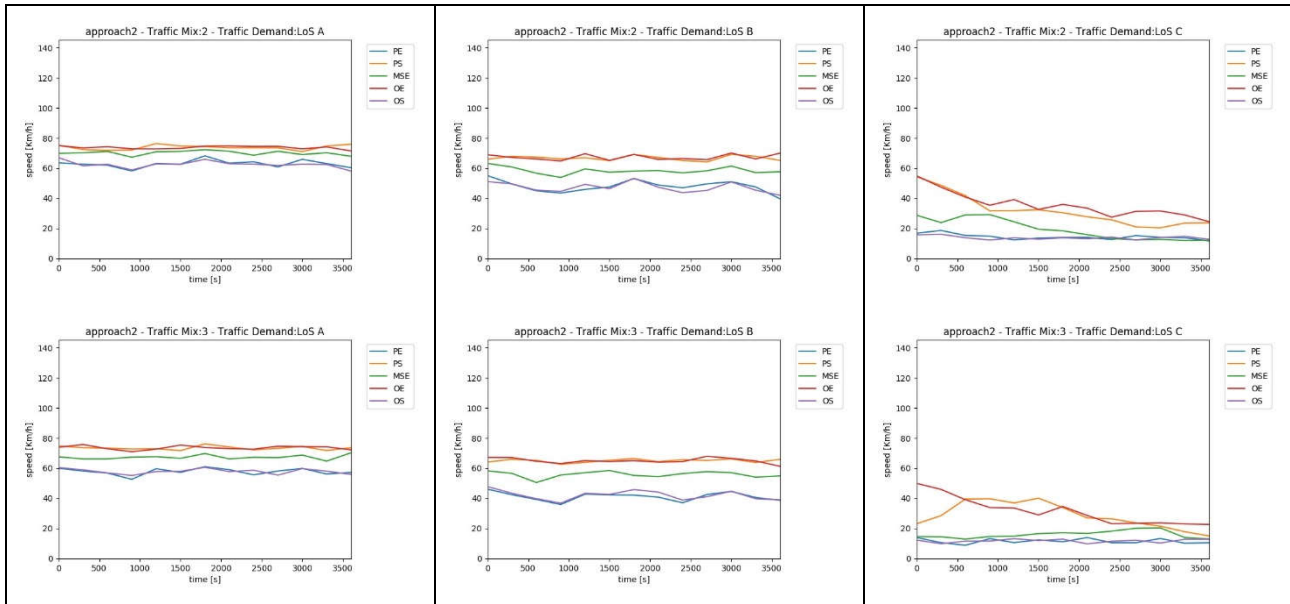
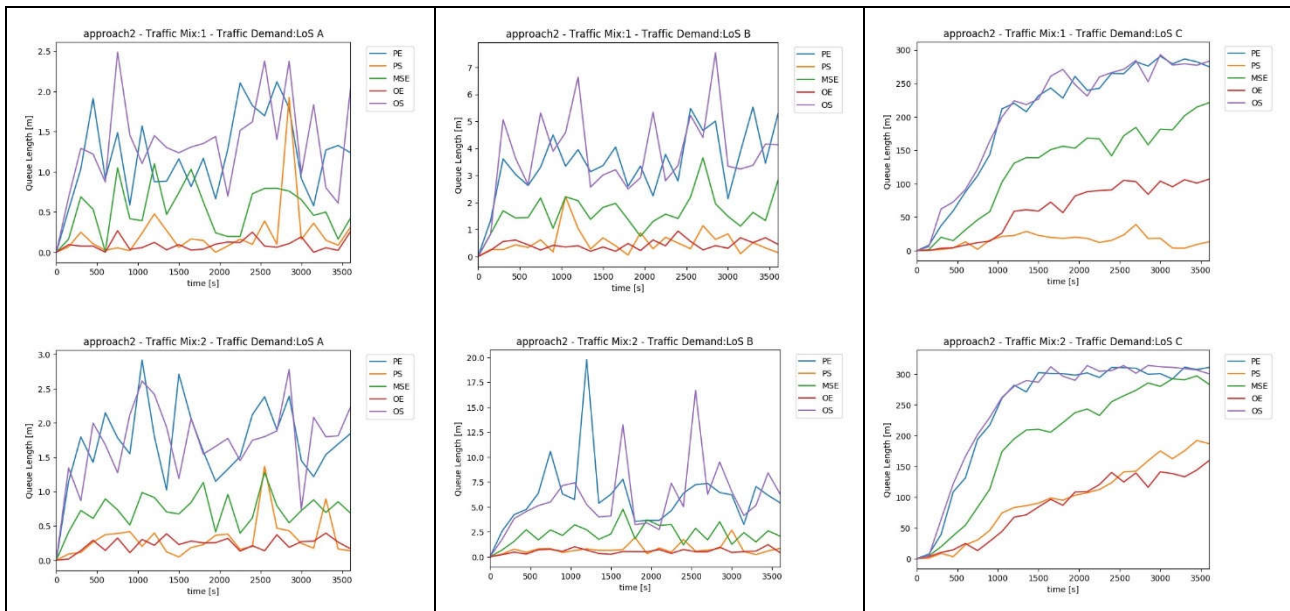


Figure 50. Average speed at the edge ‘approach_2’ for the different parameter sets. First row: varying LOS at traffic mix 1; second row: varying LOS at traffic mix 2; third row: varying LOS at traffic mix 3.

The breakdown occurring for LOS C is also reflected in terms of spillback formed along edge ‘approach_2’ (**Figure 51**). Maximum queue length of approximately 320 m is observed for traffic mix 3, LOS C and parametrisation schemes PE and OS. However, long queues are created for the other parametrisation schemes as well for the aforementioned traffic mix and LOS. In general, observations regarding the local impacts coincide with the aforementioned regarding the network-wide ones.



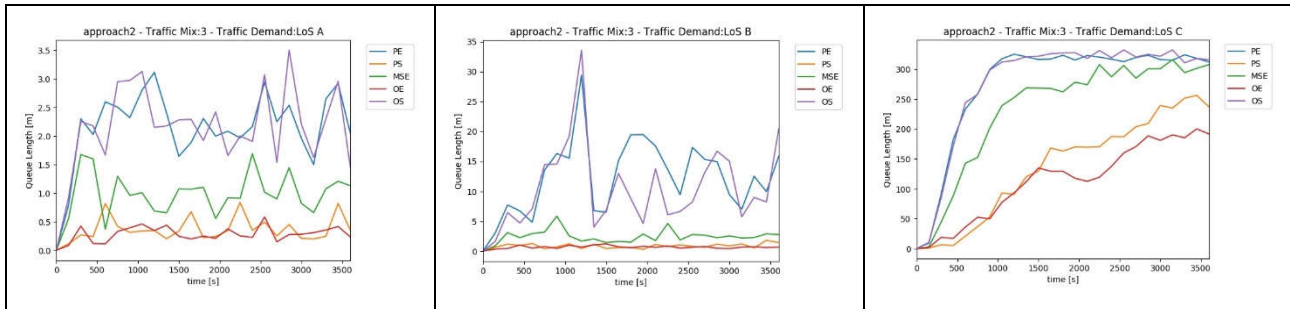
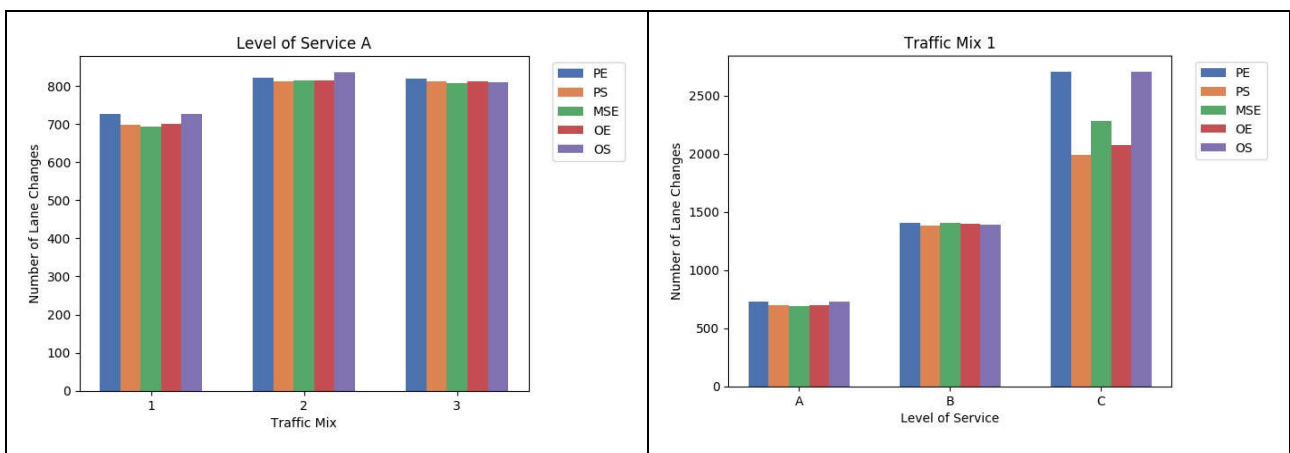


Figure 51. Average queue length at the edge ‘approach_2’ for the different parameter sets. First row: varying LOS at traffic mix 1; second row: varying LOS at traffic mix 2; third row: varying LOS at traffic mix 3.

4.4.2.2 Impacts on Traffic Dynamics

Figure 52 shows the total number of lane changes per simulated scenario. For traffic mix 1 and LOS A the number of lane changes is proportional to the number of injected vehicles in the simulation network with a constant factor of approximately one lane change per vehicle. However, for higher demand levels corresponding to lower average network speeds (LOS B and C), the lane change rate per vehicle is higher than one. It is clear that the smoother merging operations are at the lane drop, lesser lane changes are executed during the simulation. For congested conditions, conservative vehicle behaviour results in more lane changes compared to moderate or aggressive (parametrisation schemes PE and OS for traffic mixes 1 and 2, and LOS C). However, when the network is fully jammed (traffic mix 3, LOS C, and parametrisation schemes PE and OS) there is no room for tactical lane changes and the latter phenomenon vanishes. The overall picture with respect to lane changes is rather complex for this scenario and no generic conclusions can be drawn since congestion builds up upstream of the lane drop for most of the traffic mixes, traffic demand levels and parametrisation schemes.



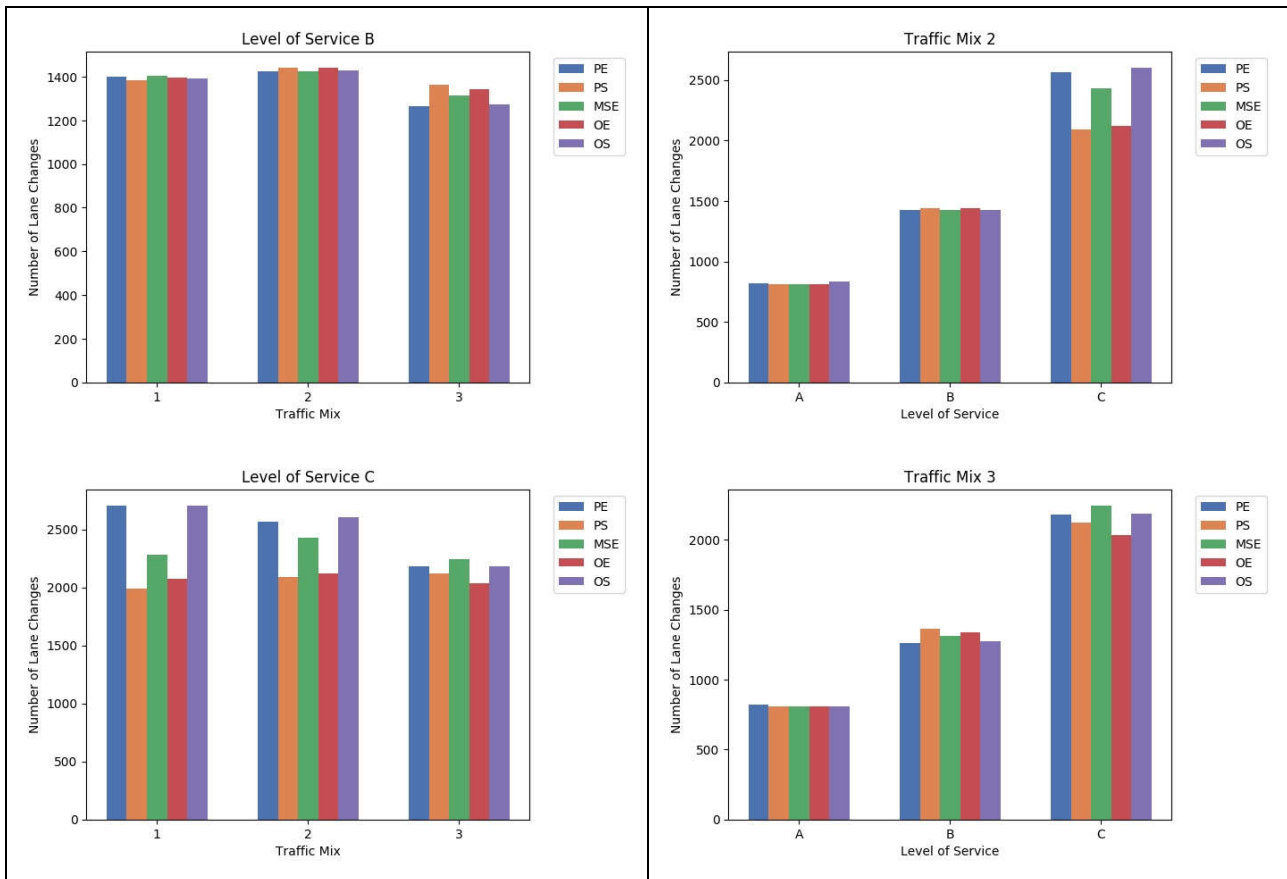


Figure 52. Number of lane changes for Scenario 4.2 (motorway network) baseline simulation experiments (varying parameter scheme, LOS, and traffic mix). Different bar colours correspond to different parameter schemes. The left column groups results by LOS, the right column by traffic mix.

4.4.2.2.3 Impacts on Traffic Safety

Figure 53 presents the average number of events with $TTC < 3.0$ s (termed ‘critical’ below). Plots in the left column indicate that the number of critical events increases with increasing traffic demand. However, it has to be noted that this increase becomes more distinct for scenarios corresponding to lower average network speed (PE and OS schemes). When the network becomes fully jammed (traffic mix 3, LOS C, and parametrisation schemes PE and OS) the latter difference in safety critical events between different parametrisation schemes diminishes since there is limited free space for lane-changing on the motorway network.

As discussed in Section 4.4.2.1.2, CAVs/CVs accept larger gaps for lane-changing compared to LVs in baseline simulation experiments. Thus, the likelihood of finding a gap to merge early on the right-most lane (open lane) is lower and finally they have to come to a full stop (emergency braking) in front of the closed lane more frequently. This phenomenon causes several rear-end conflicts which are safety critical. This tendency is more pronounced for schemes PE and OS where CAVs/CVs become more unwilling to accept short gaps for lane-changing due to the corresponding driver model parameter values. However, it has to be stressed that based on this finding (which is counter-intuitive), schemes that were expected to favour efficiency explicitly, also generate safety benefits which would be expected when driving behaviour is more conservative in general.

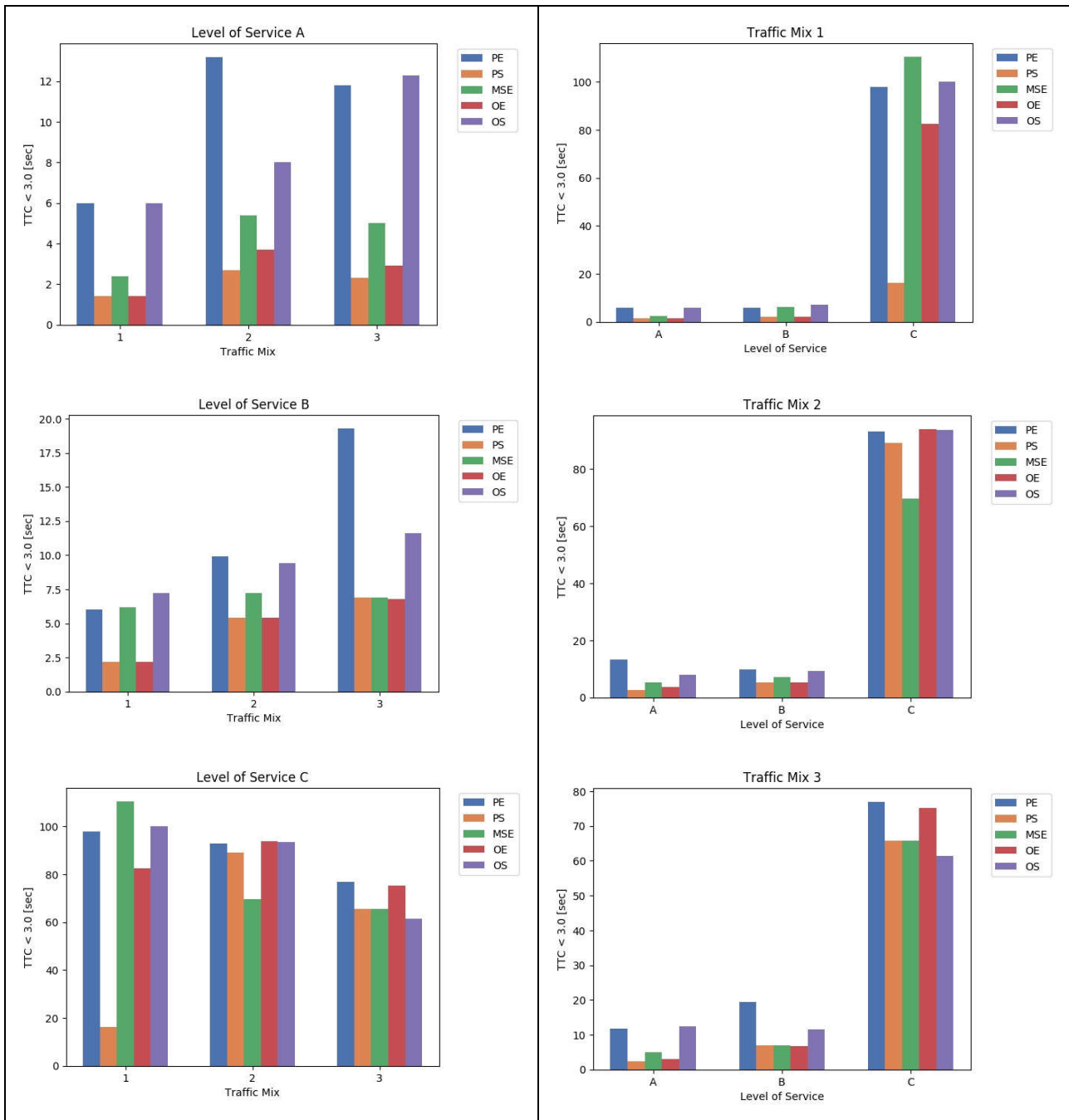


Figure 53. Average number of events with TTCs below 3.0 seconds for Scenario 4.2 (motorway network) baseline simulation experiments (varying parameter scheme, LOS, and traffic mix). Different bar colours correspond to different parameter schemes. The left column groups results by LOS, the right column by traffic mix.

4.4.2.2.4 Environmental Impacts

Figure 54 depicts average CO₂ emissions per kilometre travelled. It can be seen that CO₂/km increases as traffic efficiency decreases (**Figure 49**). For congested conditions (LOS C and parametrisation schemes PE and OS), emission levels increase dramatically due to stop-and-go traffic. Even for the same LOS and traffic mix, parametrisation schemes that favour efficiency exhibit reduced emissions levels compared to those favouring safety. This trend is uniform irrespective of the traffic demand level and traffic mix.

Moreover, it is shown that as the share of CAVs/CVs increases in the traffic mix, CO₂/km increases irrespective of the traffic demand level. The increased emission rates in the case CAVs/CVs are more in the traffic mix can be ascribed to the fact that 75% of them execute ToCs (a few leading to MRMs) at TAs, thus disturbing traffic operations at TAs as mentioned in Section 4.1.2.4. This phenomenon is more prominent for parametrisation scheme PE where driver awareness at the onset of ToC is reduced. Another reason is the fact that traffic composition is more homogeneous for traffic mix 1.

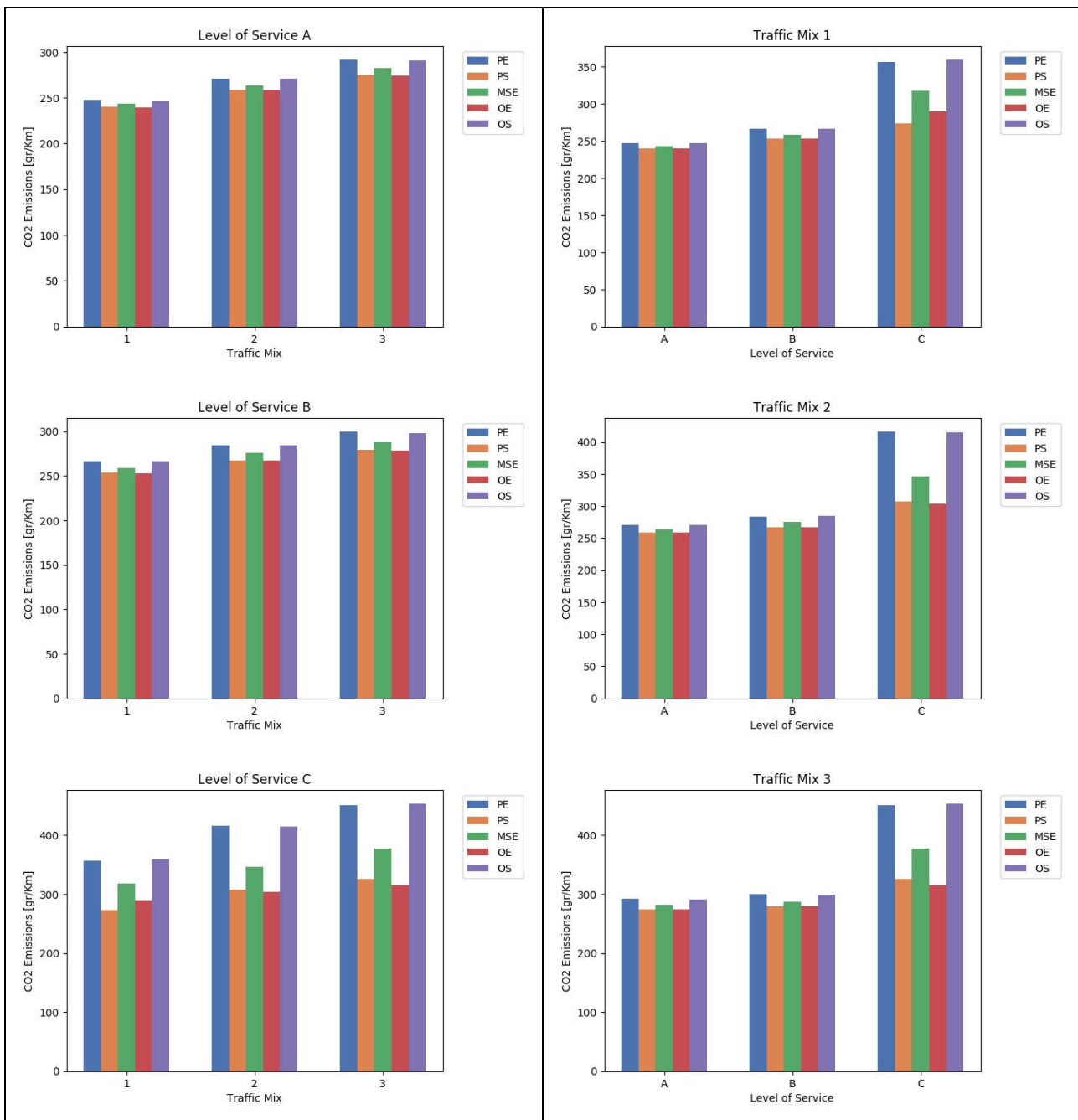


Figure 54. Average CO₂ emissions per km travelled for Scenario 4.2 (motorway network) baseline simulation experiments (varying parameter scheme, LOS, and traffic mix). Different bar colours correspond to different parameter schemes. The left column groups results by LOS, the right column by traffic mix.

4.5 Scenario 5.1: Schedule ToCs before no AD zone

4.5.1 Scenario Description

A (C)AV/CV is expected to behave more erratically after ToC. The dissimilarity between the driving behaviour during transitions and the driving behaviour shortly thereafter, might result in a significant disruption of traffic flow and safety. This effect is amplified when many ToCs occur in the same area. Hence, to avoid the latter amplification in mixed traffic scenarios, downward ToCs are distributed in time and space upstream of an area where no or limited automated driving is unavoidable (e.g., tunnels, geo-fenced areas, or complicated road works).

Figure 55 illustrates Scenario 5.1 where vehicles are approaching a no-AD zone consisting of two lanes. At some point upstream of the no-AD zone, the RSI defines through the collective perception process both the positions and speeds of vehicles and determines the optimal location and moment for CAVs/CVs to perform a downward ToC. Subsequently, ToC requests are provided to the corresponding CAVs/CVs; based on these ToC requests, CAVs/CVs perform ToCs at the desired location and time.

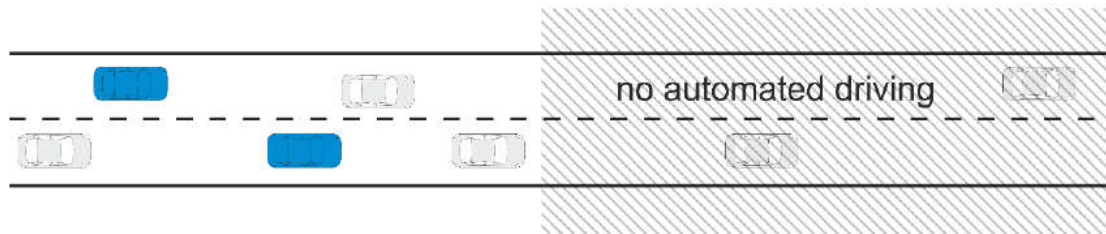


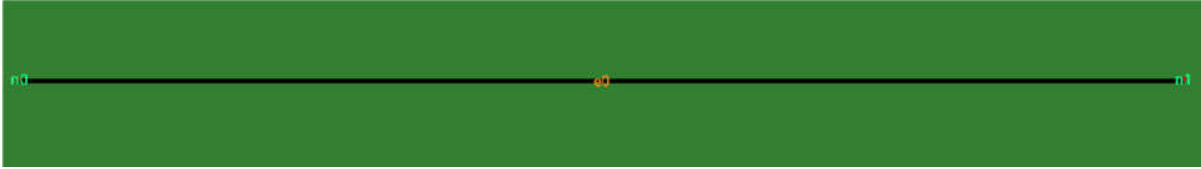
Figure 55. Schematic overview of Scenario 4.2.

Note: the figure is schematic. The blue CAVs have performed ToCs further upstream than the picture might suggest.

More details about the simulation network of Scenario 5.1 can be found in **Table 28**.

Table 28. Network configuration details for Scenario 5.1.

Scenario 5.1	Settings	Notes
Road section length	5.0 km	
Road priority	3	
Allowed road speed	27.78 m/s	• 100 km/h
Number of nodes	2	• n0 – n1
Number of edges	1	
Number of O-D relations	1	• n0 to n1
Number of lanes	2	• 2 normal lanes
Work zone location	-	
Closed edges	-	
Disallowed vehicle classes	• normal lanes: pedestrians, tram,	• from n0 to n1

	rail_urban, rail, rail_electric, ship	
Filenames	• network: TransAID_UC5-1.net.xml	
<p>Intended control of lane usage</p> <p>CAVs and other traffic are approaching a no-AD zone with 2 lanes. Starting about 3.0 km upstream from the no-AD zone, the RSI determines through collective perception the positions and speeds of vehicles and determines the optimal location and moment for CAVs to perform a downward ToC. Subsequently, ToC requests are provided to the corresponding CAVs. Based on the ToC requests, the CAVs perform ToCs at the desired location and moment in time and transition to manual mode. CVs are warned about the ToCs and possible MRMs. In the no-AD zone, the CAVs are in manual mode.</p>		
<p>Network layout</p> 		
<p>Road segments</p> <p>n0→n1: (5.000 m)</p>		

4.5.2 Results

4.5.2.1 Impacts on Traffic Efficiency

Network-wide Impacts

The results obtained for use case five using a demand of maximally LoS C for the two lane highway scenario did not show significant disruptions of the smooth traffic flow in the scenario, see **Figure 56** for some samples illustrating the average network speed, which remains approximately constant at the speed limit of 120 km/h for all scenarios and parameter schemes.

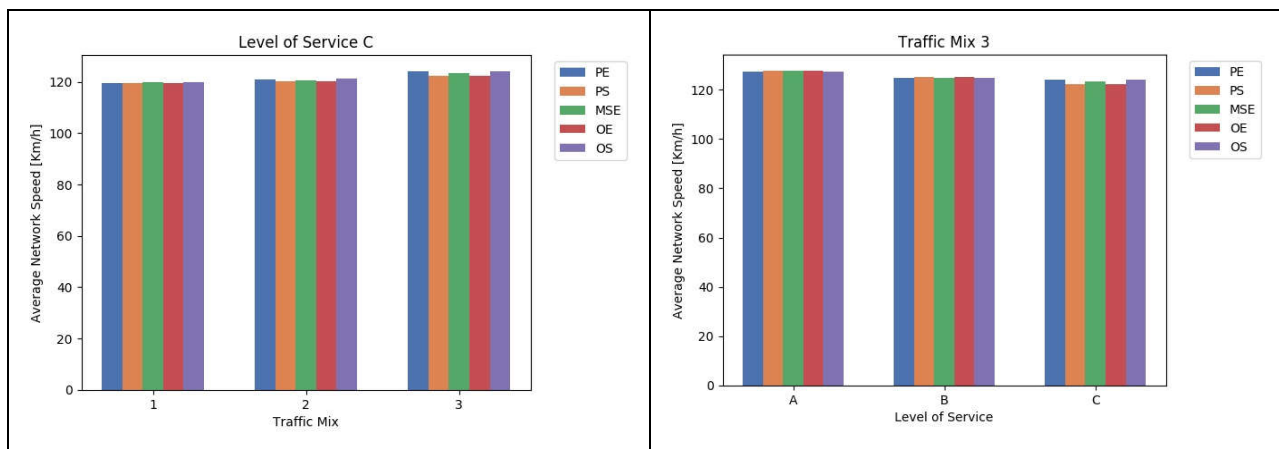


Figure 56. Average network speed for Scenario 5.1 baseline simulation experiments (varying parameter scheme, LOS, and traffic mix). Different bar colours correspond to different parameter schemes.

Local Impacts

Figure 57 reveals once more that there are no significant differences between the different scenarios. Apart from a small decrease of the free flow average speed on edge ‘e0’ for increasing demand no difference between the tested parametrisation schemes and traffic composition can be identified. This decreased average speed is due to the DVU’s varying desired speeds and the slightly increased likelihood that a DVU with a smaller desired speed impedes another one from attaining its higher desired speed if there are more vehicles are on the road.

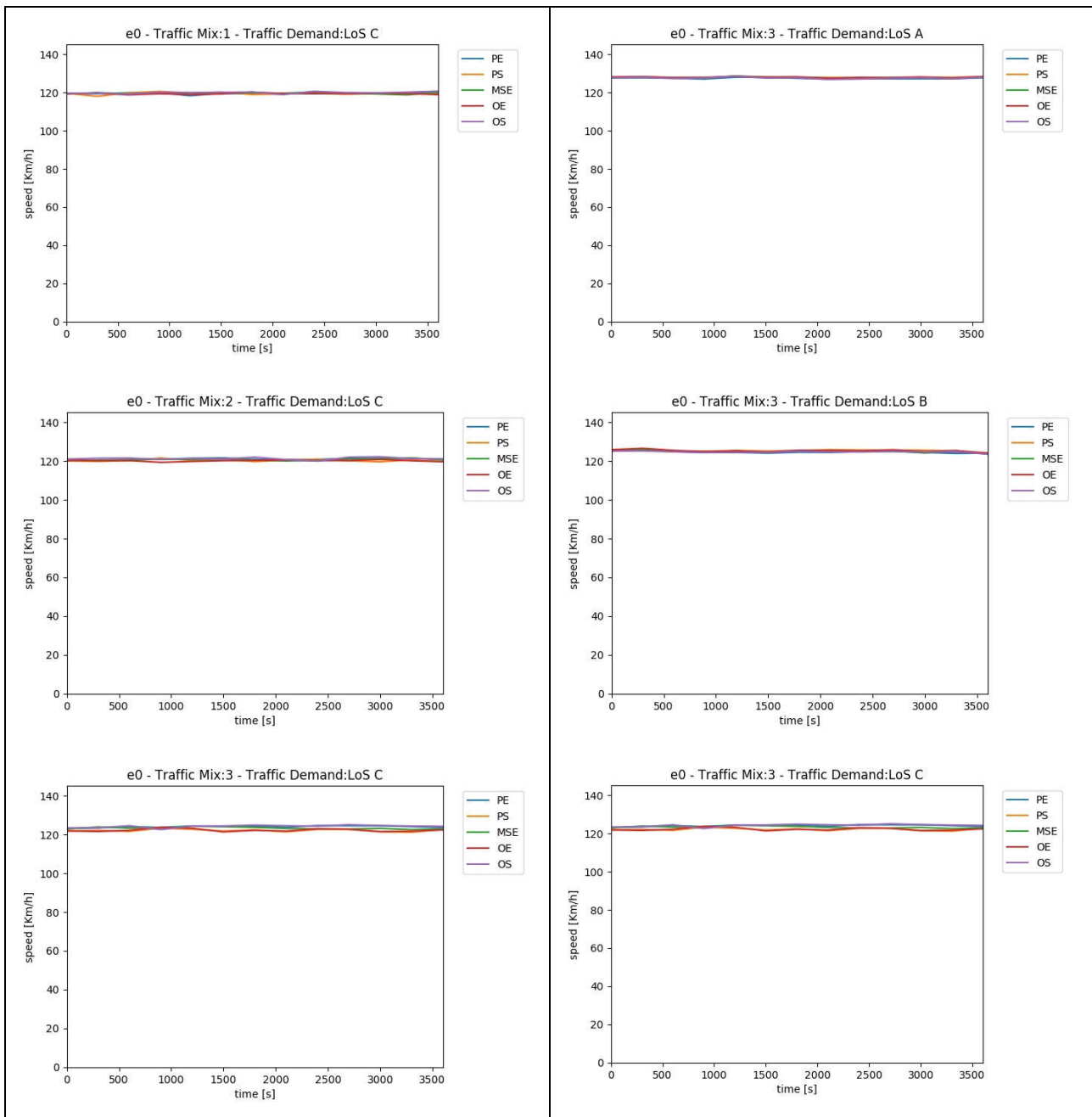


Figure 57. Average speed at the edge ‘approach_2’ for the different parameter sets. Left column: varying traffic mix at LOS C; right column: varying demand level at traffic mix 3.

4.5.2.2 Impacts on Traffic Dynamics

Figure 58 shows the total number of lane changes for each simulated scenario (accumulated over the ten executed runs). Interestingly, the number of changes decreases with an increasing share of AVs when the total demand is held constant, see left column. This may be explained by a more conservative lane change behavior of the AVs. Moreover, it does not increase linearly with the number of vehicles as might be expected. The increased number of lane changes for the parameter schemes PS and OE can be explained by the elevated willingness of DVUs to accept smaller gaps under that parameterisation.

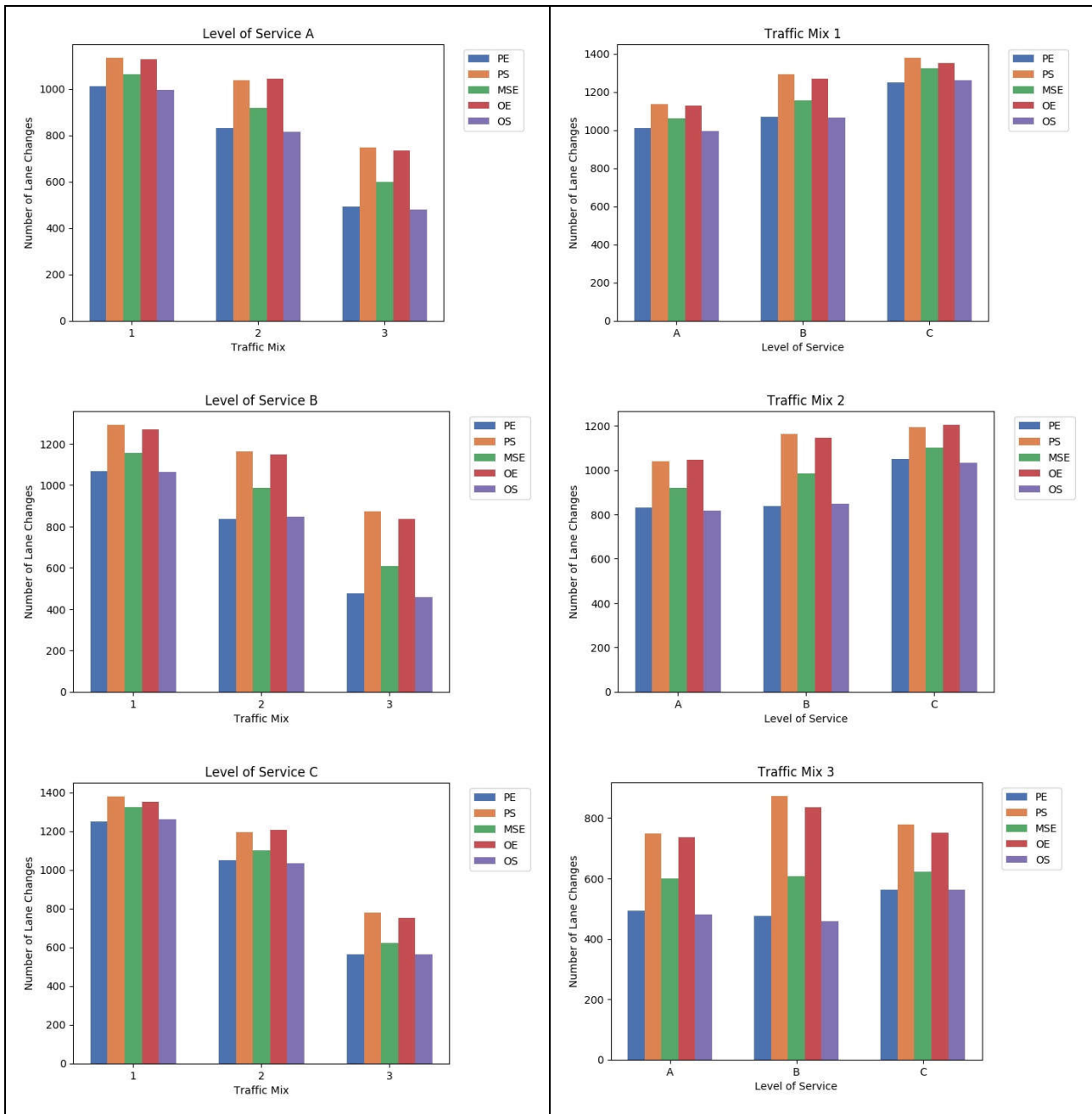


Figure 58 Number of lane changes for Scenario 5.1 baseline simulation experiments (varying parameter scheme, LOS, and traffic mix). Different bar colours correspond to different parameter schemes. The left column groups results by LOS, the right column by traffic mix.

4.5.2.3 Impacts on Traffic Safety

Due to the smoothness of the traffic flow in all scenarios, critical events (TTC below 3.0 seconds) are extremely rare for the simulated levels of demand. During all 450 runs only two instances have been observed (both for LoS C / Mix 3), see **Figure 57**.

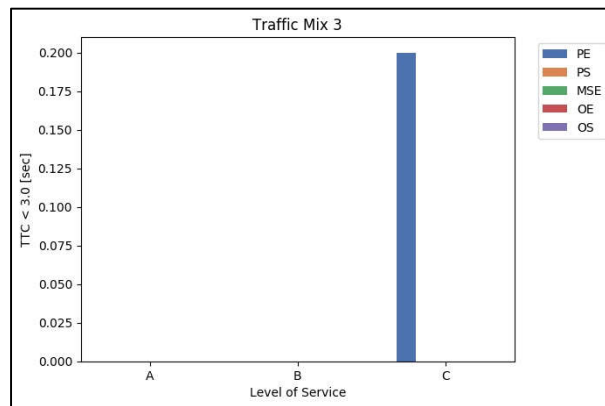
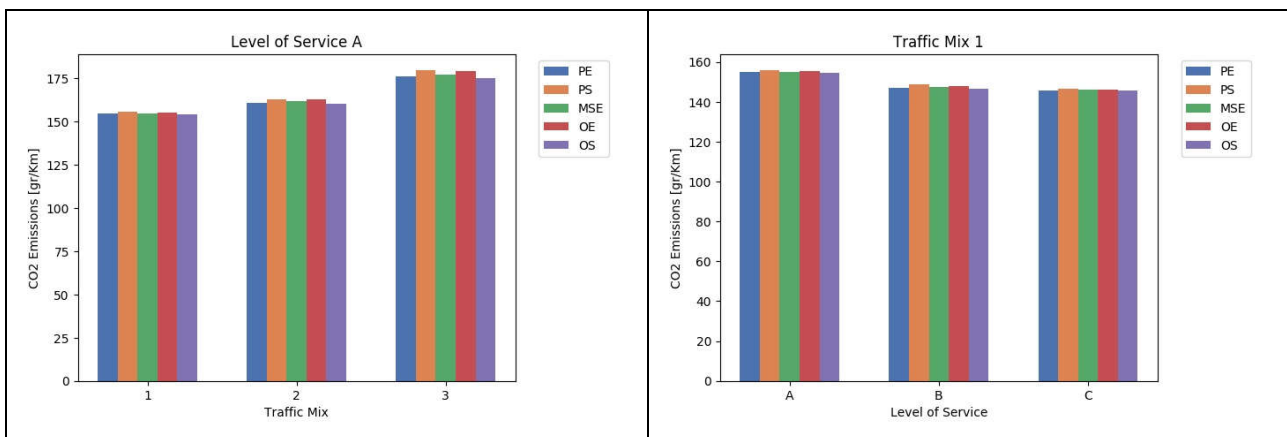


Figure 59. Average number of events with TTCs below 3.0 seconds for the different LoS with fixed traffic composition (Mix 3).

4.5.2.4 Environmental Impacts

As all scenarios exhibit highly similar dynamics, the differences between the corresponding emission levels are not large either, see **Figure 60**, which shows the average CO₂ emissions per travelled kilometre for different scenarios.

Two observations are perhaps notable. Firstly, the emissions increase with the share of CAVs/CVs in the scenario (correlating inversely with the number of lane changes, see Section 4.5.2.2). Probably, this is induced by the additional braking and accelerating occurring during ToCs and, more importantly, during MRMs. Perhaps, the slight disturbances due to not performing a lane change, which might be beneficial to the flow, also play a role. However, both factors are not reflected in the average network speed, see Section 4.5.2.1. Secondly, the emission level decreases with increasing demand, which may surprise at first glance. Keeping in mind that the situation is not congested, this is probably best explained by the slightly decreased average vehicle speeds, which correspond to a more efficient operation in terms of emissions per kilometre.



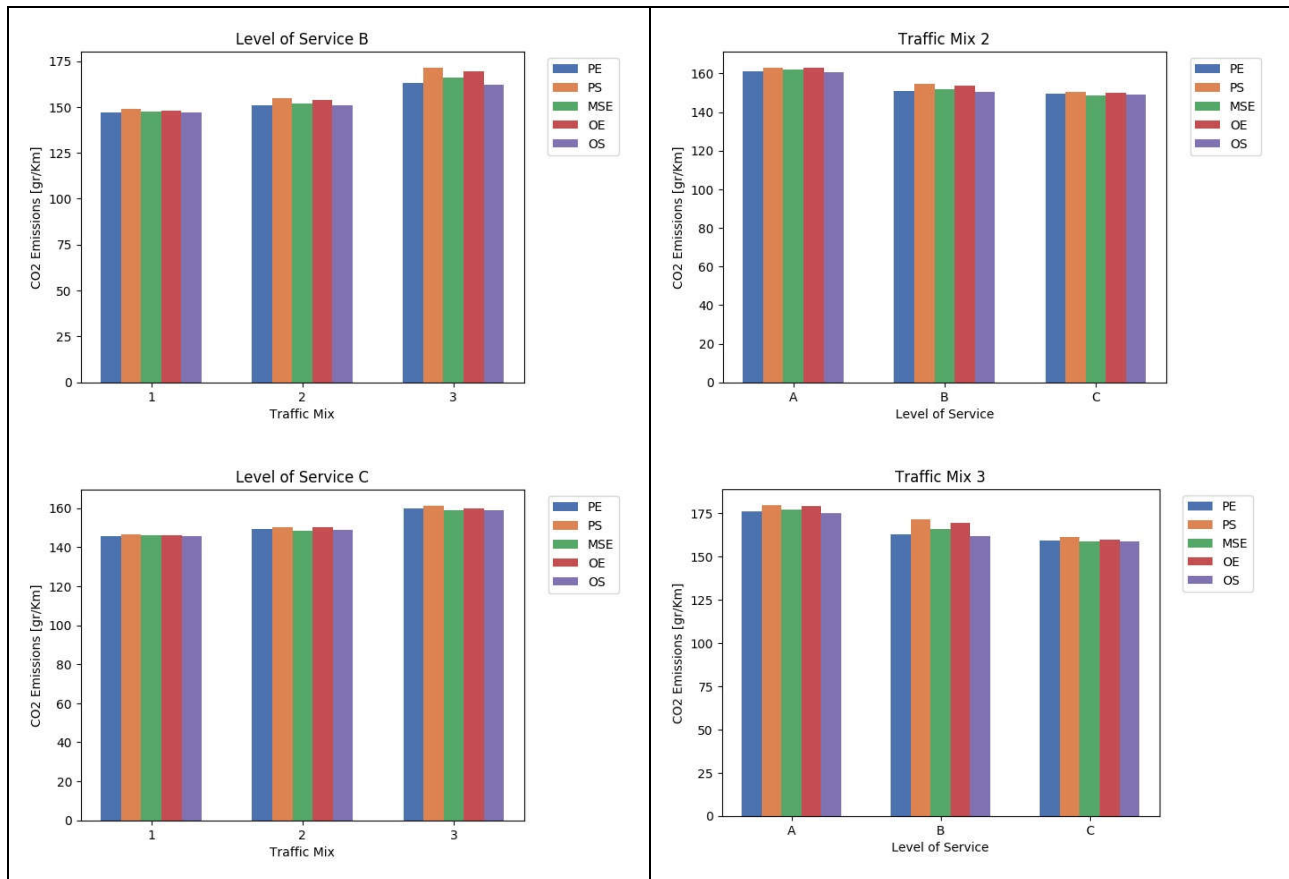


Figure 60. Average CO₂ emissions per km travelled for Scenario 5.1 baseline simulation experiments (varying parameter scheme, LOS, and traffic mix). Different bar colours correspond to different parameter schemes. The left column groups results by LOS, the right column by traffic mix.

5 Conclusions

In this Deliverable D3.1 we developed driver models to emulate vehicle automations for CAVs/CVs. These models dictate CAV/CV longitudinal motion, lateral motion, and driving behaviour during ToC/MRM. We adopted an ACC model from a previous study and modified it to ensure collision-free car-following and to simulate CAV/CV longitudinal motions in SUMO. We also parametrised SUMO's default lane change model (LC2013) to reflect the actual (OEM-specific) CAV/CV lane change behaviour by means of a sensitivity analysis. Finally, we developed a ToC/MRM model based on literature findings to mimic ToC/MRM at TAs.

Our baseline simulations experiments encompassed three distinct dimensions (the traffic demand level, the traffic mix, and the driver model parametrisation scheme) to capture the effects of ToCs/MRM for varying traffic conditions, traffic composition, and vehicle properties. We addressed six scenarios, previously defined in Deliverable D2.2, with respect to the investigation of ToC/MRM impacts at work zones (Scenarios 1.1 and 4.2), motorway merge segments (Scenarios 2.1 and 3.1), and no-AD zones (Scenario 5.1). We presented simulation results and analysed them in terms of traffic efficiency, traffic dynamics, traffic safety, and environmental impacts at TAs.

The analysis of the simulation results indicated that congestion at lane drops is highly correlated with safety-critical events. Moreover, it is found that traffic safety is further undermined as the share of CAVs/CVs in the traffic mix increases. The rationale behind this behaviour is that CAVs/CVs were simulated more conservative in terms of their lane change behaviour in comparison to LVs. Therefore, they cannot merge early enough to the desired lane, which in return leads to sudden braking in front of the dead-end lane and consequently to rear-end conflicts due to car-following. It is also noteworthy that conflicts are higher for parametrisation schemes that were expected to benefit traffic safety (PE and OS). However, since the parameter values of these schemes result in reduced merging efficiency, the aforementioned phenomenon is more pronounced.

A noteworthy finding is that parametrisation schemes OE and PS exhibit similar performance for most of the simulated scenarios and output statistics. The same applies to parametrisation schemes PE and OS. These pairs represent similar behaviour in terms of car-following and lane-changing, but different in terms of driver response to ToC/MRM (**Table 18**). Thus, it can be deduced that ToCs and MRMs do not heavily impact traffic operations given their current implementation in baseline simulation experiments. This is rather exemplified by simulation results of Scenario 5.1, where ToCs/MRMs have no effects on traffic operations given the examined demand levels, traffic mixes, and parametrisation schemes. The reason behind this behaviour can be two-fold. Firstly, the unexpectedness of MRMs for non-cooperative vehicles is only captured rudimentarily in the given model structure, and secondly, MRMs do not necessarily result in a full vehicle stop. By adapting the ToC/MRM model to incorporate more realism concerning following vehicle reaction to MRMs, and assuming MRM logic that mandates a full vehicle stop, the most deteriorating effects of ToCs/MRMs might be captured.

Simulation results also show that there is no clear relationship between lane-changing and traffic efficiency. However, it is stressed that no investigation was conducted with respect to the allocation of lane changes per reason, location, and vehicle type. This work will be done in future deliverables to identify the impacts of lane changes in the proximity and along TAs. Finally, it is demonstrated that emissions levels decrease for improved traffic efficiency, and increase significantly for stop-and-go traffic (Scenario 4.2, Motorway Network).

According to simulation results, it is clear that traffic operations are significantly degraded at lane drop locations leading to adverse impacts on traffic efficiency, safety, and environment. Thus, facilitating merging operations at lane drops by providing lane advice seems to be a promising

measure for improving traffic conditions at TAs. The latter traffic management measure was proposed by TransAID in D2.1 and will be evaluated in D3.2.

Finally, we emphasise that within the context of this Deliverable D3.1 some important assumptions were made with respect to vehicle model parameter values and respective driving behaviour for CAVs, CVs, and LVs. Thus, the investigation of ToCs/MRMs at TAs was done to a theoretical level which provided an initial understanding of traffic operations at TAs in the absence of traffic management. Simulation results indicate that a rigorous calibration of the LVs lane change behaviour is also necessary to replicate overall merging operations more accurately. Parameters pertaining to ToC/MRM model need to be also tuned in more detail based on actual CAV/CV behaviour. Moreover, an actual road network needs to be simulated (with calibrated demand) in the next project iteration to examine the effects of ToCs/MRMs in real traffic conditions.

References

- Behrisch, M., Bieker, L., Erdmann, J., & Krajzewicz, D. (2011). SUMO – Simulation of Urban MObility: An Overview. In *Proceedings of SIMUL 2011, The Third International Conference on Advances in System Simulation*. Barcelona: ThinkMind. Retrieved from <http://www.thinkmind.org/index.php?view=instance&instance=SIMUL+2011>
- Blommer, M., Curry, R., Swaminathan, R., Tijerina, L., Talamonti, W., & Kochhar, D. (2017). Driver brake vs. steer response to sudden forward collision scenario in manual and automated driving modes. *Transportation Research Part F: Traffic Psychology and Behaviour*, *45*, 93–101. <https://doi.org/10.1016/j.trf.2016.11.006>
- Blythe, P., & Curtis, A. (2004). Advanced driver assistance systems: Gimmick or reality? Presented at the 11th World Congress on ITS, Nagoya. Retrieved from https://www.researchgate.net/profile/Philip_Blythe/publication/233932657_Advanced_Driver_Assistance_Systems_gimmick_or_reality/links/56b8843f08aebbde1a7f7907.pdf
- Clark, H., & Feng, J. (2017). Age differences in the takeover of vehicle control and engagement in non-driving-related activities in simulated driving with conditional automation. *Accident Analysis & Prevention*, *106*, 468–479. <https://doi.org/10.1016/j.aap.2016.08.027>
- Cukier, R. I., Fortuin, C. M., Shuler, K. E., Petschek, A. G., & Schaibly, J. H. (1973). Study of the sensitivity of coupled reaction systems to uncertainties in rate coefficients. I Theory. *The Journal of Chemical Physics*, *59*(8), 3873–3878. <https://doi.org/10.1063/1.1680571>
- Davis, L. C. (2004). Effect of adaptive cruise control systems on traffic flow. *Physical Review E*, *69*(6). <https://doi.org/10.1103/PhysRevE.69.066110>
- de Winter, J. C. F., Happee, R., Martens, M. H., & Stanton, N. A. (2014). Effects of adaptive cruise control and highly automated driving on workload and situation awareness: A review of the empirical evidence. *Transportation Research Part F: Traffic Psychology and Behaviour*, *27*, 196–217. <https://doi.org/10.1016/j.trf.2014.06.016>
- Erdmann, J. (2014). Lane-Changing Model in SUMO. In *Proceedings of the SUMO2014 Modeling Mobility with Open Data* (Vol. 24, pp. 77–88). Berlin, Deutschland: Deutsches Zentrum für Luft- und Raumfahrt e.V. Retrieved from <http://elib.dlr.de/89233/>
- Eriksson, A., & Stanton, N. A. (2017). Takeover Time in Highly Automated Vehicles: Noncritical Transitions to and From Manual Control. *Human Factors: The Journal of the Human Factors and Ergonomics Society*, *59*(4), 689–705. <https://doi.org/10.1177/0018720816685832>
- Fuller, R. (2005). Towards a general theory of driver behaviour. *Accident Analysis & Prevention*, *37*(3), 461–472. <https://doi.org/10.1016/j.aap.2004.11.003>
- Gold, C., Damböck, D., Lorenz, L., & Bengler, K. (2013). “Take over!” How long does it take to get the driver back into the loop? *Proceedings of the Human Factors and Ergonomics Society Annual Meeting*, *57*(1), 1938–1942. <https://doi.org/10.1177/1541931213571433>
- Hasebe, K., Nakayama, A., & Sugiyama, Y. (2003). Dynamical model of a cooperative driving system for freeway traffic. *Physical Review E*, *68*(2). <https://doi.org/10.1103/PhysRevE.68.026102>

- Hausberger, S., Rexeis, M., & Luz, R. (2011). PHEM - the model of the TU Graz for the calculation of vehicle emissions and its database at Euro 5 and Euro 6. Presented at the Symposium: Emissions and potential for reduction in road traffic, Stuttgart, Germany.
- Horst, R. V. D., & Hogema, J. (1993). Time-to-Collision and Collision Avoidance Systems. Presented at the 6th ICTCT Workshop, Salzburg.
- Kesting, A., & Treiber, M. (2008). Calibrating Car-Following Models by Using Trajectory Data: Methodological Study. *Transportation Research Record: Journal of the Transportation Research Board*, 2088, 148–156. <https://doi.org/10.3141/2088-16>
- Kesting, A., Treiber, M., Schönhof, M., & Helbing, D. (2008). Adaptive cruise control design for active congestion avoidance. *Transportation Research Part C: Emerging Technologies*, 16(6), 668–683. <https://doi.org/10.1016/j.trc.2007.12.004>
- Krauß, S. (1998). *Microscopic Modeling of Traffic Flow: Investigation of Collision Free Vehicle Dynamics* (Doctoral Thesis). DLR-Forschungsbericht. Retrieved from <http://elib.dlr.de/8380/>
- Liang, C.-Y., & Peng, H. (1999). Optimal Adaptive Cruise Control with Guaranteed String Stability. *Vehicle System Dynamics*, 32(4–5), 313–330. <https://doi.org/10.1076/vesd.32.4.313.2083>
- Liu, H., Kan, X., Wei, D., Chou, F.-C., Shladover, S. E., & Lu, X.-Y. (2018). *Using Cooperative Adaptive Cruise Control (CACC) to Form High-Performance Vehicle Streams - Microscopic Traffic Modeling* (FHWA Exploratory Advanced Research Program No. Cooperative Agreement No. DTFH61-13-H-00013). University of California, Berkeley: California PATH Program.
- Louw, T., Kountouriotis, G., Carsten, O., & Merat, N. (2015). Driver Inattention During Vehicle Automation: How Does Driver Engagement Affect Resumption Of Control? In *4th International Conference on Driver Distraction and Inattention (DDI2015)*, Sydney: proceedings. ARRB Group. Retrieved from <http://eprints.whiterose.ac.uk/91858/>
- Lu, Z., Coster, X., & de Winter, J. (2017). How much time do drivers need to obtain situation awareness? A laboratory-based study of automated driving. *Applied Ergonomics*, 60, 293–304. <https://doi.org/10.1016/j.apergo.2016.12.003>
- Lu, Z., Happee, R., Cabrall, C. D. D., Kyriakidis, M., & de Winter, J. C. F. (2016). Human factors of transitions in automated driving: A general framework and literature survey. *Transportation Research Part F: Traffic Psychology and Behaviour*, 43, 183–198. <https://doi.org/10.1016/j.trf.2016.10.007>
- Marsden, G., McDonald, M., & Brackstone, M. (2001). Towards an understanding of adaptive cruise control. *Transportation Research Part C: Emerging Technologies*, 9(1), 33–51. [https://doi.org/10.1016/S0968-090X\(00\)00022-X](https://doi.org/10.1016/S0968-090X(00)00022-X)
- Merat, N., Jamson, A. H., Lai, F. C. H., & Carsten, O. (2012). Highly Automated Driving, Secondary Task Performance, and Driver State. *Human Factors: The Journal of the Human Factors and Ergonomics Society*, 54(5), 762–771. <https://doi.org/10.1177/0018720812442087>
- Merat, N., Jamson, A. H., Lai, F. C. H., Daly, M., & Carsten, O. M. J. (2014). Transition to manual: Driver behaviour when resuming control from a highly automated vehicle. *Transportation Research Part F: Traffic Psychology and Behaviour*, 27, 274–282. <https://doi.org/10.1016/j.trf.2014.09.005>

- Milanés, V., & Shladover, S. E. (2014). Modeling cooperative and autonomous adaptive cruise control dynamic responses using experimental data. *Transportation Research Part C: Emerging Technologies*, 48, 285–300. <https://doi.org/10.1016/j.trc.2014.09.001>
- Milanés, V., & Shladover, S. E. (2016). Handling Cut-In Vehicles in Strings of Cooperative Adaptive Cruise Control Vehicles. *Journal of Intelligent Transportation Systems*, 20(2), 178–191. <https://doi.org/10.1080/15472450.2015.1016023>
- Milanes, V., Shladover, S. E., Spring, J., Nowakowski, C., Kawazoe, H., & Nakamura, M. (2014). Cooperative Adaptive Cruise Control in Real Traffic Situations. *IEEE Transactions on Intelligent Transportation Systems*, 15(1), 296–305. <https://doi.org/10.1109/TITS.2013.2278494>
- Mok, B., Johns, M., Miller, D., & Ju, W. (2017). Tunneled In: Drivers with Active Secondary Tasks Need More Time to Transition from Automation. In *Proceedings of the 2017 CHI Conference on Human Factors in Computing Systems* (pp. 2840–2844). New York, NY, USA: ACM. <https://doi.org/10.1145/3025453.3025713>
- National Research Council (U.S.) (Ed.). (2010). *Highway Capacity Manual*. Washington, D.C.: Transportation Research Board, National Research Council.
- Naus, G. J. L., Vugts, R. P. A., Ploeg, J., van de Molengraft, M. J. G., & Steinbuch, M. (2010). String-Stable CACC Design and Experimental Validation: A Frequency-Domain Approach. *IEEE Transactions on Vehicular Technology*, 59(9), 4268–4279. <https://doi.org/10.1109/TVT.2010.2076320>
- Ott, L., & Longnecker, M. (2004). *A first course in statistical methods*. Belmont, CA: Thomson-Brooks/Cole.
- Punzo, V., & Ciuffo, B. F. (2011). Sensitivity Analysis of Car-following Models: Methodology and Application. Presented at the Transportation Research Board 90th Annual Meeting Transportation Research Board. Retrieved from <https://trid.trb.org/view/1092680>
- Punzo, V., Montanino, M., & Ciuffo, B. (2015). Do We Really Need to Calibrate All the Parameters? Variance-Based Sensitivity Analysis to Simplify Microscopic Traffic Flow Models. *IEEE Transactions on Intelligent Transportation Systems*, 16(1), 184–193. <https://doi.org/10.1109/TITS.2014.2331453>
- Saltelli, A. (Ed.). (2008). *Global sensitivity analysis: the primer*. Chichester, England ; Hoboken, NJ: John Wiley.
- Saltelli, A., Annoni, P., Azzini, I., Campolongo, F., Ratto, M., & Tarantola, S. (2010). Variance based sensitivity analysis of model output. Design and estimator for the total sensitivity index. *Computer Physics Communications*, 181(2), 259–270. <https://doi.org/10.1016/j.cpc.2009.09.018>
- Saltelli, A., Tarantola, S., Campolongo, F., & Ratto, M. (2002). *Sensitivity Analysis in Practice*. Chichester, UK: John Wiley & Sons, Ltd. <https://doi.org/10.1002/0470870958>
- Samuel, S., Borowsky, A., Zilberstein, S., & Fisher, D. L. (2016). Minimum Time to Situation Awareness in Scenarios Involving Transfer of Control from an Automated Driving Suite. *Transportation Research Record: Journal of the Transportation Research Board*, 2602, 115–120. <https://doi.org/10.3141/2602-14>

- Shladover, S., Su, D., & Lu, X.-Y. (2012). Impacts of Cooperative Adaptive Cruise Control on Freeway Traffic Flow. *Transportation Research Record: Journal of the Transportation Research Board*, 2324, 63–70. <https://doi.org/10.3141/2324-08>
- Sobol, I. M. (1993). Sensitivity estimates for nonlinear mathematical models. *Mathematical Modelling and Computational Experiments*, 1(4), 407–414.
- Sobol, I. M., Tarantola, S., Gatelli, D., Kucherenko, S. S., & Mauntz, W. (2007). Estimating the approximation error when fixing unessential factors in global sensitivity analysis. *Reliability Engineering & System Safety*, 92(7), 957–960. <https://doi.org/10.1016/j.ress.2006.07.001>
- Todosiev, E. P. (1963). *The action point model of the driver-vehicle system* (Ph.D. Thesis). The Ohio State University.
- Treiber, M., & Helbing, D. (2001). Microsimulations of Freeway Traffic Including Control Measures. *At - Automatisierungstechnik*, 49(11/2001). <https://doi.org/10.1524/auto.2001.49.11.478>
- Treiber, M., Hennecke, A., & Helbing, D. (2000). Congested traffic states in empirical observations and microscopic simulations. *Physical Review E*, 62(2), 1805–1824. <https://doi.org/10.1103/PhysRevE.62.1805>
- Treiber, M., & Kesting, A. (2013). *Traffic Flow Dynamics: Data, Models and Simulation*. Berlin Heidelberg: Springer-Verlag. Retrieved from [//www.springer.com/us/book/9783642324598](http://www.springer.com/us/book/9783642324598)
- van Arem, B., van Driel, C. J. G., & Visser, R. (2006). The Impact of Cooperative Adaptive Cruise Control on Traffic-Flow Characteristics. *IEEE Transactions on Intelligent Transportation Systems*, 7(4), 429–436. <https://doi.org/10.1109/TITS.2006.884615>
- VanderWerf, J., Shladover, S., Kourjanskaia, N., Miller, M., & Krishnan, H. (2001). Modeling Effects of Driver Control Assistance Systems on Traffic. *Transportation Research Record: Journal of the Transportation Research Board*, 1748, 167–174. <https://doi.org/10.3141/1748-21>
- VanderWerf, J., Shladover, S., Miller, M., & Kourjanskaia, N. (2002). Effects of Adaptive Cruise Control Systems on Highway Traffic Flow Capacity. *Transportation Research Record: Journal of the Transportation Research Board*, 1800, 78–84. <https://doi.org/10.3141/1800-10>
- Wagner, P. (2012). Analyzing fluctuations in car-following. *Transportation Research Part B: Methodological*, 46(10), 1384–1392. <https://doi.org/10.1016/j.trb.2012.06.007>
- Xiao, L., & Gao, F. (2011). Practical String Stability of Platoon of Adaptive Cruise Control Vehicles. *IEEE Transactions on Intelligent Transportation Systems*, 12(4), 1184–1194. <https://doi.org/10.1109/TITS.2011.2143407>
- Xiao, L., Wang, M., & van Arem, B. (2017). Realistic Car-Following Models for Microscopic Simulation of Adaptive and Cooperative Adaptive Cruise Control Vehicles. *Transportation Research Record: Journal of the Transportation Research Board*, 2623, 1–9. <https://doi.org/10.3141/2623-01>
- Xin, W., Hourdos, J., Michalopoulos, P., & Davis, G. (2008). The Less-Than-Perfect Driver: A Model of Collision-Inclusive Car-Following Behavior. *Transportation Research Record: Journal of the Transportation Research Board*, 2088, 126–137. <https://doi.org/10.3141/2088-14>

Young, M. S., & Stanton, N. A. (2002). Malleable Attentional Resources Theory: A New Explanation for the Effects of Mental Underload on Performance. *Human Factors: The Journal of the Human Factors and Ergonomics Society*, 44(3), 365–375.

<https://doi.org/10.1518/0018720024497709>

Young, M. S., & Stanton, N. A. (2007). Back to the future: Brake reaction times for manual and automated vehicles. *Ergonomics*, 50(1), 46–58. <https://doi.org/10.1080/00140130600980789>

Zeeb, K., Buchner, A., & Schrauf, M. (2015). What determines the take-over time? An integrated model approach of driver take-over after automated driving. *Accident Analysis & Prevention*, 78, 212–221. <https://doi.org/10.1016/j.aap.2015.02.023>

Ziegler, J., Bender, P., Schreiber, M., Lategahn, H., Strauss, T., Stiller, C., ... Zeeb, E. (2014). Making Bertha Drive-An Autonomous Journey on a Historic Route. *IEEE Intelligent Transportation Systems Magazine*, 6(2), 8–20. <https://doi.org/10.1109/MITS.2014.2306552>

Appendix A

SUMO network files were created within the context of D2.2. Information pertinent to the dimensions of the simulation experiments (three different vehicle mixes for CAVs, CVs, and LVs, three different traffic demand levels (LOS A, LOS B, LOS C), five different driver model parameter sets (PS, PE, MSE, OE, OS), all corresponding to six baseline scenarios) was input to the appropriate SUMO configuration files in D3.1.

Initially, parameter values for the driver models were specified (either in the form of constant values or normal distributions) for each parametrisation scheme, through a configuration file (**Figure A.1**). Subsequently, using the Python script ‘createVehTypeDistribution.py’, along with the corresponding configurations (text) files, the desired heterogeneous flows are generated (**Figure A.2**).

```
# Create automated vType distribution.

# Parametrization Scheme: Pessimistic Safety (PS)

#####
# Attribute distributions for the ACC model.
# Aggressive ACC.
#####
carFollowModel ; ACC
tau           ; normal(1.2, 0.1); [1.1, 1.3]
accel         ; normal(1.5, 1.0); [0.75, 2.0]
decel         ; normal(3.0, 1.0); [2.0, 4.0]
emergencyDecel ; 9.0

#####
# Generic Attributes.
#####
color; white
actionStepLength ; 0.1

#####
# Attribute distributions for the SL2015 model.
# Aggressive SL2015.
#####
lcAssertive ; normal(0.9, 0.1); [0.8, 1.0]

#####
# Attribute distributions for the TOC/MRM model.
# Conservative TOC/MRM.
#####
param; has.toc.device           ; true
param; device.toc.manualType    ; vehLVPS
param; device.toc.automatedType ; vehCAVToCPS
param; device.toc.responseTime  ; normal(7, 3); [2, 60]
param; device.toc.initialAwareness ; normal(0.3, 0.3); [0.1, 1.0]
param; device.toc.recoveryRate  ; normal(0.2, 0.1); [0.01, 0.5]
param; device.toc.mrmDecel      ; 3.0
param; device.toc.useColorScheme ; true
```

normal(mu, sd): with mu and sd being floating numbers: Normal distribution with mean mu and standard deviation sd.

Figure A.1 Configure file – defines the car-following parameter distributions for the pessimistic safety parametrisation scheme.

```

<vTypeDistribution id="vehLVMSE">
  <vType accel="1.503" actionStepLength="0.100" carFollowModel="Krauss" color="yellow" decel="3.362"
    emergencyDecel="9.000" id="vehLVMSE0" lcAssertive="1.300" sigma="0.483" speedFactor="0.905" tau="0.723"/>
  <vType accel="1.675" actionStepLength="0.100" carFollowModel="Krauss" color="yellow" decel="3.035"
    emergencyDecel="9.000" id="vehLVMSE1" lcAssertive="1.300" sigma="0.383" speedFactor="1.174" tau="1.469"/>
  <vType accel="1.069" actionStepLength="0.100" carFollowModel="Krauss" color="yellow" decel="3.810"
    emergencyDecel="9.000" id="vehLVMSE2" lcAssertive="1.300" sigma="0.671" speedFactor="1.014" tau="0.925"/>
  <vType accel="3.314" actionStepLength="0.100" carFollowModel="Krauss" color="yellow" decel="2.965"
    emergencyDecel="9.000" id="vehLVMSE3" lcAssertive="1.300" sigma="0.910" speedFactor="1.129" tau="0.821"/>
  <vType accel="2.673" actionStepLength="0.100" carFollowModel="Krauss" color="yellow" decel="2.386"
    emergencyDecel="9.000" id="vehLVMSE4" lcAssertive="1.300" sigma="0.638" speedFactor="0.864" tau="1.034"/>

```

(a)

```

</vType>
<vType accel="1.868" actionStepLength="0.100" carFollowModel="ACC" color="white" decel="2.343"
  emergencyDecel="9.000" id="vehCAVtoCMSE1" lcAssertive="0.737" tau="1.507">
  <param key="device.toc.automatedType" value="vehCAVtoCMSE"/>
  <param key="device.toc.manualType" value="vehLVMSE"/>
  <param key="has.toc.device" value="true"/>
  <param key="device.toc.mrmDecel" value="3.000"/>
  <param key="device.toc.recoveryRate" value="0.348"/>
  <param key="device.toc.initialAwareness" value="0.218"/>
  <param key="device.toc.useColorScheme" value="true"/>
  <param key="device.toc.responseTime" value="4.630"/>

```

(b)

```

</vType>
<vType accel="1.868" actionStepLength="0.100" carFollowModel="ACC" color="blue" decel="2.343"
  emergencyDecel="9.000" id="vehCVtoCMSE1" lcAssertive="0.605" tau="1.507">
  <param key="device.toc.automatedType" value="vehCVtoCMSE"/>
  <param key="device.toc.manualType" value="vehLVMSE"/>
  <param key="has.toc.device" value="true"/>
  <param key="device.toc.mrmDecel" value="3.000"/>
  <param key="device.toc.recoveryRate" value="0.348"/>
  <param key="device.toc.initialAwareness" value="0.218"/>
  <param key="device.toc.useColorScheme" value="true"/>
  <param key="device.toc.responseTime" value="0.000"/>

```

(c)

Figure A.2 Portion of the output ‘vTypeDistributions’ file including information of the driver models of each vehicle type: (a) LVs, (b) CAVs and (c) CVs.

The process of running all baseline simulation scenarios is automated, through the use of the Python script ‘batchRunner.py’ (**Figure A.3**), for all possible combinations of the different vehicle mixes, traffic demand levels, and driver model parameter sets. In addition, an important aspect of reproducing realistic results in a simulation scenario is the stochasticity introduced into the simulation experiments. SUMO uses two different RNG instances, one for random numbers used on creating vehicles and one for dynamic behaviour. In order to secure that simulation results were statistically significant, ten simulations were performed using different seeds that were randomly generated.

```
# Number of simulations per Demand/Parameter configuration
Nsim = 10
# Number of lanes (regarding the LOS) in the current scenario
Nlanes = 1

# Number of restarts if a run fails
MAXTRIES = 10

# List of genral additional files to be loaded for all runs
generalAddFiles = [".././../shapes.add.xml", ".././../closeLanes.add.xml", ".././../view.add.xml "]

# Demand levels (levelID->veh/(h*l))
demand_urban = {"los_A":735, "los_B":1155, "los_C":1617}

# levels to be used for simulations
demand_levels = demand_urban
demand_ID_map = {"los_A":0, "los_B":1, "los_C":2}

# Vehicle mix (mix_ID->class->share [in %])
veh_mixes = {"mix_0":{"LV":0.7, "CVToC":0.15, "CAVToC":0.15},
             "mix_1":{"LV":0.5, "CVToC":0.25, "CAVToC":0.25},
             "mix_2":{"LV":0.2, "CVToC":0.4, "CAVToC":0.4}}

# Parameter assumptions regarding (E)fficiency/(S)afety and (O)ptimism/(P)essimism
param_schemes = ["PS", "OS", "PE", "OE", "MSE"]

# template file for the routes
routefile_template = "routes_template.rou.xml"

# config file
config_file = "sumo.cfg"

# runner script for single runs
runner_file = "runner.py"
```

Figure A.3 Part of the Python script used for the automated running of the baseline simulation scenarios.

The collection of the simulation output files was conducted in four different XML-format files, using commands [lanechange-file](#), [summary-file](#), [emission-file](#) and [queue-file](#) in the Python script ‘batchRunner.py’, as depicted in **Figure A.4**, while the output for the SSM device is specified at the corresponding route definition file (**Figure A.5**). Finally, as illustrated in **Figure A.4**, the Python script ‘batchRunner.py’ calls the ‘runner.py’ script which triggers the ToC device for the specified vehicle types.

```
# this is the main entry point of this script
if __name__ == "__main__":
    options = get_options()
    downwardEdgeID = None
    distance = None
    # this script has been called from the command line. It will start sumo as a
    # server, then connect and run
    if options.gui:
        sumoBinary = checkBinary('sumo-gui')
    else:
        sumoBinary = checkBinary('sumo')
    # sumoBinary = checkBinary('sumo-gui')

    traci.start([sumoBinary, "-c", options.sumocfg, "--seed", options.seed,
    "--summary", "outputSummary%s"%options.suffix, "-a", options.additional, "-r", options.routes,
    "--lanechange-output", "outputLaneChanges%s"%options.suffix,
    "--queue-output", "outputQueue%s"%options.suffix])

    downwardEdgeID = "approach2"
    distance = 10.
    #~ upwardEdgeID = "e0"
    #~ upwardDist = 3500.0

    run(downwardEdgeID, distance) #, upwardEdgeID, upwardDist)

    traci.close()
    sys.stdout.flush()
```

Figure A.4 Part of the Python script ‘batchRunner.py’ including the desired commands/arguments for the generation of the output files.


```

<?xml version="1.0" encoding="UTF-8"?>
<routes
  xmlns:xsi="http://www.w3.org/2001/XMLSchema-instance"
  xsi:noNamespaceSchemaLocation="http://sumo.dlr.de/xsd/routes_file.xsd">

  <route edges="start approach1 approach2 safetyzone1 workzone safetyzone2 leave end" id="route01"/>

  <flow begin="0" departLane="random" end="3600" id="CVToC"
    probability="{CVToCprob}" route="route01" type="{CVToCtype}">
    <param key="has.ssm.device" value="true" />
    <param key="device.ssm.measures" value="TTC DRAC PET" />
    <param key="device.ssm.thresholds" value="0 0 10" />
    <param key="device.ssm.frequency" value="10" />
    <param key="device.ssm.range" value="20" />
    <param key="device.ssm.trajectories" value="false" />
    <param key="device.ssm.file" value="{ssmOutFile}" />
  </flow>

  <flow begin="0" departLane="random" end="3600" id="CAVToC"
    probability="{CAVToCprob}" route="route01" type="{CAVToCtype}">
    <param key="has.ssm.device" value="true" />
    <param key="device.ssm.measures" value="TTC DRAC PET" />
    <param key="device.ssm.thresholds" value="0 0 10" />
    <param key="device.ssm.frequency" value="10" />
    <param key="device.ssm.range" value="20" />
    <param key="device.ssm.trajectories" value="false" />
    <param key="device.ssm.file" value="{ssmOutFile}" />
  </flow>

  <flow id="LV" type="{LVtype}" route="route01" begin="0" end="3600"
    probability="{LVprob}" departLane="best" departSpeed="max">
    <param key="has.ssm.device" value="true" />
    <param key="device.ssm.measures" value="TTC DRAC PET" />
    <param key="device.ssm.thresholds" value="0 0 10" />
    <param key="device.ssm.frequency" value="10" />
    <param key="device.ssm.range" value="20" />
    <param key="device.ssm.trajectories" value="false" />
    <param key="device.ssm.file" value="{ssmOutFile}" />
  </flow>

</routes>

```

⇒ CVs

⇒ CAVs

⇒ LVs

Figure A.5 The route definition file, ‘rou.xml’, to attach an SSM device to the vehicles.